# Treatment of steel industry wastewater by an integrated ozonation and electrocoagulation process

*Thesis submitted in partial fulfillment of the requirements for the degree of*

*Doctor of Philosophy*

*By*

*Pranjal Pratim Das*

*Roll No.: 176107027*


**Department of Chemical Engineering**

**Indian Institute of Technology Guwahati**

**Guwahati – 781039, Assam, India**

# Treatment of steel industry wastewater by an integrated ozonation and electrocoagulation process

*Pranjal Pratim Das*

# Treatment of steel industry wastewater by an integrated ozonation and electrocoagulation process

*Thesis submitted in partial fulfillment of the requirements for the degree of*

*Doctor of Philosophy*

*By*

*Pranjal Pratim Das*

*Roll No.: 176107027*


**Department of Chemical Engineering**

**Indian Institute of Technology Guwahati**

**Guwahati – 781039, Assam, India**

*Dedicated to my Parents, my elder Brother, my wife and the Almighty GOD. Their Uncountable Support and Blessings has Helped Me to be the Better Person that I am Today.*

# Department of Chemical Engineering
# Indian Institute of Technology Guwahati
# Guwahati - 781039, Assam, India

# CERTIFICATE

It is certified that the work contained in the thesis entitled "**Treatment of steel industry wastewater by an integrated ozonation and electrocoagulation process**", by **Pranjal Pratim Das**, a Ph.D. student of the Department of Chemical Engineering, Indian Institute of Technology Guwahati, has been carried out under my supervision. The work documented in this thesis has not been submitted to any other University or Institute for the award of any degree or diploma.

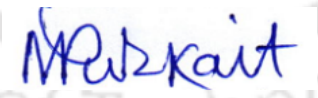

**Dr. Mihir Kumar Purkait**

Professor

Department of Chemical Engineering

Indian Institute of Technology Guwahati

Guwahati - 781039, Assam, India

Date: 10/06/2024

# *Acknowledgements*

I wish to express my sincere acknowledgement and respect to my supervisor, **Prof. Mihir Kumar Purkait** for being a source of my inspiration and guidance all throughout my research work. I am thankful to him for his useful suggestions and constant encouragement throughout my entire work period and feel fortunate enough to have worked under him all these years. He has been a moral support throughout my bad times and has always provided me with the freedom to carry out my work without any pressure in the most amicable manner.

I would like to thank my doctoral committee (DC) members, Prof. S. K. Majumder and Prof. A. K. Golder (Chemical Engineering), as well as Prof. P. K. Ghosh (Civil Engineering) for their valuable suggestions and constructive criticism, which helped me to make necessary improvements in various stages of my research work and also enhance my presentation and writing skills. Further, I would also like to express my heartfelt gratitude to the members of my PhD viva-voce committee, **Prof. Sunil Kumar Maity** (IIT Hyderabad, India), **Prof. Graham A. Gagnon** (Dalhousie University, Canada), **Prof. Subrata Kumar Majumder** (Chairperson), **Prof. Pallab Ghosh**, and **Prof. Selvaraju Narayanasamy**, for their invaluable guidance, insightful feedback, and unwavering support. Their expertise and recommendations were instrumental in refining my research and contributing to my academic development.

I am thankful to all the faculty members of the Chemical Engineering Department for their constant encouragement and support during my stay in this department. I would also like to extend my gratitude to the technical officers of my department specially, Mr. Harsaraj Biswanath and Mrs. Ritumoni Kalita, (technical officers), Mr. Lukumoni Borah and Mr. Dipak Barman (technical superintendents), Mr. Jayanta Mout (senior technical superintendent), Mr. Balen Mahanta, Mr. Debajit Borah and Mr. Pankaj Baruah (junior technical superintendents), and the office staffs, Mr. Bhagya Boro and Ms. Chinmayee Pathak. The experimental works presented in this thesis as well as all the official paper works would never have been possible

without the help of these proficient technicians. I am also thankful to the Central Instruments Facility, IITG for analysing all my samples with the utmost precision and timely disposition.

I extend my sincere thanks to my lab seniors Dr. Murchana Changmai and Dr. Piyal Mondal for helping me out innumerable times with my work. My labmates specially, Mr. Niladri S. Samanta, Mr. Ankush D. Sontakke, Mr. Anweshan, Mrs. Deepti, and Mr. Simons Dhara, along with all my juniors provided constant support during my work and helped me in having a pleasant work environment in the lab with their untimely help, support and valuable cooperation. I would also like to extend my gratitude to all the research scholars of the Chemical Engineering department for helping me out whenever I approached them with any queries or requirements.

I would also like to thank **Tata Steel Limited, India** for giving me the opportunity to work with them in creating a better sustainable water environment.

I have no words to thank **the almighty GOD** who was and will always remain my source of strength and wisdom.

Last but not the least; I would like to thank my father **Mr. Tapan Kumar Das**, my mother, **Mrs. Iva Dutta Das**, my elder brother **Mr. Parashar Olymen** and my wife **Mrs. Punampriya Borgohain** for supporting me at every step of my Ph.D. My parents have always believed in me and moulded me into the strong and independent person that I am today. My wife has always been a moral support during my time of weakness and I could not thank God enough for bestowing me with such a supportive family. Their love, affection, blessings and sacrifices made me stronger to overcome my hurdles and achieve my target.

*Pranjal Pratim Das*

# *Abstract*

Steel industries are one among the major industries which contribute to the world's economic growth. Over the years, steel production has been ramping up steadily, so there has been a significant increase in wastewater discharge. These wastewaters can vary depending on the specific units and processes used for a particular steel plant. The generation of wastewater in steel industries occurs from various unit operations like blast furnace, coke oven converters, electric arc furnace, ladle refining, rolling mills, quenching and tempering, among others. The presence of cyanide, phenol, oil and grease, iron, ammonia-N, chlorides, sulphates, and colored compounds are pervasive in such type of wastewaters, particularly from the coke oven converters and cold rolling mill units. Chemical coagulation and biological methods are typically employed for treating such highly impure and contaminated effluent generated from the coke oven converters in the Tata steel industry. Anaerobic and aerobic digestion, sequential batch reactors, bio-filters and activated sludge process are some of the most commonly used biological methods. The water that is obtained after the biological oxidation treatment is known as the biological oxidation treated (BOT) wastewater. Although, biological treatments can be effective in reducing the organic loads and some inorganic components in steel industry wastewater; however, the presence of coloured compounds and different recalcitrant pollutants, may require additional treatment methods, to be effectively removed from the wastewater. Similarly, the oil emulsion wastewater from cold rolling mills (CRM) of Tata steel industry is one of the unavoidable sector, where further treatment is needed before being released into the environment. A typical discharge of CRM wastewater contains high concentrations of oil & grease, phenol, iron and COD. Other compounds in small quantities may also be present viz. various salts of chromium, copper, nickel, and zinc, depending

upon the steel composition. Therefore, there is an urge for a more efficient, economical and facile technique for the treatment of toxic contaminated wastewaters from steel industry.

Ozonation is a widely used technique for both water and wastewater treatment due to its effectiveness in removing a wide range of contaminants and disinfecting water. It can significantly improve the biodegradability and degrade the refractory organic compounds from both water and wastewater via oxidative reactions either through direct molecular ozone or indirect $HO^{\bullet}$ free radicals formed in a chain reaction mechanism. However, the generation of ozone requires higher energy consumption, which may increase the overall operating cost of the process. Therefore, the use of a pre/post treatment method may be helpful in addressing the economic challenges and increasing the performance efficiency of the overall process. In view of this, the thesis work describes the combined effect of ozonation and electrocoagulation methods for the treatment of BOT wastewater. Due to the recalcitrant nature of the pollutants, treating BOT wastewater with only one treatment system is insufficient. However, the drawbacks of a single method can be resolved by using the combined treatment, resulting in a more effective treatment process and improved outcomes. The BOT wastewater consisting of coloured compounds, iron, and ammonia-N from Tata Steel Industry, India was considered here. The effects of operating variables like ozone generation rate, current density and treatment time on pollutant removal were analyzed for the hybrid process. The experimental conditions such as 1.33 mg $s^{-1}$ (ozone generation rate), 40 min (ozonation time), 100 A $m^{-2}$ (current density), and 30 min (electrolysis time) were found to be optimum for reducing all the pollutant concentrations (iron, ammonia-N, and colour) below their respective permissible limits of surface water quality. The removal capacity of the hybrid process was found to be 98.2%, 90.6%, and 62.8% for colour, iron, and ammonia-N, respectively. A kinetic

study was performed for the degradation of the pollutants during the hybrid process. The pseudo-first-order kinetic model was found to be best suited for the analysis with the $R^2$ value of about 0.99 for iron, ammonia-N, and colour, respectively, at an optimum ozone generation rate of 1.33 mg $s^{-1}$. Further, an image processing software (Image J Software, 9.0) was utilized for analyzing the bubble size in which the sauter mean diameter of the microbubble was found to be 425 µm, and the range of the microbubble size varied between 20 µm and 650 µm. Finally, the cost analysis study showed that the proposed hybrid process was found to be economical compared to other reported literature.

The work also focuses on the treatment of cyanide and phenol rich steel plant wastewater from Tata Steel Industry, India by hybrid ozonation assisted electrocoagulation method. The steel plant wastewater consisted of high cyanide and phenol concentrations along with chlorides, COD and BOD. The removal efficiency was found to be inadequate when the electrocoagulation or ozonation process was performed separately for the removal of cyanide. However, a combination of ozonation and electrocoagulation showed highly satisfactory results. The effects of operating variables viz. ozone generation rate, current density, and analysis time on pollutant removal were primarily analyzed for the hybrid process. The experimental operating condition was optimized and was seen that ozone generation rate of 1.33 mg $s^{-1}$, ozonation time of 40 min, a current density of 100 A $m^{-2}$, and electrolysis time of 30 min were sufficient for reducing the pollutant concentration below its permissible limits. The removal efficiencies of the combined process at optimum conditions were 99.8%, 99.5%, 94.7%, 95%, and 46.5% for cyanide, phenol, COD, BOD, and chloride, respectively. A kinetic study was performed for the degradation of the pollutants during ozonation. The pseudo first-order kinetic model was found to be best suited for the analysis

## Abstract

with the highest $R^2$ value of 0.99 for cyanide, COD, BOD, and chloride, respectively. Further, the mass transfer study illustrates an increase in the dissolved ozone concentration in the solution for an increase in the volumetric mass transfer coefficient, $K_l$ a. Finally, the cost estimation study of the hybrid process was carried out and compared with that of the other reported literature.

Further, the work establishes the performance of standalone ozonation and electrocoagulation processes for the treatment of CRM wastewater consisting of phenol, COD, BOD, iron, and oil content from Tata Steel Industry, India. The operational variables of both the standalone processes, viz. current density, ozone generation rate, and treatment time, were addressed to analyse its effect on the removal efficiency of each process separately. Optimum experimental conditions of 200 A $m^{-2}$ (current density), 1.12 mg $s^{-1}$ (ozone generation rate), and 30 min (treatment time) were adequate in lowering the amount of all the pollutant content below their respective discharge limits. It was observed that, the electrocoagulation process proved to be more efficient (98% phenol, 97.5% iron, 90.5% COD, 85.7% BOD, and 88% oil & grease) compared to ozonation (93.5% phenol, 86.5% iron, 70% COD, 74.3% BOD, and 62% oil & grease) in terms of pollutant removal rate for the target wastewater. The electrocoagulated flocs were then characterized to analyse its particle size and confirm the presence of pollutants removed during the process. The kinetic study conducted showed that pseudo first-order reaction fitted best with the highest $R^2$ of 0.99 for phenol, COD, BOD, iron, and 0.98 for oil & grease. Moreover, mass transfer analysis for ozonation indicates an increase in the volumetric mass transfer coefficient ($K_l$ a) with an increase in the ozone generation rate. The cost of ozonation process was found to be about six times than that of electrocoagulation. Nevertheless, the efficiencies and operating costs for both the standalone processes were found to be satisfactory compared to other methods reported in the literature.

# Research Publications

## 1. Journal Publications:

### 1.1 Journal Articles Published (Related to the thesis work)

1. **Das, P. P.**, Anweshan, Mondal, P., & Purkait, M. K. (2021). Integrated ozonation assisted electrocoagulation process for the removal of cyanide from steel industry wastewater. **Chemosphere**, 263, 128370. https://doi.org/10.1016/j.chemosphere.2020.128370
2. **Das, P. P.**, Anweshan, & Purkait, M. K. (2021). Treatment of cold rolling mill (CRM) effluent of steel industry. **Separation and Purification Technology**, 274, 119083. https://doi.org/10.1016/j.seppur.2021.119083
3. **Das, P. P.**, Mondal, P., Anweshan, & Purkait, M. K. (2021). Treatment of steel plant generated biological oxidation treated (BOT) wastewater by hybrid process. **Separation and Purification Technology**, 258, 118013. https://doi.org/10.1016/j.seppur.2020.118013
4. **Das, P. P.**, Sharma, M., & Purkait, M. K. (2022). Recent progress on electrocoagulation process for wastewater treatment: A review. **Separation and Purification Technology**, 292, 121058. https://doi.org/10.1016/j.seppur.2022.121058
5. **Das, P. P.**, Dhara, S., Samanta, N. S., & Purkait, M. K. (2024). Advancements on ozonation process for wastewater treatment: A comprehensive review. **Chemical Engineering & Processing: Process Intensification**, 202, 109852. https://doi.org/10.1016/j.cep.2024.109852
6. Bharti, M., **Das, P. P.**, & Purkait, M. K. (2023). A review on the treatment of water and wastewater by electrocoagulation process: Advances and emerging applications. **Journal of Environmental Chemical Engineering**, 11, 111558. https://doi.org/10.1016/j.jece.2023.111558

7. Changmai, M., **Das, P. P.**, Mondal, P., & Purkait, M. K. (2022). Hybrid electrocoagulation–microfiltration technique for treatment of nanofiltration rejected steel industry effluent. **International Journal of Environmental Analytical Chemistry**, 102, 62-83. https://doi.org/10.1080/03067319.2020.1715381

**1.2. Journal Articles Published (Apart from the thesis work)**

8. Sharma, M., **Das, P. P.**, Sood, T., Chakraborty, A., & Purkait, M. K. (2021). Ameliorated polyvinylidene fluoride based proton exchange membrane impregnated with graphene oxide, and cellulose acetate obtained from sugarcane bagasse for application in microbial fuel cell. **Journal of Environmental Chemical Engineering**, 9, 106681. https://doi.org/10.1016/j.jece.2021.106681
9. Sharma, M., **Das, P. P.**, Sood, T., Chakraborty, A., & Purkait, M. K. (2022). Reduced graphene oxide incorporated polyvinylidene fluoride/cellulose acetate proton exchange membrane for energy extraction using microbial fuel cells. **Journal of Electroanalytical Chemistry**, 907, 115890. https://doi.org/10.1016/j.jelechem.2021.115890
10. Dhara, S., Samanta, N. S., **Das, P. P.**, Uppaluri, R. V. S., & Purkait, M. K. (2023). Ravenna Grass-Extracted Alkaline Lignin-Based Polysulfone Mixed Matrix Membrane (MMM) for Aqueous Cr (VI) Removal. **ACS Applied Polymer Materials**, 5, 6399-6411. https://doi.org/10.1021/acsapm.3c00999
11. Shekhar Samanta, N., **Das, P. P.**, Dhara, S., & Purkait, M. K. (2023). An Overview of Precious Metal Recovery from Steel Industry Slag: Recovery Strategy and Utilization. **Industrial & Engineering Chemistry Research**, 62, 9006–9031. https://doi.org/10.1021/acs.iecr.3c00604

## 2. Book Chapter Publications:

### 2.1 Book Chapters Published (Related to the thesis work)

1. **Das, P. P.**, Sontakke, A. D., & Purkait, M. K. (2023). Electrocoagulation process for wastewater treatment: Applications, challenges, and prospects, in: M. Shah (Ed.), Development in Wastewater Treatment Research and Processes, **Elsevier**, 23-48. https://doi.org/10.1016/B978-0-323-95684-0.00015-4
2. **Das, P. P.**, Dhara, S., & Purkait, M. K. (2023). Hybrid electrocoagulation and ozonation techniques for industrial wastewater treatment, in: M. Shah (Ed.), Sustainable Industrial Wastewater Treatment and Pollution Control, **Springer Nature**, 107-128. https://doi.org/10.1007/978-981-99-2560-5_6
3. **Das, P. P.**, Mondal, P., & Purkait, M. K. (2022). Treatment of industrial wastewater utilizing standalone and integrated advanced oxidation processes, in: M. Shah (Ed.), Advanced Oxidation Processes for Wastewater Treatment, **Taylor & Francis,** 1-15. https://doi.org/10.1201/9781003165958
4. **Das, P. P.**, Baite, T. N., & Purkait, M. K. (2024). Industrial Wastewater Treatment by Electrocoagulation Process, in: M. Shah (Ed.), Environmental Approach to Remediate Refractory Pollutants from Industrial Wastewater Treatment Plant, **Elsevier**, 55-73. https://doi.org/10.1016/B978-0-443-13884-3.00019-6
5. **Das, P. P.**, & Purkait, M. K. (2024). Removal of industrial wastewater contaminants by ozonation process, in: M. Shah (Ed.), Environmental Approach to Remediate Refractory Pollutants from Industrial Wastewater Treatment Plant, **Elsevier**, 75-89. https://doi.org/10.1016/B978-0-443-13884-3.00025-1

6. **Das P.P.**, Dhara, S., & Purkait, M. K. (2024). Ozone-based oxidation processes for the removal of pharmaceutical products from wastewater, in: M. Shah & P. Ghosh (Eds.), Emerging Technologies for Removal of Pharmaceuticals and Personal Care Products: State of the Art, Challenges and Future Perspectives, **Elsevier**, 287-308. https://doi.org/10.1016/B978-0-443-19207-4.00003-3
7. **Das, P. P.**, Sontakke, A. D., Samanta, N. S., & Purkait, M. K. (2023). Emerging Contaminants in Wastewater: Eco-Toxicity and Sustainability Assessment, in: M. Shah (Ed.), Industrial Wastewater Reuse: Applications, Prospects and Challenges, **Springer Nature**, 63-87. https://doi.org/10.1007/978-981-99-2489-9_4
8. Samanta, N.S., **Das, P. P.**, & Purkait, M. K. (2023). Recycle of water treatment plant sludge and its utilization for wastewater treatment, in: M. Sillanpaa, & K. Gurung (Eds.), Resource Recovery in Drinking Water Treatment, **Elsevier**, 239-264. https://doi.org/10.1016/B978-0-323-99344-9.00010-4

**2.2 Book Chapters Published (Apart from the thesis work)**

9. **Das, P. P.**, Nair, D., & Purkait, M. K. (2023). Industrial Wastewater to Biohydrogen Production via Potential Bio-refinery Route, in: M. Shah (Ed.), Biorefinery for Water and Wastewater Treatment, **Springer Nature**, 159-179. https://doi.org/10.1007/978-3-031-20822-5_8
10. Sharma, M., **Das, P. P.**, & Purkait, M. K., Ghangrekar, M. M. (2024). Scaling-up of bioelectrochemical process for simultaneous wastewater treatment and energy extraction, in: D. A. Jadhav, M. Behera, & M. Shah (Eds.), Advances in Environmental Electrochemistry, **Elsevier**, 123-141. https://doi.org/10.1016/B978-0-443-18820-6.00007-2

## 3. Authored Book Publications:

### 3.1 Authored Books Published (Related to the thesis work)

1. Purkait, M. K., Mondal, P., & **Das, P. P.**, Wastewater Treatment in Steel Industries: Case Studies, Advances, and Prospects. Publisher: **Taylor & Francis** (2023).

   **Book ISBN: 978-1003366263**

2. Purkait, M. K., **Das, P. P.**, & Sharma, M., Electrocoagulation Based Treatment of Water and Wastewater: Overview and Applications. Publisher: **Elsevier** (2024).

   **Book ISBN: 978-0443138935**

### 3.2 Authored Books Accepted (Related to the thesis work)

3. Purkait, M. K., **Das, P. P.**, & Bharti, M., Electrocoagulation: Fundamentals and Applications in Water and Wastewater Treatment. Publisher: **Taylor & Francis** (2024).

   **(Book accepted, Status: In-Press)**

4. Purkait, M. K., & **Das, P. P.**, Ozone-based disinfection of water and wastewater: Advancements and applications. Publisher: **Elsevier** (2024). **(Book accepted, Status: In-Press)**

### 3.3 Authored Books Published (Apart from the thesis work)

5. Purkait, M. K., Sharma, M., **Das, P. P.**, & Chang, C. T., Blue Energy Extraction Using Salinity Gradients: A Critical Evaluation of Case Studies. Publisher: **Elsevier** (2024).

   **Book ISBN: 978-0443216138**

6. Purkait, M. K., Mondal, P., Samanta, N. S., & **Das, P. P.**, Waste-Based Zeolite: Synthesis and Environmental applications. Publisher: **Elsevier** (2024). **Book ISBN: 978-0443223167**

7. Purkait, M. K., Duarah, P., & **Das, P. P.**, Recovery of Bioactives from Food Wastes. Publisher: **Taylor & Francis** (2023). **Book ISBN: 978-1003315469**

## 4. Conferences/ Seminars attended:

1. **Das, P. P.**, & Purkait, M. K. "Hybrid Ozonation assisted Electrocoagulation process for the Treatment of Steel Industry Wastewater" at **International Conference** on Advances in Chemical, Biological and Environmental Engineering **(ICACBEE-2021)**, 23rd - 24th April, 2021, NIT Jaipur.
2. **Das, P. P.**, & Purkait, M. K. "An integrated approach for the analysis of biological oxidation treated (BOT) wastewater of steel plant: Parametric study and cost estimation" at **International Conference** on Advances in Sustainable Research for Energy and Environmental Management **(ASREEM-2021)**, 6th - 8th August, 2021, NIT Surat.
3. **Das, P. P.**, & Purkait, M. K. "Treatment of Steel Industry Effluent by Ozonation-assisted Electrocoagulation: Mass Transfer and Kinetic Study" at **National Conference** on Recent Innovations in Chemical Engineering **(RICE-2021)**, 8th - 9th February, 2021, NIT Bhopal.
4. **Das, P. P.**, & Purkait, M. K. "Treatment of Steel Industry Wastewater" at **National Conference** on Issues and Challenges in Water Treatment and Allied Research for Sustainable Environment **(Water-2020)**, 23rd - 25th January, 2020, IIT Guwahati.
5. **Das, P. P.**, & Purkait, M. K. "Integrated Water Treatment Process for Industrial Wastewater Reclamation and Reuse" at **National Conference** on Raising Agro-processing and Integrating Novel technologies for Boosting Organic Wellness **(RAINBOW-2020)**, 1st February 2020, Tezpur university.

# CONTENTS

**CONTENTS**

# LIST OF FIGURES

## LIST OF FIGURES

# LIST OF TABLES

# *Nomenclature*

## Notations

| | |
|---|---|
| $A$ | Area of the electrodes |
| $C_p^0$ | Initial pollutant concentration |
| $d_{32}$ | Sauter mean bubble diameter |
| $E_{EO}$ | Electrical energy per order |
| $F$ | Faraday's constant |
| $HO^{\bullet}$ | Hydroxyl radicals |
| $I$ | Current |
| $k_{obs}$ | Observed first-order rate constant |
| $K_d$ | Diffusion coefficient of ozone |
| $K_l\, a$ | Volumetric mass transfer coefficient of ozone |
| $m_1$ | Weight of the electrodes after the experiment without cleaning |
| $m_2$ | Weight of the electrodes after the experiment with cleaning |
| M.W | Molecular mass of Aluminum |
| $p$ | Cost of electrodes |
| $Q_{energy}$ | Electrical energy consumption |
| $Q_{electrode}$ | Electrode materials consumption |
| $q$ | Electricity cost |
| $\%R$ | Percentage removal |
| $t$ | Treatment time |
| $V$ | Voltage |
| $V_L$ | Volume of wastewater |
| $X_e$ | Equilibrium concentration of dissolved ozone in the solution |

# Chapter 1

# Introduction

# Chapter 1

# Introduction

*The present chapter provides an overview of the treatment techniques viz. ozonation and electrocoagulation adopted for the analysis of various steel industry wastewater. A detailed discussion on the importance of operational parameters of both the techniques such as current density, ozone flow rate, reaction time, solution pH, and electrode spacing in improving their performance efficiency have been clearly depicted. The integration of ozonation and electrocoagulation have been explored to create a highly efficient and reliable technique for the treatment of industrial wastewater. Wastewaters from various unit operations of Tata steel industry were treated by both standalone and hybrid ozone assisted electrocoagulation technique. A brief description on the types of wastewater considered were also summarized. All the toxic contaminants in the target wastewaters were successfully eliminated, ensuring compliance with the water quality standards and regulatory requirements. A preliminary cost analysis has been included to understand the economic involvement of the proposed hybrid technique. Altogether, this chapter presents a detailed literature review on the various aspects of steel plant wastewater treatment including the source of target wastewater, techniques involved, operating parameters and contaminant effects on human health.*

## 1.1 Background

Water is the most fundamental requirement of life and is used to conduct numerous household and industrial activities. However, around 2 billion people in the world lacks convenient access to safe drinking water and an average of 7.8 million people die every year due to poor water hygiene and sanitation. Moreover, drought affects around 55 million people annually, which in turn causes

more than US$5 billion of economic loss. Since 1980, the annual usage of water has increased by 1%, and this trend is expected to continue until 2050 [1]. The rapid progress in industrial sectors viz. mining, distillery, tannery, pharmaceutical, fertiliser, and textile industries among others as well as an increase in urbanization, population growth, and living standards has resulted in the formation of refractory and toxic pollutants containing wastewater, which has further caused water shortages throughout the world in recent years. Such refractory pollutants are distinguished by high chemical and biological oxidation demand contents and are defiant to biological treatments because of their low biodegradability index. Even the presence of a small quantity of these non-biodegradable organic compounds in wastewater poses substantial risks to the human health since they are regarded as potential endocrine disruptors, and carcinogens. Industries are the primary source though which such hazardous and non-biodegradable pollutants are released into the environment [2]. On an average, the industries discharge between 300 and 400 million tons of waste consisting of refractory organics, heavy metals, toxic sludge, and micro-pollutants into the global water bodies annually, thereby posing a greater risk to both human beings and aquatic species. Therefore, it is crucial to treat industrial wastewaters on an urgent basis. The removal of refractory organics, toxic heavy metals, pharmaceuticals, pesticides, oil & grease from industrial wastewaters pose a significant challenge for the current treatment technologies since the working mechanism of conventional wastewater treatment systems are designed based on organic loads [3]. Thus, it is crucial to integrate biodegradability enhancement with mineralization of refractory organics to successfully treat different types of industrial wastewater. The schematic outline of a typical wastewater treatment plant is shown in Figure 1.1.

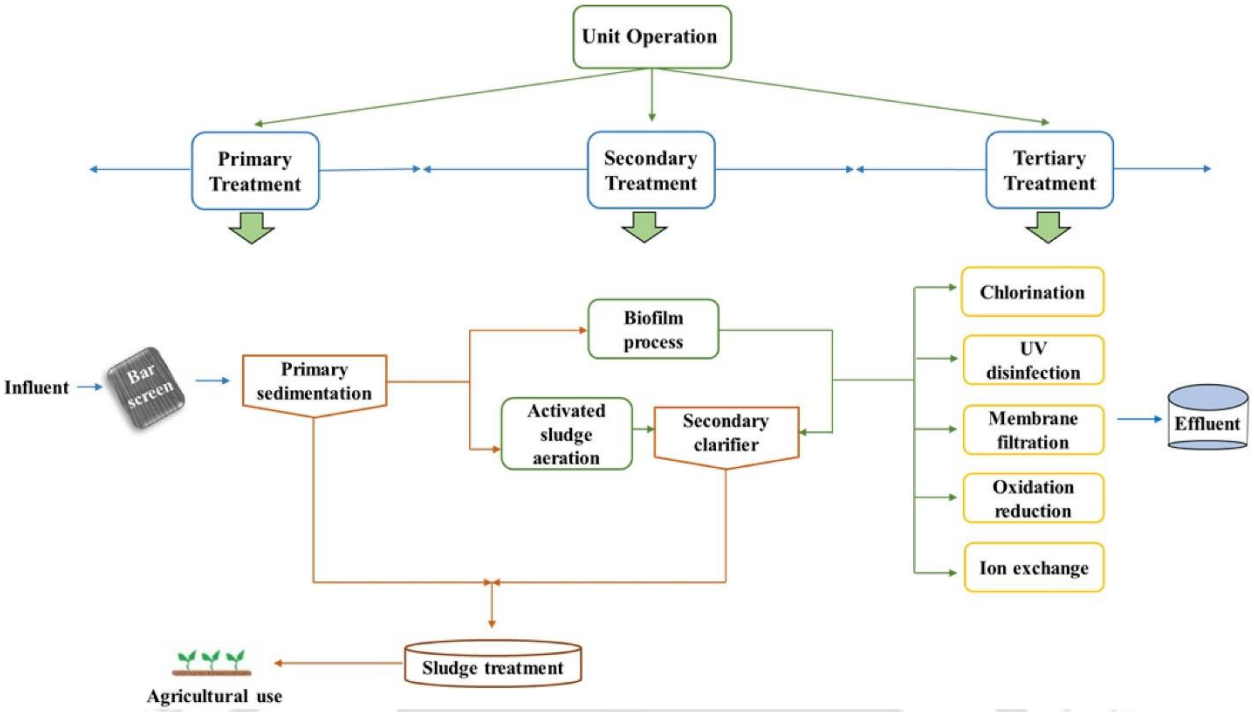


**Fig. 1.1:** Flowchart of a conventional wastewater treatment system

Ozonation is a class of advanced oxidation process that can significantly improve the biodegradability and remove the refractory organic compounds from both water and wastewater by oxidative reactions either through direct molecular ozone (acidic conditions) or indirect $HO^{\bullet}$ free radicals (alkaline conditions) formed in a chain reaction mechanism [4]. Ozone is an immensely reactive and unstable allotrope of $O_2$ with a pungent odour. It effectively decomposes the larger organic molecules into short chain intermediate products during the process. These intermediate products effectively permeate the cell walls of microbes and can be easily biodegraded due to the enhancement in biological oxidation rate by smaller size molecules, thus improving the pollutant degradation efficiency. Further, ozonation causes the solubilization of sludge and decreases the overall biomass yield [5]. However, the use of ozone alone cannot achieve complete mineralization of several refractory organic compounds. Also, the generation of ozone

requires higher energy consumption, which in turn increases the overall operating cost of the process. As such, the use of a pre/post treatment method may be helpful in increasing the overall mineralization rate and to address the economic challenges [6]. Electrocoagulation has been reported to be a potential approach for treating both water and wastewater because it is flexible, easy to operate, and can degrade a variety of contaminants. Electrocoagulation is very effective even in the removal of the tiniest colloidal particles via application of an electric field, responsible for assisting in coagulation and flotation of the contaminants. Due to its high removal rate and cost-effectiveness, electrocoagulation is considered as a viable alternative to various water treatment processes for the treatment of highly contaminated wastewaters. As no chemical coagulant is added, electrocoagulation does not pose any risk of secondary contaminant generation unlike chemical coagulation. Also, the particle size of the metal hydroxide flocs produced during the process are stable and large that can be easily separated via decantation or simple filtration [7]. These flocs contain less water (acid resistant compound), thus making it easier to remove them via filtration.

## 1.2 Ozone oxidation process

Since the early 20th century, ozone (bluish gas) has been broadly utilized to treat drinking water and industrial wastewater. The use of ozone has emerged as a very promising wastewater treatment alternative that produces zero amount of sludge along with the formation of oxygen and water as end products via residual ozone decomposition [8]. The application of ozone for the treatment of various wastewater is shown in Table 1.1. The most commonly used technique for producing ozone depends entirely on the corona discharge principle, that involves the use of high voltage discharge in a dried/cooled gaseous (air or $O_2$) environment. It electrically charges the oxygen molecules to a higher energy state, thereby causing the molecules to break apart. The resultant free

oxygen atoms then react with other available oxygen molecules to produce ozone [9]. The ozone oxidation is governed by several operating parameters, viz. ozone flow rate, reaction time, and solution pH, that determine the process effectiveness. However, the ideal values of these parameters may differ depending on the target contaminants. Therefore, proper optimization is required to ensure the desired outcome of the ozonation process. The schematic diagram of the ozonation process is shown in Figure 1.2.

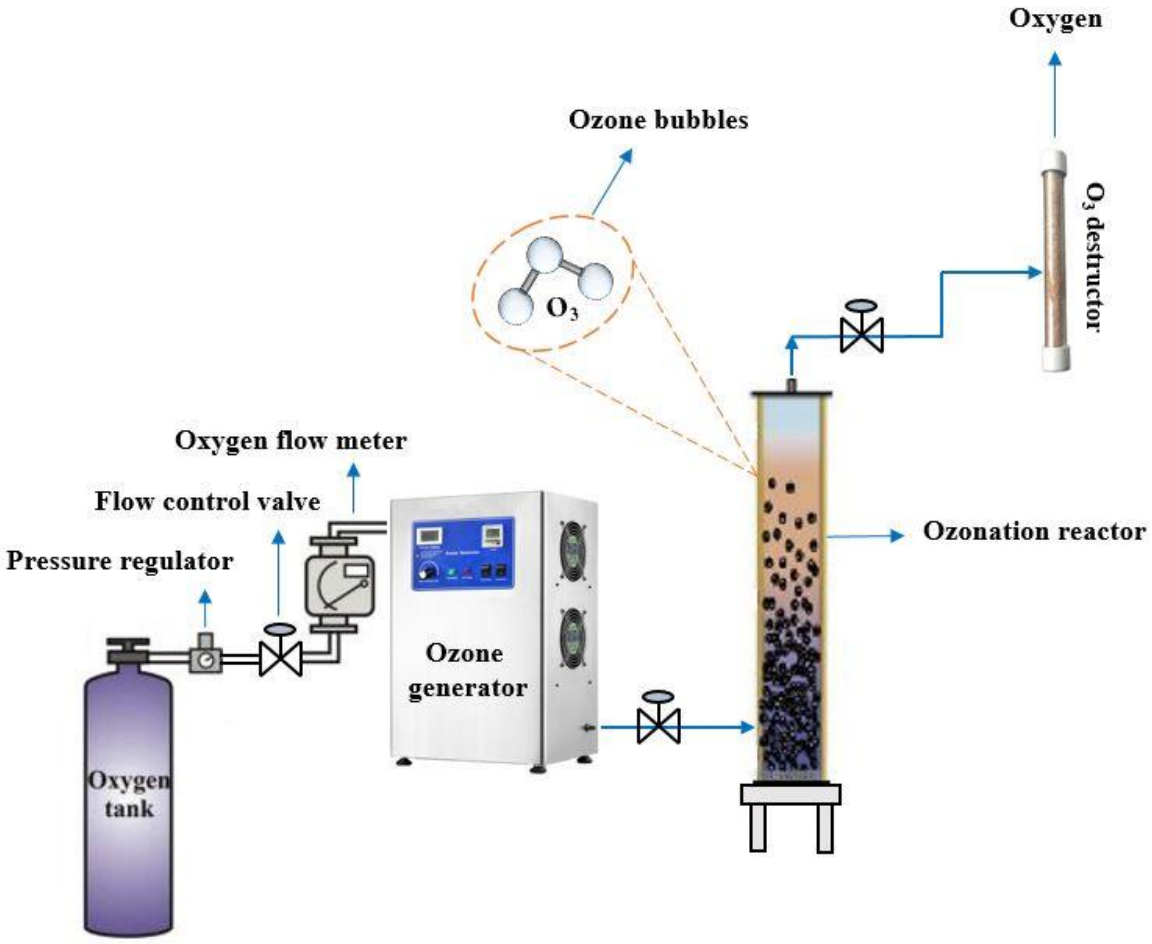


**Fig. 1.2:** Schematic layout of the ozonation process

**Table 1.1.** Application of ozone in wastewater treatment

| Types of wastewater | Experimental conditions | Results | References |
|---|---|---|---|
| Textile wastewater | Volume flow rate: 5 $m^3 h^{-1}$, Ozone dose: 35 mg $L^{-1}$, COD: 147.5 mg $L^{-1}$, pH: 7.4-7.9, Reaction time: 1.27 h, Temperature: 35°C | The COD and TSS content were reduced by 50% and 70% respectively. | [10] |
| Pulp and paper wastewater | Volume: 1 L, pH: 7.9, Ozone dose: 1100 mg $L^{-1}$ COD: 1310 mg $L^{-1}$, Reaction time: 10 min, Temperature: 20°C | 20% removal of COD with around 50% removal of lignin, colour and turbidity were obtained. | [11] |
| Winery wastewater | Volume: 9 L, pH: 4, Ozone flow rate: 100 mg $min^{-1}$, COD: 4650 mg $L^{-1}$, Reaction Time: 3 h, Temperature: 27°C | The degradation rates of COD and total carbon were 12% and 37% respectively. | [12] |
| Synthetic pharmaceutical wastewater | Volume: 1 L, pH: 7.8, Ozone dose: 3 mg $L^{-1}$, Clofibric acid: 1.8 µg $L^{-1}$, Reaction Time: 10 min, Temperature: 23°C | The clofibric acid and bezafibrate were reduced up to 40% and 50% respectively. | [13] |
| Acrylic fiber manufacturing wastewater | Volume: 6 L, Ozone flow rate: 0.5 L $min^{-1}$, $NH_3$-N: 67 mg $L^{-1}$, pH: 8, Reaction Time: 2 h, Temperature: 20°C | Removal rates of around 42% and 21% were obtained for COD and $NH_3$-N respectively. | [14] |

| | | | |
|---|---|---|---|
| Oil sands affected pit water | Volume: 8.5 L, pH: 8.31, Ozone dose: 30 mg $L^{-1}$ Naphthenic acid: 19.7 mg $L^{-1}$, Reaction Time: 48 h, Temperature: 23°C | A reduction of 67.5% naphthenic acid and 20.7% acid-extractable fraction were obtained. | [15] |
| Synthetic anti-inflammatory drug wastewater | Volume: 1 L, pH: 6.3, Ozone dose: 15.3 g $m^{-3}$, Ibuprofen: 200 mg $L^{-1}$, Reaction Time: 1 h, Temperature: 25°C | The ibuprofen content was reduced by 86% with a mineralization rate of 15%. | [16] |
| Landfill leachate | Volume: 3.5 L, Ozone dose: 66.7 g $m^{-3}$, DOC: 523 mg $L^{-1}$, pH: 7-8, Reaction Time: 25 min, Temperature: 23°C | 78% reduction in UV-254 absorbing compounds with 23% DOC removal were achieved. | [17] |
| Textile wastewater | Volume: 2 L, pH: 8.0, Ozone flow rate: 120 L $h^{-1}$, Dye content: 400 mg $L^{-1}$, Reaction time: 26 min, Temperature: 20°C | The degradation of COD and colour content were observed to be around 41% and 90% respectively. | [18] |

### 1.2.1 Operational parameters

#### *1.2.1.1 Ozone flow rate*

It is crucial to select an adequate ozone flow rate for the oxidation of the target contaminants to effectively optimize the ozone doses. High ozone doses substantially enhances the $HO^{\bullet}$ radical production, which improves the rate of mineralization and the degradation efficiency of the process. Higher ozone flow rates can enhance the disinfection efficiency of ozone-based processes

for water and wastewater purification by increasing the dissolved ozone content in the solution [19]. As a result, ozone-based treatments can degrade the refractory contaminants more quickly, thereby reducing the treatment time and increasing productivity. Ozone generators with higher flow rates can handle larger volumes of water, making them ideal for large-scale applications. However, higher ozone doses require more energy to produce and deliver ozone, which can significantly increase the operating cost. Besides, it is difficult to control the ozone distribution at higher flow rates, resulting in uneven treatment and reduced process effectiveness. Also, higher ozone flow rates can put more strain on ozone generators and other equipment, which can increase maintenance and repair costs over time [20]. The energy consumption can be lowered by adequately optimizing the ozone doses supplied to the aqueous solution. The volumetric mass transfer rate of ozone from the gaseous to the aqueous phase should be effectively monitored and controlled to reduce the uneven treatment of the target solution. Besides, the use of a pre or post-treatment process can reduce the adverse effects of high ozone flow rates on the maintenance and functioning of ozone generators [21].

### *1.2.2 Solution pH*

The solution pH is a vital parameter as it regulates the mass transfer rate and ozone decomposition during the ozonation process. The removal efficiency of ozonation significantly relies upon the pH of the solution since it controls the reaction pathway of ozone. In an alkaline medium, the reaction mechanism undergoes a radical pathway and forms high amount of $OH^{\bullet}$ free radicals, whereas, in an acidic medium, it undergoes a selective direct reaction pathway [8]. The $HO^{\bullet}$ radical has an oxidation potential of 2.8 V, much higher than the molecular ozone (2.1 V). As such, a higher solution pH is needed to improve the ozone decomposition rate and produce more $HO^{\bullet}$ radicals, which increases the oxidation of recalcitrant organic compounds and leads to higher pollutant

removal. The electric charge properties of surface $HO^{\bullet}$ groups at the catalyst interface are also governed by the solution pH. However, ozone oxidation results in the generation of acidic by-products (inorganic acids along with organic anions) [22]. The solution pH becomes highly acidic during oxidation due to the reaction of ozone with the degraded products generated via $OH^-$ anions and $HO^{\bullet}$ radicals (typically carboxylic acids). The pH reduction is very prominent in the initial stage of oxidation due to higher ozone consumption. As such, the solution pH should be properly maintained at alkaline conditions to enhance the pollutant degradation efficiency. The integration of ozone with a post treatment method especially electrocoagulation can substantially increase the solution pH from acidic to alkaline condition. The production of $OH^-$ anions at the cathode surface and the evolution of $H_2$ gas at the cathode vicinity may be credited to the increased solution pH during the process. Besides, an equilibrium state can be attained after a certain alkaline pH because of the buffering capability of $M(OH)_n$ / $M(OH)_n^-$ coagulants [23].

### *1.2.3 Reaction time*

The reaction time plays a substantial role in governing the rate of contaminant degradation during ozonation. Prolonged reaction time can increase the duration of contact between ozone and the contaminants, leading to an enhanced removal performance of the ozonation process [24]. It can also improve the disinfection rate by destroying a wider range of microbes, viz. bacteria, viruses, and protozoa. Also, an increase in reaction time can lead to reduced chemical usage, as it may be possible to achieve the desired level of treatment with lower ozone doses. Besides, the effectiveness of ozone can be maximized by using a recirculation system to ensure that the water is exposed to ozone for a longer period, or a dissolved ozone system can be employed, where ozone is added to water in the form of tiny bubbles, thereby increasing the contact time between the two

[25]. Although a longer treatment time can enhance the ozonation performance, increasing the reaction time beyond a certain period can have adverse effects on the process removal rate. It is worth noting that prolonged reaction time can also result in higher energy consumption which in turn enhances the operating cost. It can also increase the production of undesirable by-products, viz. bromate and aldehydes. However, the use of larger reaction tanks or increasing the flow rate of water through the reaction tanks can improve the interaction between ozone and the water being treated, thus reducing the reaction time of the process [26]. Besides, optimizing the solution pH and process temperature or using a catalyst considerably lowers the treatment time since these parameters affect the reaction rate of ozone with the organic contaminants. Also, the combination of ozone with post/pre-water treatment methods can significantly reduce the overall reaction time.

### 1.2.2 Challenges of ozone oxidation process

#### *1.2.2.1 Energy requirement*

Although the ozonation process is very efficient in oxidizing the toxic contaminants from various wastewater sources, challenges such as high energy requirement and intermediate formation during ozonation need to be resolved before considering a large-scale implementation of such hybrid approaches. Since the degradation of wastewater contaminants by ozonation is an energy-intensive process, it is regarded as one of the most crucial parameters while evaluating the ozone-based treatment of wastewater [27]. Most of the energy consumption during ozonation arises from the high electrical energy needed for ozone production and its subsequent treatment process. The international union of pure and applied chemistry (IUPAC) has recommended two figures of merit for the use of electricity by AOPs, viz. (i) electrical energy per order ($E_{EO}$): the unit of electricity (kWh) needed to lower the pollutant content by one order of magnitude (90%) in 1 $m^3$ of wastewater, and (ii) electrical energy per mass ($E_{EM}$): the unit of electricity (kWh) needed to lower

the amount of pollutant by one kg. $E_{EO}$ is typically used for determining the electrical energy of advanced oxidation processes because of the presence of trace organic pollutants in low concentrations [28]. For batch ozonation process, $E_{EO}$ can be calculated as shown below [29]:

$$E_{EO} = \frac{P \times t \times 100}{V \times log(\frac{Ci}{Cf})} \quad (1.1)$$

$$\ln(\frac{Ci}{Cf}) = k' \times t \quad (1.2)$$

Here P = power required (kW), t = treatment time (min), V = sample volume (L), $C_i$ and $C_f$ = initial and final pollutant concentrations, respectively, and $k'$ = reaction rate constant ($min^{-1}$) of pseudo first-order kinetics. As per equation (2), $E_{Eo}$ for various AOPs can be evaluated primarily via log $(\frac{Ci}{Cf})$ irrespective of the type of oxidation processes. The physico-chemical and structural characteristics, along with the concentration variation of the target pollutants, significantly affect the outcome of log $(\frac{Ci}{Cf})$. The ozone doses required for the removal of organic pollutants are highly diverse because of the variations in their reaction rate constant towards molecular ozone or $OH^{\bullet}$ radicals [30]. Thus, the $E_{EO}$ values may significantly vary during the oxidation of multiple wastewater pollutants.

#### *1.2.2.2 Intermediate formation*

During the ozonation of wastewater, bromate is primarily produced from bromide oxidation via direct ozone attack or indirect radical pathway. Bromate production may increase due to the sequential or simultaneous contribution of $OH^{\bullet}$ radicals and molecular ozone to the oxidation process. Bromate formation is a major challenge during ozonation, especially in water sources containing bromide. Bromate may also be produced when $Br^{\bullet}$ is formed during the reaction between $HO^{\bullet}$ radicals and $Br^{-}$, although this hypothesis needs to be confirmed [31]. Pre-treatment

of water can remove bromide ions, thus reducing the potential for bromate formation. Maintaining the solution pH between 6-8 during ozonation can also inhibit the bromate formation. Besides, the in-situ formation or incorporation of reducing agents, especially hydrogen peroxide and the reduction in ozone doses can minimize the bromate formation by converting bromate to bromide. Hypobromous acid (HOBr) on deprotonation forms hypobromite anion ($BrO^-$), which reacts with $H_2O_2$ to convert back to bromide through immediate supply and accumulation during the process [32]. The in-situ formation of $H_2O_2$ due to the recombination of $HO_2^\bullet$ radicals produced during ozone decomposition results in the generation of more $HO^\bullet$ radicals while lowering the bromate production. Low $H_2O_2$ concentrations may be inadequate to convert the $BrO^-$ ions to bromide. On the other hand, higher concentrations of $H_2O_2$ effectively hinder the bromate production; however, it also reduces the pollutant oxidation rate by scavenging the $OH^\bullet$ free radicals [33]. In addition, the electrochemical formation of in-situ $H_2O_2$ during ozone assisted electrocoagulation process can also considerably reduce the bromate production rate.

## 1.3 Electrocoagulation process

Electrocoagulation is an electrochemical process that is widely used in water and wastewater treatment for the removal of various contaminants, including suspended solids, colloids, metals, and organic compounds. Electrocoagulation involves the application of an electrical current to electrodes immersed in the water or wastewater to facilitate coagulation and flocculation. It has gained popularity as a sustainable and cost-effective alternative to traditional coagulation methods [34]. It consists of atleast two electrodes (usually made of aluminum or iron) connected to a direct current (DC) power supply to provide the necessary voltage for the electrodes. Both the voltage and current are crucial parameters for optimizing the process. When a direct current is applied, the

electrodes release ions into the water, initiating electrolysis. During electrolysis, metal ions (e.g., $Al^{3+}$ or $Fe^{2+}$) are released from the electrodes. These ions neutralize the charged particles in the water, destabilizes them and forms coagulants. The coagulants generated cause the suspended particles, colloids, and dissolved contaminants to aggregate. Subsequent flocculation enhances the particle size, making them easier to settle or be removed by either decantation or simple filtration [35]. The schematic layout of the electrocoagulation process is shown in Figure 1.3.

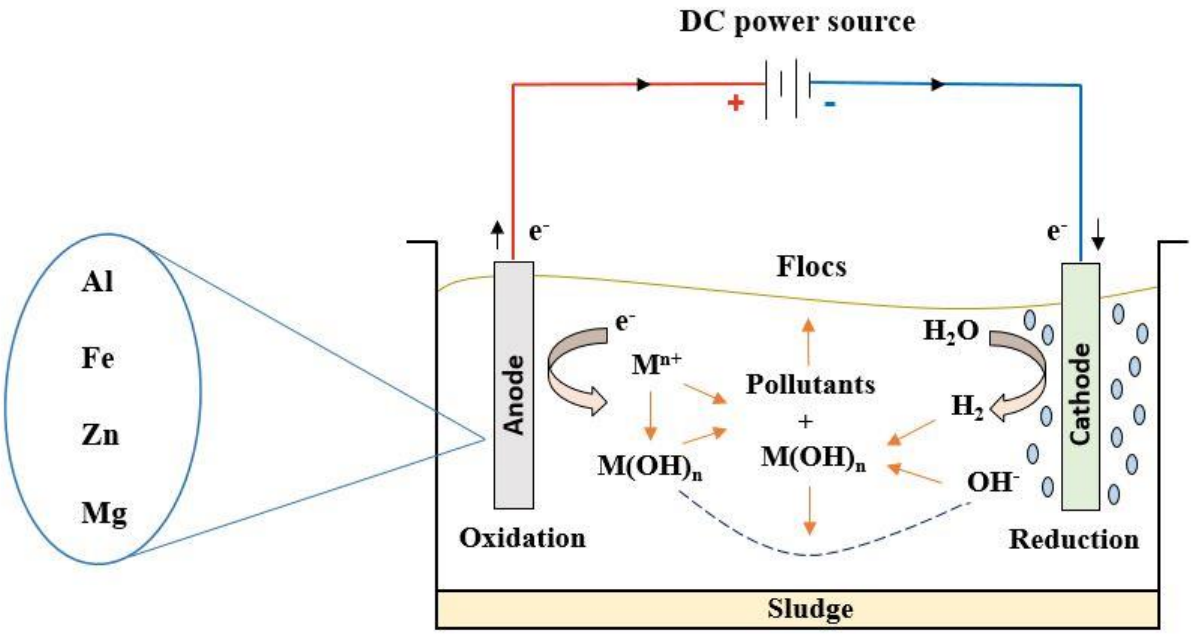


**Fig. 1.3:** Schematic diagram of the electrocoagulation process

### 1.3.1 Electrode materials

#### *1.3.1.1 Aluminium and iron electrodes*

Aluminium (Al) is commonly employed as an electrode material during the EC process. Application of current density leads to the formation of aluminium cations ($Al^{3+}$) via dissolution of sacrificial anodes. The anodic and cathodic reaction using aluminium electrodes are shown in

Eqs. 1–3 [36]. The metal concentration in the solution increases due to electro-dissolution and eventually precipitates at the bottom of EC chamber as metal hydroxides. $Al^{3+}$ ions undergo a complex equilibrium with various monomeric and polymeric species viz. $Al(OH)_3$, $Al(OH)^{2+}$, $Al\,(OH)_4^-$, $Al\,(OH)_2^+$, $Al_6\,(OH)_{15}^{3+}$, $Al_7\,(OH)_{17}^{4+}$, $Al_8\,(OH)_{20}^{4+}$, $Al_{13}\,(OH)_{34}^{5+}$ and $Al_{13}O_4\,(OH)_{24}^{7+}$ depending upon the solution pH [37]. However, $Al(OH)_3$ produced via complex precipitation mechanisms is primarily responsible for the formation of flocculates and aggregates.

At anode:

$$Al\,(s) \rightarrow Al^{3+}\,(aq) + 3e^- \quad (1.3)$$

At cathode:

$$3H_2O + 3e^- \rightarrow \frac{3}{2}\,H_2\,(g) + OH^-\,(aq) \quad (1.4)$$

Overall:

$$Al^{3+}\,(aq) + 3H_2O \rightarrow Al(OH)_3\,(s) + 3H^+ \quad (1.5)$$

Similarly, utilization of applied potential across the iron (Fe) electrodes leads to the production of in-situ coagulants via electro-dissolution of sacrificial electrodes. Hydroxyl ions are generated at the anode vicinity via reduction, whereas $H_2$ bubbles are produced at the cathode vicinity via oxidation, which assist in driving the generated floc to the water surface. The anodic and cathodic reaction using Fe electrodes are shown in Eqs. 4–6. At low solution pH and oxygenated water, ferrous ions are easily transformed into ferric ions [38]. Depending upon the pH, the electrogenerated ferric ions undergoes hydrolysis reaction to form different monomeric and polymeric species in the solution viz. $Fe(OH)_3$, $Fe(H_2O)_5OH^{2+}$, $Fe(H_2O)_6^{3+}$, $Fe(H_2O)_4(OH)_2^+$, $Fe(OH)^{4-}$, $Fe_2(H_2O)_6(OH)_4^{2+}$ and $Fe_2(H_2O)_8(OH)_2^{4+}$. These Fe complexes have a very strong tendency to polymerize at a pH range of 3–7. Moreover, the primary complex formed viz.

$Fe(OH)_3$ remains in the aqueous solution as gelatinous suspension, thereby assisting in the removal of wastewater contaminants by either electrostatic attraction or complexation phenomenon with subsequent coagulation [39].

At anode:

$$Fe\,(s) \rightarrow Fe^{2+}\,(aq) + 2e^{-} \quad (1.6)$$

At cathode:

$$2H_2O + 2e^{-} \rightarrow H_2\,(g) + 2OH^{+}\,(aq) \quad (1.7)$$

Overall:

$$4Fe^{2+} + 10H_2O + O_2\,(aq) \rightarrow 4Fe(OH)_3\,(s) + 8H^{+} \quad (1.8)$$

Al and Fe electrodes are widely preferred among all the other electrodes in EC process due to their high pollutant removal efficiency, cost-effectiveness and easy availability. The high performance of Al and Fe electrodes is associated with the reduction in the electrical double layer by higher charge valency of $Al^{3+}$ and $Fe^{3+}$ ions as compared to copper, zinc and magnesium, thereby assisting even more in the coagulation-flocculation process [40]. Although the use of Fe electrodes can minimize the cost of the EC process as compared to Al electrodes, however, it may develop a reddish-brown tinge to the treated EC samples, which in turn produces a turbid solution. On the other hand, Al electrode constitutes high strength to weight ratio, corrosion resistant property and high electrical conductivity. Also, it does not impart any colour to the treated solution and can easily outperform Fe electrode in terms of removal efficiency depending upon the wastewater [41]. As such, the selection of appropriate electrode material based on the targeted pollutants and cost-benefit analysis is very important.

### *1.3.1.2 Other miscellaneous electrodes*

In addition to Al and Fe electrodes, utilization of copper (Cu) as an electrode material also assist in the removal of various wastewater pollutants during electrocoagulation. A comparative analysis carried out between Al and Cu electrodes reported that, Cu electrodes provide higher removal efficiency against Al electrodes and uniform corrosion was observed at the surface of Cu electrodes after the treatment. During the utilization of Cu electrodes in electrocoagulation process, typical $H_2$ formation takes place at the cathode vicinity, while copper cations ($Cu^{2+}$) ions were simultaneously released at the anode [42]. Eqs. 10–12 represent the reactions that occur during electrocoagulation process using Cu electrodes, at which $Cu^{2+}$ ions and $Cu(OH)_2$ are generated in situ to act as a coagulant in the removal of wastewater contaminants. Hydrolysis of $Cu^{2+}$ and $Cu^{3+}$ ions lead to the formation of both monomeric and polymeric species viz. $CuOH^{2+}$, $Cu(OH)_2^+$, $Cu(OH)_4^-$, $Cu_2(OH)_2^{4+}$, $Cu(H_2O)_2^+$, $Cu(H_2O)_4(OH)_2^+$ and $Cu(H_2O)_5OH^{2+}$. The colloidal particles (net negative charge) are adsorbed onto the surface of $Cu(OH)_2$, which get neutralized and subsequently precipitates due to its heavy mass [43].

Moreover, several studies have also suggested the use of alternate anodic materials viz. magnesium (Mg) and zinc (Zn) during electrocoagulation. The principle is similar as stated formerly for Al, Fe and Cu electrodes, which consist of anodic dissolution for Mg and Zn respectively) followed by coagulation and precipitation. Depending upon the solution pH, the generated ions ($Mg^{2+}$ and $Zn^{2+}$) further lead to the formation of its corresponding hydroxides viz. $Mg(OH)_2$ and $Zn(OH)_2$ [44]. Al and Fe ions consist of higher charge valency as compared to Mg and Zn ions, thereby allowing for an improved coagulation process with low coagulant concentrations. On the other hand, the assessment of other electrochemically produced coagulants is based on the coagulant residual concentrations present in the treated water. For example, the United States Environmental

Protection Agency (USEPA) recommends the limiting Al concentration to 0.2 mg/L, whereas the limit for Mg is set at 30 mg/L, to avoid any health related issues [38].

### 1.3.2 Operational parameters

#### *1.3.2.1 Current density*

Current density or current applied per effective electrode surface area is considered a very significant parameter determining the electrocoagulation performance. During the application of EC process, current density regulates the rate of electron release, occurring as a result of metal ion dissociation from the electrodes. The range of applied current density may differ depending upon the types of effluent. This variation in current density is mostly due to the changes in ionic interaction, caused by the type of contaminants present in the effluent [45]. In most cases, the applied current density in EC process may typically vary from 0.01 to 880 A $m^{-2}$. Despite the fact that, the applied current density closely corresponds to the release and dissociation of metal ions in solution, however, a surplus of current may considerably reduce the performance of EC process by allowing in-situ secondary reactions along with the formation of colloidal charge reversal due to overdosing of coagulants [46]. Such phenomenon has the potential to shorten the electrode life span and formation of a thin film layer on the electrode surface, thereby lowering the process efficiency. Thus, the current density should be suitably optimized based on the target contaminants to achieve the desirable treatment performance. Also, the use of larger electrode surface area at lower or optimized current density can overcome the aforementioned challenges [47].

#### *1.3.2.2 Inter-electrode distance*

In EC process, the inter-electrode distance is considered to be a very crucial parameter, as it governs the electrostatic field between the cathodes and anodes. A decrease in the inter-electrode

distance eventually increases the electrostatic field. Thus, the metal hydroxides which assist in the formation of flocs to promote coagulation deteriorates due to the intense collisions caused by the high electrostatic attraction. Consequently, at a shorter inter-electrode distance, the efficiency of the EC process significantly increases [48]. However, an increase in the electrode distance leads to higher resistance to mass transfer and slow charge transfer. Higher inter-electrode distance delays the subsequent production of metal hydroxide based flocs due to low electrostatic forces. Excessive electrode distance also lowers the process efficiency, thereby resulting in high power consumption to compensate for the slower release of metal ions between the cathodes and anodes. As such, it is very important to operate the electrocoagulation process at an optimal inter-electrode distance. In most of cases, the optimum range of inter-electrode distance typically vary from 0.5–1 cm depending upon the types of wastewater [49].

#### *1.3.2.3 Solution pH*

The solution pH plays a very significant role in determining the performance of EC process. The solution pH greatly controls the release and formation of coagulants during the EC process. The effect of pH is directly associated with the formation of coagulants in solution, which exhibits several species in equilibrium viz. metal ionic complexes and monomeric/polymeric hydroxide-complexes. The variety and quantity of such complexes are important since they all exhibit different interactions with wastewater contaminants, thereby providing different coagulant performances. Also, the monomeric and polymeric species formed at highly alkaline condition shows very low adsorption capacity [50]. For instance, the species formed at highly alkaline conditions for Fe and Al electrodes viz. $Fe(OH)_4^-$ and $Al(OH)_4^-$ respectively performs very poorly with regards to adsorption efficiency. On the other hand, $Fe(OH)_3^-$ and $Al(OH)_3^-$ formed under neutral and slightly alkaline/acidic conditions significantly enhance the adsorption capacity of the

coagulants. Thus, the solution pH has a considerably influence on the physiochemical characteristics of coagulants viz. (i) particle size of coagulant species and (ii) solubility and electrical conductivity of metal hydroxides [51]. Also, the net charges and electrostatic interactions of the pollutants are directly influenced by the protonation/deprotonation (based on pKa values) of its functional groups. As such, the double layer gets altered which in turn affects the coagulant formation. Besides, the evolution of $H_2$ at the cathode vicinity and the formation of $OH^-$ ions considerably increases the solution pH. However, inappropriate pH conditions may alter the double layer, which in turn may decrease the coagulant formation [52]. Therefore, the variation in solution pH needs to be effectively optimized according to different physico-chemical nature of the target pollutants and the effluent characteristics in order to improve the pollutant adsorption capacity of the coagulant species throughout the EC process.

#### *1.3.2.4 Electrode configuration*

The electrode configuration mode not only affects the pollutant removal efficiency but also the operational cost and energy consumption of the EC process. The most commonly used electrode arrangements are bipolar electrodes in serial connection (BP-S) and monopolar electrodes in serial (MP-S) and parallel connection (MP-P). The arrangement of various electrode connection modes in an EC reactor is shown in Figure 1.4. Depending on the electrical polarity, each electrode in a monopolar configuration mode functions as either cathode or anode in the electrochemical cell. In case of MP-P connection, the sacrificial anodes are interlinked directly with one another in the EC cell; besides the cathodes are also connected in a similar configuration [53]. Meanwhile, in MP-S connection, each set of electrode (anode-cathode) is connected internally; however, they are not linked to the outer electrodes. In BP-S connection, the electrodes which are monopolar (except the

outer electrodes) exhibit different polarity at each of the electrode vicinity, based on the charges of previous electrodes. The bipolar electrodes are always connected in series configuration. It is worth noting that, series connection necessitates the use of higher potential difference, while the same current is spread across all electrodes. Two electrochemical cells act together in a bipolar electrode configuration, resulting in a higher surface area compared to monopolar configuration [54]. This adequately favours the anodic oxidation in bipolar mode which in turn improves the efficiency of the electrocoagulation process. On the other hand, the efficiency of monopolar electrode configuration is considerably lower with the same applied current density for both connections due to the less available surface area. Besides, the electric current in parallel connection is distributed among all the electrode interconnection as a function of its resistance. Nevertheless, parallel connection mode provides significant benefits in terms of energy consumption. Taken together, the BP-S connection mode aids in high pollutant removal, whereas use of MP-P connection provides low cost of operation [55]. Therefore, it is necessary to adequately select and optimize the electrode configurations to minimize the energy consumption and achieve the desired treatment performance.

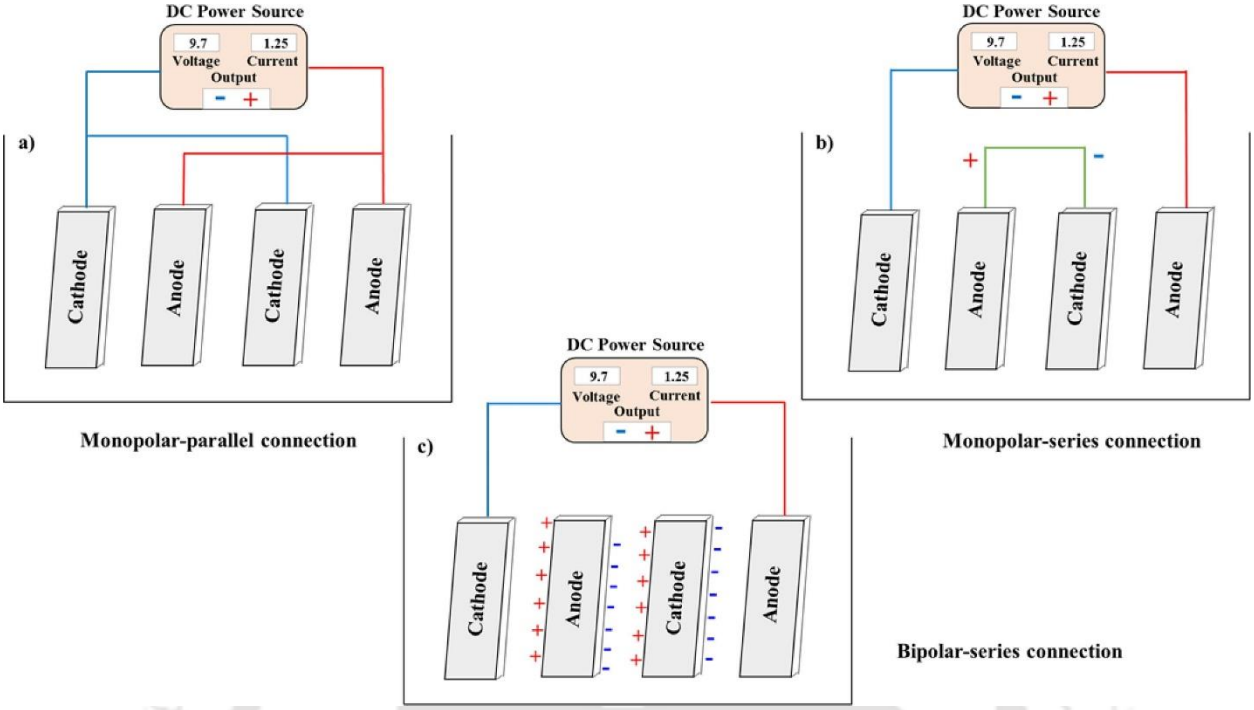


**Fig. 1.4:** Different electrode configurations in an electrochemical cell. (a) monopolar-parallel connection, (b) monopolar-series connection and (c) bipolar-series connection

## 1.4 Ozone assisted electrocoagulation process

Ozone assisted electrocoagulation is an advanced wastewater treatment process that combines electrocoagulation and ozone oxidation to efficiently remove a wide range of contaminants. The synergy between these two processes enhances the removal of pollutants from water and wastewater. Ozone assisted electrocoagulation process typically consumes less energy compared to ozonation alone, making it more energy-efficient. The use of electrocoagulation as a post treatment process could completely mineralize the complex species in the solution by mitigating the intermediate by-products formed during ozonation [56]. The integrated process can be designed to be scalable and adaptable to various water treatment scenarios, including small-scale applications, such as point-of-use household drinking water treatment, as well as larger treatment

facilities such as industrial or municipal wastewater treatment, making it an appropriate water and wastewater treatment system. Besides, the integrated process is capable of meeting stringent water quality standards and regulatory requirements, by efficiently removing heavy metals, pesticides, surfactants, pathogens and microorganisms from different types of contaminated water sources [57]. Table 1.2 shows the benefits of combining electrocoagulation with various water treatment techniques. Among the wide array of available applications of the ozone assisted electrocoagulation process, few have been briefed down below:

**Industrial wastewater treatment**: Ozone-assisted electrocoagulation is widely used in industrial settings to treat wastewater produced by different manufacturing processes. It can effectively remove heavy metals, organic pollutants, oil & grease, and other toxic chemicals commonly found in industrial effluents [56].

**Grey water treatment**: Ozone-assisted electrocoagulation can also be applied for the treatment of grey water to enhance the removal of suspended solids, detergents, organic matter, and pathogens. It can improve the overall water quality before being discharged into the water bodies or for reuse [57].

**Distillery wastewater treatment**: Ozone-assisted electrocoagulation is extensively used for the treatment of distillery wastewater. It can completely degrade the organic matter, heavy metals, colour, suspended solids, nutrients, and volatile organic compounds (VOCs) present in the wastewater, thus minimizing its environmental impact [58].

**Groundwater treatment**: Contaminated groundwater can be treated using ozone-assisted electrocoagulation to remove various pollutants, such as heavy metals, sulphate, chloride, pesticides, and volatile organic compounds (VOCs). It is particularly useful for cleaning up groundwater at industrial sites or areas with historical pollution [59].

**Surface water treatment**: Ozone-assisted electrocoagulation can be employed to treat surface water sources, such as ponds, lakes, rivers, and reservoirs, to remove suspended solids, pathogens, dissolved oxygen, algae, and antibiotics. This is critical for ensuring a reliable source of clean water for municipalities and industries [60].

**Textile wastewater treatment**: The textile industry produces wastewater containing surfactants, colorants, dyes, suspended solids, and organic chemicals. Ozone-assisted electrocoagulation can assist in decolorizing and removing these harmful pollutants, ensuring compliance with the regulatory standards [61].

**Table 1.2:** Combination of electrocoagulation with different water treatment methods

| Hybrid methods | Types of wastewater | Pollutants | Operating conditions | | Removal efficiency | Improvement in process performance via hybrid method | References |
|---|---|---|---|---|---|---|---|
| | | | EC | Oxidation | | | |
| $O_3$/EC | Steel industry wastewater | Cyanide, COD and BOD | Current density = 50-150 A $m^{-2}$, Electrode distance = 0.005 m, Reaction time = 30 min, pH = 7.7, Electrode connection = BP-S | Ozone generation rates = 1.00-1.33 mg/s, Reaction time = 40 min | The removal rate for cyanide, COD and BOD were 62%, 60% and 61% respectively | An improved removal rate of 99.8% cyanide, 94.7% COD and 95% BOD were achieved. The operating cost of the overall process was 5.822 US$ $m^{-3}$. | [62] |
| $O_3$/EC | Grey water | COD, TOC and Escherichia coli (E.coli) | Current density = 5-20 mA $cm^{-2}$, Electrode distance = 2 cm, Reaction time = 60 min, pH = 7 | Ozone concentration = 22.3 -56 mg/L, Treatment time = 60 min | A COD removal rate of 77% and TOC of 64.5% were obtained. | The removal rates of E. coli, COD and TOC were 89%, 86% and 70.2% respectively. The total cost of the process was found to be 1.9 US$ $m^{-3}$. | [57] |

| | | | | | | | |
|---|---|---|---|---|---|---|---|
| EO/EC | Groundwater | Nitrate and Ammonium ion ($NH_4^+$-N) | Current density = 40 mA $cm^{-2}$, Electrode distance = 0.3 cm, Reaction time = 60 min, pH = 7.8 | Current density = 75 mA $cm^{-2}$, Hydraulic retention time = 25-50 min, Volumetric flow rate = 4-8 mL/min | The removal efficiency of nitrate content varied between 90 and 100% over a 60 min of treatment time. Also, an increase in the $NH_4^+$-N ion content up to 6.7 mg/L was seen. | The concentration of the $NH_4^+$-N ion was completely removed (100%) at a volumetric flow rate of 4 mL $min^{-1}$. No toxic by-products were formed. | [63] |
| EO/EC | Synthetic deep aquifer | Trace organic compounds (TrOCs) | Current density = 5.55 mA $cm^{-2}$, Electrode distance = 1 cm, Electrolysis time = 5 min, pH = 6, Electrode connection = MP-P | Current density = 14.8 mA $cm^{-2}$, Treatment time = 20 min, pH = 7.5 | The removal rates of trimethoprim and benzyldimethyl-decylammonium chloride were~10% & 5% respectively. | An improved removal efficiency of~ 87% TMP and~ 70% BAC-C10 were obtained. The electrical energy per order ($E_{EO}$) was found to be around 10–75 kWh $m^{-3}$. | [64] |
| Peroxi-EC | Pharmaceutical wastewater | COD | Current density = 1.7- | $H_2O_2$ content = 300 mg/L | The removal of COD from the | The removal rate was increased to around | [65] |

| | | | | | | | |
|---|---|---|---|---|---|---|---|
| | | | 1.9 mA $cm^{-2}$, Electrode distance = 2.5 cm, Reaction time = 60 min, pH = 7, Electrode connection = BP-S | | treated wastewater was observed to be 34.2%. | 58% (residual 205 mg $L^{-1}$). Also, the energy consumption was reduced by 50.6%. | |
| Peroxi-EC | Industrial park treatment plant | COD, Colour and Total coliform count | Current density = 14.2 mA $cm^{-2}$, Electrode distance = 2.5 cm, Electrolysis time = 30 min, pH = 2.8, Electrode connection = MP-P | Amount of $H_2O_2$ added = 40 mL 0.6 $L^{-1}$ | A COD removal rate of 56% was obtained. | The removal rates of COD, colour and total coliform count were found to be 78%, 97% & 99.9% respectively. | [66] |

## 1.5 State of the art

With a brief overview of the contemporary research, this section summarizes the outcome of various literatures so as to identify few potential areas of research that needs to be addressed for this thesis work. The state of the art has been presented for both standalone and hybrid ozone assisted electrocoagulation methods used for the treatment of highly contaminated water and wastewater.

### 1.5.1 Ozone assisted electrocoagulation process for the removal of cyanide and phenol from steel industry wastewater

The steel industry contributes enormously to the economic development of the world. However, due to its high manufacturing rate, the generation of wastewater in steel industries is enormous. These wastewaters can vary depending on the specific units and processes used in a particular steel plant. The generation of wastewater in steel industries occurs from various unit operations like smelting of pig iron in a blast furnace, coke oven, ladle refining, rolling mills, quenching and tempering, shearing, pickling and scaling among others. The presence of cyanide is pervasive in such type of wastewaters, particularly from the blast furnace discharges [67]. Cyanide exists in wastewater mainly in two forms, HCN and $CN^-$ ions. The permissible limit of cyanide into surface water is less than 0.2 mg $L^{-1}$. Cyanide is a highly toxic compound that, when present in wastewater or in the environment, can pose significant health risks to human beings. The adverse effects of cyanide exposure are well-documented and can be severe. Ingesting or inhaling even small amounts of cyanide can lead to acute poisoning. Symptoms can develop within minutes and include headache, dizziness, seizures, nausea, vomiting and respiratory failure. Cyanide-contaminated water can also lead to chronic health effects. Chronic exposure to cyanide may result

in long-term health effects, including neurological problems, thyroid dysfunction, and damage to the cardiovascular system [68]. Therefore, wastewaters with high cyanide content should only be discharged into the environment once its recommended limit is reached. Besides, the presence of phenol and its compounds are very significant in coke oven and rolling mill wastewaters of steel plants refineries. The permissible limit of phenol in potable water is 0.5 μg $L^{-1}$, whereas the discharge limit for surface water is 1 mg $L^{-1}$. High concentration of phenol in drinking as well as surface water results in considerable health concerns amongst human beings, and animals. Phenol is a strong irritant to the skin, eyes, and respiratory tract. Exposure to even relatively low concentrations of phenol can cause skin and eye irritation, leading to redness, burning, and pain. Ingestion, inhalation, or dermal exposure to higher concentrations of phenol can result in systemic toxicity. Symptoms may include headache, dizziness, nausea, vomiting, abdominal pain, and in severe cases, cardiovascular and neurological effects [69]. As such, it becomes necessary to prevent the release of wastewaters with high phenol content into the natural water bodies without proper treatment. Further, the presence of chlorides, a major environmental pollutant found in ladle furnace wastewater, also causes harmful effects on human beings like hypertension, dehydration, and diarrheal symptoms among others. Apart from these, some of the adverse effects of chlorides within the steel industry involve blockage of pipes, demineralization, corrosion, and scaling. The permissible limit of chloride is 1000 mg $L^{-1}$ for surface water. High chloride concentrations can also harm aquatic eco-system, particularly freshwater invertebrates and fish by disrupting the osmoregulation and physiology of these species [70]. Thus, strict monitoring and regulation of chloride contaminated wastewaters must be done before being discharged into the environment.

#### *1.5.1.1 Literature review*

There are numerous reports on the treatment of real industrial effluents based on different techniques. Amongst these, the most commonly used techniques are adsorption [71], chemical precipitation , nanotechnology [72], UV-irradiation, membrane filtration [73] and biological treatment [74]. Although the afore-mentioned techniques are widely used, however, a deep insight into all these methods indicate various drawbacks, associated with each of the them [75]. Also, it is well established that the individual/standalone techniques have several limitations in effectively treating real industrial effluents with multiple contaminants due to its complex nature. In this context, various combinational and/or hybrid techniques have received remarkable attention due to their high degradation efficiency, faster reaction rate, reduced treatment time, and minimal operational cost.

Ozone is one of the most potential alternatives that have attracted researchers to treat highly contaminated effluents from different industrial sources. The utilization of ozone can be categorized into a strong oxidant and a powerful disinfectant. Highly reactive molecular ozone, as well as hydroxyl radicals produced during the reaction mechanism is primarily responsible for the oxidation process [5]. By increasing the inhibitor concentration, the ozone reaction becomes more inclined towards direct reaction. Therefore, either a direct ozone attack and/or an indirect free radical reaction (generation of hydroxyl radicals via ozone decomposition) signifies the phenomenon of ozone reaction with various inorganic and organic compounds, resulting in their efficient removal from the effluent [76]. Similarly, electrocoagulation has been studied intensively by various researchers for its effectiveness in removing toxic wastewater contaminants. This method primarily involves three vital steps, i.e., an electrolytic reaction at the electrode surface, in-situ coagulant production, and adsorption of colloidal particles onto the produced metal

hydroxide flocs, followed by precipitation. The contaminant removal from the aqueous solution was further aided by the production of hydrogen gas (cathode) and oxygen gas (anode) during the process via floatation phenomenon. The selection of proper electrode materials is essential for effective removal of the target contaminants [37]. Aluminum and iron are often utilized as electrode materials, as both the materials exhibit better results compared to other electrodes.

Even though the ozonation process is highly efficient; however, the use of ozone alone to treat highly contaminated industrial effluents necessitate higher ozone doses which consumes a lot of energy and may also result in incomplete mineralization due to intermediate by-product formation. Nevertheless, integration of a pre/post treatment method with ozone may significantly aid in reducing its high operational cost and enhancing the overall process efficiency [6]. In view of this, electrocoagulation is considered as a viable pre/post treatment method to ozonation due to its high removal rate and cost-effectiveness. As such, the synergy between these two processes results in low energy consumption and mitigation of the intermediate by-products, making the hybrid ozone assisted electrocoagulation approach highly promising and energy-efficient. Besides, it is capable of meeting stringent water quality standards and regulatory requirements, by efficiently removing both organic and inorganic pollutants from different types of contaminated water sources [77].

#### *1.5.1.2 Scope of research*

Highly toxic contaminants in industrial wastewater necessitates the use of strict regulations and proper wastewater management practices. Although several studies have been conducted on the treatment of real industrial effluents by different techniques; however, it is envisaged that the use of hybrid ozone assisted electrocoagulation process for the analysis of cyanide and phenol rich steel plant wastewater has not been investigated yet. As such, the cyanide and phenol rich wastewater was collected from Tata steel industry (India). A combination of ozone and

electrocoagulation was adopted for the simultaneous removal of cyanide, phenol, and chloride from Tata steel plant wastewater. Variation of ozone flow rate, current density, treatment time and solution pH was studied to evaluate the degradation pattern of the contaminants by the proposed hybrid approach. Kinetic modelling and mass transfer study were performed during the ozonation process to predict the movement of ozone gas between different phases. The relation between the increased ozone concentration in the solution and the volumetric mass transfer coefficient ($K_l$ a) was also determined. Finally, a preliminary economic analysis was carried out to assess the total energy consumption and the cost-effectiveness of the hybrid ozone assisted electrocoagulation process.

### 1.5.2 Treatment of steel plant generated biological oxidation treated (BOT) wastewater to remove colour, ammonia-N and iron

Steel industries generate various types of wastewater during their production stage. These wastewaters can vary depending upon the unit operations and processes used in a particular steel plant. The wastewaters generated are toxic, hazardous, and contains persistent colour and foul odour. Typically, chemical precipitation and biological oxidation methods are used for treating such contaminated wastewaters in Tata steel industry (India) [78]. The water that is obtained after the biological oxidation of coke oven effluent is known as the biological oxidation treated (BOT) wastewater. Although it is biologically treated; however, the presence of iron, colour, and ammonia-N in high concentrations are most prevalent in BOT wastewater. Ammonia is a crucial environmental pollutant found in steel plant wastewater, which exists in either of the two forms depending on the pH: unionized ammonia ($NH_3$) and ionized ammonia ($NH_4^+$). The lethal concentration of ammonia for aquatic organisms varies from 0.2 to 2.0 mg $L^{-1}$, while the

permissible limit of ammonia in the surface water is 50 mg $L^{-1}$. High concentration of ammonia in the natural water bodies not only leads to eutrophication but is also harmful to human beings, animals, and plants. Prolonged contact with ammonia contaminated wastewater can cause skin irritation, redness, dermatitis, and even chemical burns in extreme cases [79]. Ingestion or exposure to high ammonia concentrations can irritate the gastrointestinal tract, leading to symptoms like nausea, vomiting, and abdominal pain. Thus, it is crucial to restrict the discharge of wastewaters with high ammonia content into the environment without proper treatment. Besides, iron content in steel plant wastewater can be intolerable in terms of discoloration, turbidity, and unpleasant odour. While these aesthetic issues are not directly harmful to human health, yet they can be unappealing and affect public perception of water quality. The permissible limit of iron in drinking water and surface water is 0.3 mg $L^{-1}$ and 1.0 mg $L^{-1}$, respectively. Consuming water with excessive iron content may lead to gastrointestinal issues, such as stomach cramps, nausea, and diarrhoea. Also, chronic exposure to iron contaminated wastewater can result in iron overload or hemochromatosis [80]. This condition can have various health effects, including joint pain, fatigue, liver damage, and diabetes. As such, high levels of iron contaminated wastewaters should only be released into the natural water bodies once its recommended limit is reached. Apart from these major contaminants, the primary concern emerges from the presence of residual colour, generated from the coke oven plant of the steel industry. The permissible limit of colour in surface water is 300 Hazen. Discharge of the coloured wastewater is a major source of problem as it can pose a threat to aquatic life and, by extension to human health if they are used for drinking or agricultural purposes. The coloured compounds in wastewater can promote the growth of specific algae species, leading to harmful algal blooms that can release toxins into the water and affect both the aquatic life and drinking water sources [81]. Also, coloured wastewater

can reduce light penetration, potentially impacting the photosynthesis in aquatic plants and thus altering the food chain. Therefore, the presence of residual colour in wastewaters should be strictly monitored and controlled before being discharged into the environment.

#### *1.5.2.1 Literature review*

The steel industry has fuelled the economic development of the entire world for more than a century and a half. Over the years, steel production has been ramping up steadily, so there has been a significant increase in effluent discharge. In the steel manufacturing sector, around 90% of the water (on average, 88% for an integrated steel mill and 94% for an electric arc furnace-based plant) is released after cleaning and/or cooling of various units and are often reused by other utilities in the steel plant. On average, Tata steel industry (India) consumes 25 $m^3$ of water per ton of steel produced, generating wastewater at 5 $m^3$ per hour of operation [67]. Tata steel manufacturing plant generates wastewater from different unit operations, such as coke oven, blast furnace, ladle refining, continuous casting, rolling mills, annealing, shearing, galvanizing and coating, as well as several other auxiliary processes [82,83]. Amongst these various operations, the BOT wastewater obtained after the biological oxidation of coke oven plant effluent is one of the unavoidable sector of Tata steel industry, where further treatment and neutralization is required before it can be released into the environment. Anaerobic and aerobic digestion, sequential batch reactors, bio-filters and activated sludge process are some of the biological treatment methods generally used in the steel industry. Although, biological treatments can be effective in reducing the organic loads and some inorganic components in steel industry wastewater; however, the presence of coloured compounds and recalcitrant pollutants, may require additional treatment methods, to be effectively removed from the wastewater [84].

Therefore, there is a need for a more reliable, highly efficient, and scalable technology that is sustainable, eco-friendly, and cost-effective with high capacity throughput. Ozone assisted electrocoagulation is an advanced wastewater treatment technology that combines the benefits of electrocoagulation and ozone oxidation to effectively remove a wide range of toxic contaminants. The reason may be attributed to its high oxidative ability, fast reaction rate, easy operation, simple equipment design, low energy consumption and minimum cost of operation [61]. The hybrid process can be designed to be scalable and adaptable to various water treatment scenarios, including small-scale applications, such as point-of-use household drinking water treatment, as well as larger treatment facilities such as industrial or municipal wastewater treatment, making it an appropriate water and wastewater treatment system [85]. Thus, it is versatile and can be tailored to address the specific treatment requirements and challenges of highly contaminated wastewaters from steel industry.

#### *1.5.2.2 Scope of research*

Wastewater from various unit operations of steel manufacturing plants are a major concern to the research and development section of an industry. Although several studies have been conducted on the removal of toxic contaminants from various industrial wastewater; however, it is envisaged that the treatment of biological oxidation treated (BOT) wastewater from steel industry via hybrid ozone assisted electrocoagulation process has not been investigated yet. As such, the BOT wastewater obtained after the biological oxidation of coke oven effluent from Tata Steel industry (India) was considered here. A combination of ozone and electrocoagulation was adopted for the simultaneous removal of ammonia-N, iron and coloured compounds from the BOT wastewater. The efficiency of the hybrid approach was evaluated at various operating parameters viz. ozone flow rate, current density, treatment time, and solution pH to effectively remove the target

contaminants. Kinetic modelling and size determination study of ozone microbubbles were carried out to predict the degradation performance of the ozonation process under different conditions. The corrosion of electrodes and variation in film thickness during the electrocoagulation process was also estimated. Finally, a preliminary cost estimation was carried out to evaluate the total energy requirement and the mass of electrode material used during the hybrid ozone assisted electrocoagulation process.

### 1.5.3 Treatment of cold rolling mill (CRM) wastewater of steel industry to remove phenol, iron and oil & grease content

Steel industry wastewaters are generated through various processes within the steel manufacturing plant. These wastewaters can be complex and highly polluted due to the presence of heavy metals, oil & grease, suspended solids, and various chemical compounds. Managing and treating steel plant wastewater is crucial to minimize the environmental impact and comply with regulatory standards [86]. Amongst the various contaminated wastewater generated, the oil emulsion wastewater from cold rolling mills (CRM) of Tata steel industry (India) is one of the unavoidable sector, where further treatment is needed before being released into the environment. A typical discharge of CRM wastewater contains high concentrations of oil & grease, phenol, iron and COD. Other compounds may also be present such as various salts of chromium, copper, and nickel, depending upon the steel composition. The presence of oil & grease in water can be very harmful to both human beings and aquatic species. Oil & grease can provide a suitable environment for the growth of harmful microorganisms, including bacteria and viruses. These contaminated water can increase the risk of waterborne diseases in both infants and adults. The permissible limit of oil & grease in surface water is 10 mg $L^{-1}$. Dermal exposure to high levels of oil and grease may result

in dermatitis, respiratory disorders, and chronic health issues [87]. Besides, the presence of phenol in drinking as well as surface water results in considerable health concerns amongst human beings, and animals. Exposure to even relatively low concentrations of phenol can cause skin and eye irritation, leading to redness, burning, and pain. The permissible limit of phenol in potable water is 0.5 μg $L^{-1}$, whereas the discharge limit for surface water is 1 mg $L^{-1}$. Ingestion, inhalation, or dermal exposure to higher concentrations of phenol can result in systemic toxicity. Symptoms may include headache, dizziness, nausea, vomiting, abdominal pain, and in severe cases, cardiovascular and neurological effects [69]. Further, iron contaminated wastewater can be intolerable in terms of discoloration, turbidity, and unpleasant odour. While these aesthetic issues are not directly harmful to human health, yet they can be unappealing and affect public perception of water quality. The permissible limit of iron in drinking water and surface water is 0.3 mg $L^{-1}$ and 1.0 mg $L^{-1}$, respectively. Consuming water with excessive iron content may lead to gastrointestinal issues, such as stomach cramps, nausea, and diarrhoea. Also, chronic exposure to iron contaminated wastewater can result in iron overload or hemochromatosis [80]. Therefore, wastewaters with such toxic contaminants should only be discharged into the environment once the water quality standards and regulatory requirements are complied.

#### *1.5.3.1 Literature review*

The steel manufacturing sector is one of the largest manufacturing industries globally, producing over 1.8 billion tons of steel annually. Tata steel industry (India) produces steel through several methods, including basic oxygen furnace (BOF), electric arc furnace (EAF), and secondary refining (ladle furnace) process. The choice of method depends on factors such as the desired steel quality (ductility and hardness), steel types (sheets and bars), and specialty steels (stainless steel and high strength alloys) among others [88]. The produced steel then undergoes continuous casting

before being subjected to final rolling (hot and cold rolling) operations. Cold rolling is a crucial operation in the steel industry that involves reducing the thickness of steel sheets or strips while improving their surface finish and mechanical properties with various sub-processes like pickling, rolling, annealing, and tempering. Cold rolling mill (CRM) is often used to produce high-quality steel products with increased hardness and tensile strength [89]. During the operation, the steel strip may be lubricated with oil or emulsion to reduce friction and prevent surface defects. Cooling is also applied to maintain product quality and control the temperature of the steel strip. As such, a substantial quantity of oily wastewater is released, out of which the oil emulsion wastewater from cold rolling mill is the most problematic to tackle. The CRM wastewaters are residues from the cold rolling operation and exhibit great carbonation potential due to their alkaline characteristics. It requires proper treatment to achieve the standard water quality parameter before being discharged into the environment [90]. Some of the prevalent techniques used for the treatment of CRM wastewater include membrane separation [91], magnetic filtration [92], chemical coagulation [93], and biological treatment [94]. However, there are various pitfalls associated with each of the technique amid good outcomes.

In view of this, ozonation and electrocoagulation methods have received significant recognition for effectively treating highly contaminated wastewaters from various industries. Also, both these methods have a high success rate in the separation of oil & grease from oily emulsions compared to other available techniques [95,96]. Electrocoagulation process is based on the phenomenon of electrochemistry, in which oxidation or loss of electrons takes place at the anode, whereas reduction or gain of electrons occurs at the cathode surface. It is very effective even in the removal of the tiniest colloidal particles via application of an electric field, responsible for assisting in coagulation and flotation of the contaminants. It has gained popularity as a sustainable and cost-

effective alternative to traditional coagulation methods [7]. Similarly, ozone has also emerged as a promising wastewater treatment alternative that produces zero amount of sludge along with the formation of oxygen and water as end products via residual ozone decomposition. Depending upon the pH, the dominant oxidants viz. molecular ozone (acidic conditions) and hydroxyl radical (alkaline conditions) are primarily responsible for the oxidation of various organic and inorganic compounds in the wastewater [76]. It is often used as a tertiary or advanced treatment step in wastewater treatment plants to address specific water quality concerns.

#### *1.5.3.2 Scope of research*

Environmental regulations are crucial for steel plant wastewaters to ensure that the treatment processes involved meets the required discharge standards. Although several techniques have been reported on the removal of various industrial wastewater contaminants; however, it is envisaged that the use of either ozonation or electrocoagulation process for the treatment of oily CRM wastewater from steel industry has not been investigated yet. As such, the CRM wastewater generated from the cold rolling operation of Tata steel industry (India) was considered here. Both ozonation and electrocoagulation were carried out separately for the simultaneous removal of oil & grease, phenol, and iron from the CRM wastewater, followed by a feasibility study. The performance efficiencies based on the pollutant removal rate and economic analysis were compared to obtain a highly efficient and cost-effective technique for the target wastewater. The degradation rate of the pollutants was evaluated at different experimental variables such as current density, ozone flow rate, treatment time, and solution pH. Kinetic modelling of the pollutants showed that, pseudo first-order reaction model fitted perfectly for the analysis. Mass transfer analysis was conducted to predict the effect of volumetric mass transfer coefficient ($K_l$ a) on pollutant degradation. Several characterization study of sludge and electrode materials were also

performed. Finally, a preliminary cost estimation was carried out to obtain a basic understanding of the economic involvement of both the processes.

## 1.6 Scope and objectives of the present work

This thesis is focused on the treatment of wastewaters from different units and processes of steel manufacturing plant by standalone and hybrid ozone assisted electrocoagulation technique. The main objectives are:

1. Hybrid ozone assisted electrocoagulation technique for the treatment of cyanide and phenol rich steel plant wastewater.
2. Removal of ammonia-N, iron and colour from steel plant generated biological oxidation treated (BOT) wastewater via hybrid ozone assisted electrocoagulation.
3. Treatment of oil, phenol, and iron rich cold rolling mill (CRM) wastewater of steel plant by standalone electrocoagulation and ozonation techniques.

## 1.7 Organization of the thesis

To accomplish the above objectives, the thesis has been organized in six chapters. A brief content of each chapter is given below:

**Chapter 1** addresses the state of the art literature, research motivation of present work, possible scope of research, along with the objectives and organization of the thesis. **Chapter 2** describes the materials and experimental methods used for the present study. The unit operations and source of the wastewater considered were elaborately discussed. The mechanism and reactor set-up of both ozonation and electrocoagulation methods were covered. It also includes the characterization techniques used for the analysis of the wastewater samples. **Chapter 3** discusses the effectiveness of the hybrid ozone assisted electrocoagulation technique in treating cyanide and phenol rich steel

plant wastewater. Variation of ozone flow rate, current density, treatment time and solution pH was studied to evaluate the degradation pattern of the contaminants by the proposed hybrid approach. Kinetic modelling of the pollutants showed that, pseudo first-order reaction model fitted perfectly for the analysis. Mass transfer study was performed during ozonation to predict the movement of ozone gas between different phases. The co-relation between the increased ozone concentration and the volumetric mass transfer coefficient ($K_l$ a) was also determined. **Chapter 4** presents the treatment of steel plant generated BOT wastewater to remove ammonia-N, iron and coloured compounds. A combination of ozone and electrocoagulation was adopted for the simultaneous removal of the target contaminants. Kinetic study and size determination of ozone microbubbles were carried out to predict the degradation performance of the ozonation process under different conditions. The corrosion of electrodes and variation in film thickness during the electrocoagulation process was also estimated. Finally, an economic analysis was carried out to evaluate the total energy consumption and the cost-effectiveness of the hybrid technique. **Chapter 5** evaluates the performance of standalone electrocoagulation and ozonation techniques for the simultaneous removal of oil & grease, phenol, and iron from CRM wastewater of steel manufacturing plant. The degradation rate of the pollutants was evaluated at different experimental variables such as current density, ozone flow rate, treatment time, and solution pH. Mass transfer analysis was carried out to predict the effect of volumetric mass transfer coefficient ($K_l$ a) on pollutant degradation. To determine the morphological and functional properties of the wastewater generated sludge, different characterization techniques were also performed. Finally, a cost estimation was done to understand the economic involvement of both the techniques. **Chapter 6** outlines the inferences drawn from the experimental chapters presented in this thesis along with few recommendations towards scope for future work.

## References:

[1] A. Almukdad, M.A. Hafiz, A.T. Yasir, R. Alfahel, A.H. Hawari, Unlocking the application potential of electrocoagulation process through hybrid processes, J. Water Process Eng. 40 (2021) 101956. https://doi.org/10.1016/j.jwpe.2021.101956.

[2] G. Mao, Y. Han, X. Liu, J. Crittenden, N. Huang, U.M. Ahmad, Technology status and trends of industrial wastewater treatment: A patent analysis, Chemosphere. 288 (2022) 132483. https://doi.org/10.1016/j.chemosphere.2021.132483.

[3] M. Pei, B. Zhang, Y. He, J. Su, K. Gin, O. Lev, G. Shen, S. Hu, State of the art of tertiary treatment technologies for controlling antibiotic resistance in wastewater treatment plants, Environ. Int. 131 (2019) 105026. https://doi.org/10.1016/j.envint.2019.105026.

[4] M. Priyadarshini, I. Das, M.M. Ghangrekar, L. Blaney, Advanced oxidation processes: Performance, advantages, and scale-up of emerging technologies, J. Environ. Manage. 316 (2022) 115295. https://doi.org/10.1016/j.jenvman.2022.115295.

[5] S. Lim, J.L. Shi, U. von Gunten, D.L. McCurry, Ozonation of organic compounds in water and wastewater: A critical review, Water Res. 213 (2022) 118053. https://doi.org/10.1016/j.watres.2022.118053.

[6] S.N. Malik, P.C. Ghosh, A.N. Vaidya, S.N. Mudliar, Hybrid ozonation process for industrial wastewater treatment: Principles and applications: A review, J. Water Process Eng. 35 (2020). https://doi.org/10.1016/j.jwpe.2020.101193.

[7] D.T. Moussa, M.H. El-Naas, M. Nasser, M.J. Al-Marri, A comprehensive review of electrocoagulation for water treatment: Potentials and challenges, J. Environ. Manage. 186 (2017) 24–41. https://doi.org/10.1016/j.jenvman.2016.10.032.

[8] C. V. Rekhate, J.K. Srivastava, Recent advances in ozone-based advanced oxidation

processes for treatment of wastewater- A review, Chem. Eng. J. Adv. 3 (2020) 100031. https://doi.org/10.1016/j.ceja.2020.100031.

[9] B. Mennad, Z. Harrache, K. Yanallah, D. Amir Aid, A. Belasri, Effect of the anode material on ozone generation in corona discharges, Vacuum. 104 (2014) 29–32. https://doi.org/10.1016/j.vacuum.2013.12.005.

[10] L. Qi, X. Wang, Q. Xu, Coupling of biological methods with membrane filtration using ozone as pre-treatment for water reuse, Desalination. 270 (2011) 264–268. https://doi.org/10.1016/j.desal.2010.11.054.

[11] M. Mänttäri, M. Kuosa, J. Kallas, M. Nyström, Membrane filtration and ozone treatment of biologically treated effluents from the pulp and paper industry, J. Memb. Sci. 309 (2008) 112–119. https://doi.org/10.1016/j.memsci.2007.10.019.

[12] M.S. Lucas, J.A. Peres, G. Li Puma, Treatment of winery wastewater by ozone-based advanced oxidation processes (O3, O3/UV and O3/UV/H2O2) in a pilot-scale bubble column reactor and process economics, Sep. Purif. Technol. 72 (2010) 235–241. https://doi.org/10.1016/j.seppur.2010.01.016.

[13] T.A. Ternes, M. Meisenheimer, D. McDowell, F. Sacher, H.J. Brauch, B. Haist-Gulde, G. Preuss, U. Wilme, N. Zulei-Seibert, Removal of pharmaceuticals during drinking water treatment, Environ. Sci. Technol. 36 (2002) 3855–3863. https://doi.org/10.1021/es015757k.

[14] T. Zheng, Q. Wang, T. Zhang, Z. Shi, Y. Tian, S. Shi, N. Smale, J. Wang, Microbubble enhanced ozonation process for advanced treatment of wastewater produced in acrylic fiber manufacturing industry, J. Hazard. Mater. 287 (2015) 412–420. https://doi.org/10.1016/j.jhazmat.2015.01.069.

[15] Y. Shi, C. Huang, K.C. Rocha, M.G. El-Din, Y. Liu, Treatment of oil sands process-affected water using moving bed biofilm reactors: With and without ozone pretreatment, Bioresour. Technol. 192 (2015) 219–227. https://doi.org/10.1016/j.biortech.2015.05.068.

[16] A.D. Coelho, C. Sans, S. Esplugas, M. Dezotti, Ozonation of NSAID: A Biodegradability and Toxicity Study, Ozone Sci. Eng. 32 (2010) 91–98. https://doi.org/10.1080/01919510903508162.

[17] S.K. Singh, C.M. Moody, T.G. Townsend, Ozonation pretreatment for stabilized landfill leachate high-pressure membrane treatment, Desalination. 344 (2014) 163–170. https://doi.org/10.1016/j.desal.2014.03.011.

[18] K. Turhan, Z. Turgut, Decolorization of direct dye in textile wastewater by ozonization in a semi-batch bubble column reactor, Desalination. 242 (2009) 256–263. https://doi.org/10.1016/j.desal.2008.05.005.

[19] F. Nawaz, Y. Xie, H. Cao, J. Xiao, Y. Wang, X. Zhang, M. Li, F. Duan, Catalytic ozonation of 4-nitrophenol over an mesoporous α-MnO2 with resistance to leaching, Catal. Today. 258 (2015) 595–601. https://doi.org/10.1016/j.cattod.2015.03.044.

[20] J. Huang, X. Wang, Z. Pan, X. Li, Y. Ling, L. Li, Efficient degradation of perfluorooctanoic acid (PFOA) by photocatalytic ozonation, Chem. Eng. J. 296 (2016) 329–334. https://doi.org/10.1016/j.cej.2016.03.116.

[21] L. Yang, M. Sheng, Y. Li, W. Xue, K. Li, G. Cao, A hybrid process of Fe-based catalytic ozonation and biodegradation for the treatment of industrial wastewater reverse osmosis concentrate, Chemosphere. 238 (2020) 124639. https://doi.org/10.1016/j.chemosphere.2019.124639.

[22] J. Wang, H. Chen, Catalytic ozonation for water and wastewater treatment: Recent

advances and perspective, Sci. Total Environ. 704 (2020) 135249. https://doi.org/10.1016/j.scitotenv.2019.135249.

[23] H. Li, Y. Huang, S. Cui, Removal of alachlor from water by catalyzed ozonation on Cu/Al2O3 honeycomb, Chem. Cent. J. 7 (2013) 1–6. https://doi.org/10.1186/1752-153X-7-143.

[24] G. Gao, J. Shen, W. Chu, Z. Chen, L. Yuan, Mechanism of enhanced diclofenac mineralization by catalytic ozonation over iron silicate-loaded pumice, Sep. Purif. Technol. 173 (2017) 55–62. https://doi.org/10.1016/j.seppur.2016.09.016.

[25] G. Manterola, I. Uriarte, L. Sancho, The effect of operational parameters of the process of sludge ozonation on the solubilisation of organic and nitrogenous compounds, Water Res. 42 (2008) 3191–3197. https://doi.org/10.1016/j.watres.2008.03.014.

[26] C. Chen, C. Han, P. Wang, S. Guo, G. Yan, Q.X. Li, Investigation on Titanium Silicalite ETS-4 Catalyzed Ozonation for Chemicals in Wastewater, Exemplified With 4-Chlorophenol, CLEAN – Soil, Air, Water. 44 (2016) 1644–1651. https://doi.org/https://doi.org/10.1002/clen.201500282.

[27] M. Mehrjouei, S. Müller, D. Möller, Catalytic and photocatalytic ozonation of tert-butyl alcohol in water by means of falling film reactor: Kinetic and cost-effectiveness study, Chem. Eng. J. 248 (2014) 184–190. https://doi.org/10.1016/j.cej.2014.03.047.

[28] J.R. Bolton, K.G. Bircher, W. Tumas, C.A. Tolman, Figures-of-merit for the technical development and application of advanced oxidation technologies for both electric- and solar-driven systems (IUPAC Technical Report), Pure Appl. Chem. 73 (2001) 627–637. https://doi.org/doi:10.1351/pac200173040627.

[29] N. Daneshvar, A. Aleboyeh, A.R. Khataee, The evaluation of electrical energy per order

(EEo) for photooxidative decolorization of four textile dye solutions by the kinetic model, Chemosphere. 59 (2005) 761–767. https://doi.org/10.1016/j.chemosphere.2004.11.012.

[30] Z. Liu, S. Hosseinzadeh, N. Wardenier, Y. Verheust, M. Chys, S. Van Hulle, Combining ozone with UV and H2O2 for the degradation of micropollutants from different origins: lab-scale analysis and optimization, Environ. Technol. (United Kingdom). 40 (2019) 3773–3782. https://doi.org/10.1080/09593330.2018.1491630.

[31] A. Latifoglu, M.D. Gurol, The effect of humic acids on nitrobenzene oxidation by ozonation and O3/UV processes, Water Res. 37 (2003) 1879–1889. https://doi.org/10.1016/S0043-1354(02)00583-3.

[32] G.A. de Vera, J. Keller, W. Gernjak, H. Weinberg, M.J. Farré, Biodegradability of DBP precursors after drinking water ozonation, Water Res. 106 (2016) 550–561. https://doi.org/10.1016/j.watres.2016.10.022.

[33] Y. Mao, D. Guo, W. Yao, X. Wang, H. Yang, Y.F. Xie, S. Komarneni, G. Yu, Y. Wang, Effects of conventional ozonation and electro-peroxone pretreatment of surface water on disinfection by-product formation during subsequent chlorination, Water Res. 130 (2018) 322–332. https://doi.org/10.1016/j.watres.2017.12.019.

[34] A.A. Al-Raad, M.M. Hanafiah, Removal of inorganic pollutants using electrocoagulation technology: A review of emerging applications and mechanisms, J. Environ. Manage. 300 (2021) 113696. https://doi.org/10.1016/j.jenvman.2021.113696.

[35] I.D. Tegladza, Q. Xu, K. Xu, G. Lv, J. Lu, Electrocoagulation processes: A general review about role of electro-generated flocs in pollutant removal, Process Saf. Environ. Prot. 146 (2021) 169–189. https://doi.org/10.1016/j.psep.2020.08.048.

[36] N. Abdul Rahman, A. Albania Linus, U.J. Gilan, E.E. Jihed, N.K.M.F. Kumar, A. Yassin,

A. Philip, Experimental study of batch electrocoagulation treatment of peat water in Sarawak with aluminium electrodes, IOP Conf. Ser. Mater. Sci. Eng. 778 (2020) 012126. https://doi.org/10.1088/1757-899X/778/1/012126.

[37] A. Tahreen, M.S. Jami, F. Ali, Role of electrocoagulation in wastewater treatment: A developmental review, J. Water Process Eng. 37 (2020) 101440. https://doi.org/10.1016/j.jwpe.2020.101440.

[38] S. Garcia-Segura, M.M.S.G. Eiband, J.V. de Melo, C.A. Martínez-Huitle, Electrocoagulation and advanced electrocoagulation processes: A general review about the fundamentals, emerging applications and its association with other technologies, J. Electroanal. Chem. 801 (2017) 267–299. https://doi.org/10.1016/j.jelechem.2017.07.047.

[39] J.N. Hakizimana, B. Gourich, M. Chafi, Y. Stiriba, C. Vial, P. Drogui, J. Naja, Electrocoagulation process in water treatment: A review of electrocoagulation modeling approaches, Desalination. 404 (2017) 1–21. https://doi.org/10.1016/j.desal.2016.10.011.

[40] E. Jafari, M.R. Malayeri, H. Brückner, P. Krebs, Impact of operating parameters of electrocoagulation-flotation on the removal of turbidity from synthetic wastewater using aluminium electrodes, Miner. Eng. 193 (2023) 108007. https://doi.org/10.1016/j.mineng.2023.108007.

[41] M. Kobya, O.T. Can, M. Bayramoglu, Treatment of textile wastewaters by electrocoagulation using iron and aluminum electrodes, J. Hazard. Mater. 100 (2003) 163–178. https://doi.org/10.1016/S0304-3894(03)00102-X.

[42] A.K. Prajapati, P.K. Chaudhari, D. Pal, A. Chandrakar, R. Choudhary, Electrocoagulation treatment of rice grain based distillery effluent using copper electrode, J. Water Process Eng. 11 (2016) 1–7. https://doi.org/10.1016/j.jwpe.2016.03.008.

[43] N.A. Rahman, A.A. Linus, E.E. Jihed, U. Jata, N.K.M.F. Kumar, A. Philip, A. Yassin, A. Parabi, Experimental Studies on Continuous Electrocoagulation Treatment of Peat Water in Sarawak with Copper Electrodes, Int. J. Integr. Eng. 13 (2021) 168–176. https://doi.org/10.30880/ijie.2021.13.02.019.

[44] R. Kamaraj, S. Vasudevan, Evaluation of electrocoagulation process for the removal of strontium and cesium from aqueous solution, Chem. Eng. Res. Des. 93 (2015) 522–530. https://doi.org/10.1016/j.cherd.2014.03.021.

[45] D. Ghosh, H. Solanki, M.K. Purkait, Removal of Fe(II) from tap water by electrocoagulation technique, J. Hazard. Mater. 155 (2008) 135–143. https://doi.org/10.1016/j.jhazmat.2007.11.042.

[46] X. Chen, P. Ren, T. Li, J.P. Trembly, X. Liu, Zinc removal from model wastewater by electrocoagulation: Processing, kinetics and mechanism, Chem. Eng. J. 349 (2018) 358–367. https://doi.org/10.1016/j.cej.2018.05.099.

[47] S. Bener, Ö. Bulca, B. Palas, G. Tekin, S. Atalay, G. Ersöz, Electrocoagulation process for the treatment of real textile wastewater: Effect of operative conditions on the organic carbon removal and kinetic study, Process Saf. Environ. Prot. 129 (2019) 47–54. https://doi.org/10.1016/j.psep.2019.06.010.

[48] V. Khandegar, A.K. Saroha, Electrocoagulation for the treatment of textile industry effluent - A review, J. Environ. Manage. 128 (2013) 949–963. https://doi.org/10.1016/j.jenvman.2013.06.043.

[49] O. Sahu, B. Mazumdar, P.K. Chaudhari, Treatment of wastewater by electrocoagulation: A review, Environ. Sci. Pollut. Res. 21 (2014) 2397–2413. https://doi.org/10.1007/s11356-013-2208-6.

[50] T.H. Kim, C. Park, E.B. Shin, S. Kim, Decolorization of disperse and reactive dyes by continuous electrocoagulation process, Desalination. 150 (2002) 165–175. https://doi.org/10.1016/S0011-9164(02)00941-4.

[51] P. Ganesan, J. Lakshmi, G. Sozhan, S. Vasudevan, Removal of manganese from water by electrocoagulation: Adsorption, kinetics and thermodynamic studies, Can. J. Chem. Eng. 91 (2013) 448–458. https://doi.org/10.1002/cjce.21709.

[52] S. Vasudevan, J. Lakshmi, G. Sozhan, Effects of alternating and direct current in electrocoagulation process on the removal of cadmium from water, J. Hazard. Mater. 192 (2011) 26–34. https://doi.org/10.1016/j.jhazmat.2011.04.081.

[53] N. Modirshahla, M.A. Behnajady, S. Mohammadi-Aghdam, Investigation of the effect of different electrodes and their connections on the removal efficiency of 4-nitrophenol from aqueous solution by electrocoagulation, J. Hazard. Mater. 154 (2008) 778–786. https://doi.org/10.1016/j.jhazmat.2007.10.120.

[54] M. Kobya, F. Ulu, U. Gebologlu, E. Demirbas, M.S. Oncel, Treatment of potable water containing low concentration of arsenic with electrocoagulation: Different connection modes and Fe-Al electrodes, Sep. Purif. Technol. 77 (2011) 283–293. https://doi.org/10.1016/j.seppur.2010.12.018.

[55] D. Ghosh, C.R. Medhi, M.K. Purkait, Treatment of fluoride containing drinking water by electrocoagulation using monopolar and bipolar electrode connections, Chemosphere. 73 (2008) 1393–1400. https://doi.org/10.1016/j.chemosphere.2008.08.041.

[56] P. Asaithambi, A.R.A. Aziz, W.M.A.B.W. Daud, Integrated ozone—electrocoagulation process for the removal of pollutant from industrial effluent: Optimization through response surface methodology, Chem. Eng. Process. Process Intensif. 105 (2016) 92–102.

https://doi.org/10.1016/j.cep.2016.03.013.

[57] G. Barzegar, J. Wu, F. Ghanbari, Enhanced treatment of greywater using electrocoagulation/ozonation: Investigation of process parameters, Process Saf. Environ. Prot. 121 (2019) 125–132. https://doi.org/10.1016/j.psep.2018.10.013.

[58] P. Asaithambi, M. Susree, R. Saravanathamizhan, M. Matheswaran, Ozone assisted electrocoagulation for the treatment of distillery effluent, Desalination. 297 (2012) 1–7. https://doi.org/10.1016/j.desal.2012.04.011.

[59] P. V. Nidheesh, J. Scaria, D.S. Babu, M.S. Kumar, An overview on combined electrocoagulation-degradation processes for the effective treatment of water and wastewater, Chemosphere. 263 (2021) 127907. https://doi.org/10.1016/j.chemosphere.2020.127907.

[60] F. Yan, L. An, X. Xu, W. Du, R. Dai, A review of antibiotics in surface water and their removal by advanced electrocoagulation technologies, Sci. Total Environ. 906 (2024) 167737. https://doi.org/10.1016/j.scitotenv.2023.167737.

[61] L. Bilińska, K. Blus, M. Gmurek, S. Ledakowicz, Coupling of electrocoagulation and ozone treatment for textile wastewater reuse, Chem. Eng. J. 358 (2019) 992–1001. https://doi.org/10.1016/j.cej.2018.10.093.

[62] P.P. Das, A. Anweshan, P. Mondal, A. Sinha, P. Biswas, S. Sarkar, M.K. Purkait, Integrated ozonation assisted electrocoagulation process for the removal of cyanide from steel industry wastewater, Chemosphere. 263 (2021) 128370. https://doi.org/10.1016/j.chemosphere.2020.128370.

[63] A.K. Benekos, F.E. Tziora, A.G. Tekerlekopoulou, S. Pavlou, Y. Qun, A. Katsaounis, D. V. Vayenas, Nitrate removal from groundwater using a batch and continuous flow hybrid

Fe-electrocoagulation and electrooxidation system, J. Environ. Manage. 297 (2021) 113387. https://doi.org/10.1016/j.jenvman.2021.113387.

[64] D.R. Ryan, E.K. Maher, J. Heffron, B.K. Mayer, P.J. McNamara, Electrocoagulation-electrooxidation for mitigating trace organic compounds in model drinking water sources, Chemosphere. 273 (2021) 129377. https://doi.org/10.1016/j.chemosphere.2020.129377.

[65] S. Farhadi, B. Aminzadeh, A. Torabian, V. Khatibikamal, M. Alizadeh Fard, Comparison of COD removal from pharmaceutical wastewater by electrocoagulation, photoelectrocoagulation, peroxi-electrocoagulation and peroxi-photoelectrocoagulation processes, J. Hazard. Mater. 219–220 (2012) 35–42. https://doi.org/10.1016/j.jhazmat.2012.03.013.

[66] C. Barrera-Díaz, B. Frontana-Uribe, B. Bilyeu, Removal of organic pollutants in industrial wastewater with an integrated system of copper electrocoagulation and electrogenerated H2O2, Chemosphere. 105 (2014) 160–164. https://doi.org/10.1016/j.chemosphere.2014.01.026.

[67] R. Mukherjee, M. Mondal, A. Sinha, S. Sarkar, S. De, Application of nanofiltration membrane for treatment of chloride rich steel plant effluent, J. Environ. Chem. Eng. 4 (2016) 1–9. https://doi.org/10.1016/j.jece.2015.10.038.

[68] E. Jaszczak, Ż. Polkowska, S. Narkowicz, J. Namieśnik, Cyanides in the environment—analysis—problems and challenges, Environ. Sci. Pollut. Res. 24 (2017) 15929–15948. https://doi.org/10.1007/s11356-017-9081-7.

[69] A. Mohd, Presence of phenol in wastewater effluent and its removal: an overview, Int. J. Environ. Anal. Chem. 102 (2022) 1362–1384. https://doi.org/10.1080/03067319.2020.1738412.

[70] K.F. Cao, Z. Chen, Y.H. Wu, Y. Mao, Q. Shi, X.W. Chen, Y. Bai, K. Li, H.Y. Hu, The noteworthy chloride ions in reclaimed water: Harmful effects, concentration levels and control strategies, Water Res. 215 (2022) 118271. https://doi.org/10.1016/j.watres.2022.118271.

[71] A. Dey, R. Singh, M.K. Purkait, Cobalt ferrite nanoparticles aggregated schwertmannite: A novel adsorbent for the efficient removal of arsenic, J. Water Process Eng. 3 (2014) 1–9. https://doi.org/10.1016/j.jwpe.2014.07.002.

[72] P. Mokhtari, M. Ghaedi, K. Dashtian, M.R. Rahimi, M.K. Purkait, Removal of methyl orange by copper sulfide nanoparticles loaded activated carbon: Kinetic and isotherm investigation, J. Mol. Liq. 219 (2016) 299–305. https://doi.org/10.1016/j.molliq.2016.03.022.

[73] V.K. Bulasara, H. Thakuria, R. Uppaluri, M.K. Purkait, Effect of process parameters on electroless plating and nickel-ceramic composite membrane characteristics, Desalination. 268 (2011) 195–203. https://doi.org/10.1016/j.desal.2010.10.025.

[74] I. Oller, S. Malato, J.A. Sánchez-Pérez, Combination of Advanced Oxidation Processes and biological treatments for wastewater decontamination-A review, Sci. Total Environ. 409 (2011) 4141–4166. https://doi.org/10.1016/j.scitotenv.2010.08.061.

[75] V.L. Dhadge, C.R. Medhi, M. Changmai, M.K. Purkait, House hold unit for the treatment of fluoride, iron, arsenic and microorganism contaminated drinking water, Chemosphere. 199 (2018) 728–736. https://doi.org/10.1016/j.chemosphere.2018.02.087.

[76] C.G. Joseph, Y.Y. Farm, Y.H. Taufiq-Yap, C.K. Pang, J.L.H. Nga, G. Li Puma, Ozonation treatment processes for the remediation of detergent wastewater: A comprehensive review, J. Environ. Chem. Eng. 9 (2021) 106099.

https://doi.org/10.1016/j.jece.2021.106099.

[77] M.A. Ahangarnokolaei, P. Attarian, B. Ayati, H. Ganjidoust, L. Rizzo, Life cycle assessment of sequential and simultaneous combination of electrocoagulation and ozonation for textile wastewater treatment, J. Environ. Chem. Eng. 9 (2021) 106251. https://doi.org/10.1016/j.jece.2021.106251.

[78] R. Mukherjee, S. De, Preparation, characterization and application of powdered activated carbon-cellulose acetate phthalate mixed matrix membrane for treatment of steel plant effluent, Polym. Adv. Technol. 27 (2016) 444–459. https://doi.org/https://doi.org/10.1002/pat.3690.

[79] R.R. Karri, J.N. Sahu, V. Chimmiri, Critical review of abatement of ammonia from wastewater, J. Mol. Liq. 261 (2018) 21–31. https://doi.org/10.1016/j.molliq.2018.03.120.

[80] N. Khatri, S. Tyagi, D. Rawtani, Recent strategies for the removal of iron from water: A review, J. Water Process Eng. 19 (2017) 291–304. https://doi.org/10.1016/j.jwpe.2017.08.015.

[81] K.G. Pavithra, S.K. P., V. Jaikumar, S.R. P., Removal of colorants from wastewater: A review on sources and treatment strategies, J. Ind. Eng. Chem. 75 (2019) 1–19. https://doi.org/10.1016/j.jiec.2019.02.011.

[82] S. Johnson, L. Deng, E. Gençer, Environmental and economic evaluation of decarbonization strategies for the Indian steel industry, Energy Convers. Manag. 293 (2023) 117511. https://doi.org/10.1016/j.enconman.2023.117511.

[83] V. Colla, I. Matino, T.A. Branca, B. Fornai, L. Romaniello, F. Rosito, Efficient use of water resources in the steel industry, Water (Switzerland). 9 (2017) 1–15. https://doi.org/10.3390/w9110874.

[84] A. Rawat, A. Srivastava, A. Bhatnagar, A.K. Gupta, Technological advancements for the treatment of steel industry wastewater: Effluent management and sustainable treatment strategies, J. Clean. Prod. 383 (2023) 135382. https://doi.org/10.1016/j.jclepro.2022.135382.

[85] M.A. Ahangarnokolaei, B. Ayati, H. Ganjidoust, Simultaneous and sequential combination of electrocoagulation and ozonation by Al and Fe electrodes for DirectBlue71 treatment in a new reactor: Synergistic effect and kinetics study, Chemosphere. 285 (2021) 131424. https://doi.org/10.1016/j.chemosphere.2021.131424.

[86] R. Garg, S.K. Singh, Treatment technologies for sustainable management of wastewater from iron and steel industry — a review, Environ. Sci. Pollut. Res. 29 (2022) 75203–75222. https://doi.org/10.1007/s11356-022-23051-3.

[87] S. Jamaly, A. Giwa, S.W. Hasan, Recent improvements in oily wastewater treatment: Progress, challenges, and future opportunities, J. Environ. Sci. (China). (2015) 15–30. https://doi.org/10.1016/j.jes.2015.04.011.

[88] Deepti, A. Sinha, P. Biswas, S. Sarkar, U. Bora, M.K. Purkait, Separation of chloride and sulphate ions from nanofiltration rejected wastewater of steel industry, J. Water Process Eng. 33 (2020) 101108. https://doi.org/10.1016/j.jwpe.2019.101108.

[89] Y. Kimura, N. Fujita, Y. Matsubara, K. Kobayashi, Y. Amanuma, O. Yoshioka, Y. Sodani, High-speed rolling by hybrid-lubrication system in tandem cold rolling mills, J. Mater. Process. Technol. 216 (2015) 357–368. https://doi.org/10.1016/j.jmatprotec.2014.10.002.

[90] Y. Zhang, F. Gan, M. Li, J. Li, S. Li, S. Wu, New Integrated Processes for Treating Cold-Rolling Mill Emulsion Wastewater, J. Iron Steel Res. Int. 17 (2010) 32–35.

https://doi.org/10.1016/S1006-706X(10)60110-0.

[91] C.R. Symons, Treatment of cold-mill wastewater by ultra-high-rate filtration, Water Pollut. Control Fed. 43 (1971) 2280–2286. https://doi.org/doi.org/10.1109/WPCF.1975.101453.

[92] J.A. Oberteuffer, I. Wechsler, P.G. Marston, M.J. Mcnallan, High gradient magnetic filtration of steel mill process and waste waters, IEEE Trans. Magn. 11 (1975) 1591–1593. https://doi.org/10.1109/TMAG.1975.1058803.

[93] J.T. Alexander, F.I. Hai, T.M. Al-aboud, Chemical coagulation-based processes for trace organic contaminant removal: Current state and future potential, J. Environ. Manage. 111 (2012) 195–207. https://doi.org/10.1016/j.jenvman.2012.07.023.

[94] T. Zheng, X. Lin, J. Xu, J. Ren, D. Sun, Y. Gu, J. Huang, Enhanced nitrogen removal of steel rolling wastewater by constructed wetland combined with sulfur autotrophic denitrification, Sustain. 13 (2021) 1–13. https://doi.org/10.3390/su13031559.

[95] L.G. De Araujo, E.S.A.P. Prado, F. De Souza Miranda, R. Vicente, A.S. Da Silva Sobrinho, G.P. Filho, J.T. Marumo, Physicochemical modifications of radioactive oil sludge by ozone treatment, J. Environ. Chem. Eng. 8 (2020) 104128. https://doi.org/10.1016/j.jece.2020.104128.

[96] M. Changmai, M. Pasawan, M.K. Purkait, Treatment of oily wastewater from drilling site using electrocoagulation followed by microfiltration, Sep. Purif. Technol. 210 (2019) 463–472. https://doi.org/10.1016/j.seppur.2018.08.007.

# Chapter 2

# Materials and experimental methods

# Chapter 2
# Materials and experimental methods

*This chapter depicts the use of different materials and treatment techniques for the degradation of toxic contaminants from Tata steel industry wastewaters. The sources of biological oxidation treated (BOT) and cold rolling mill (CRM) wastewaters were elaborately described to understand the unit operations of iron and steel industry. Also, the types of chemicals and electrode materials used during the analysis and experiments have been clearly depicted. In the experimental methods, the mechanism and reactor set-up of the ozonation and electrocoagulation techniques as well as the need for the integration of both the treatment approaches have been critically assessed and summarized. Further, the working principle of the analytical techniques (atomic absorption spectrometry and photometry) and their use in determining the pollutant concentration from the target wastewaters were covered in details. More importantly, to understand the morphological and functional properties of the wastewater generated sludge, different characterization techniques were also taken into consideration. In general, this chapter covers all the necessary materials and experimental methods including analytical and characterization techniques for improving the reusability of the highly contaminated wastewaters, which can assist the subsequent chapters in effectively carrying out the thesis work.*

## 2.1 Materials

### 2.1.1 Steel industry wastewater and its source

Steel industries generate various types of wastewater during their production stage. These wastewaters can vary depending upon the specific unit operations and processes utilized in any

particular steel plant. Some common types of wastewater generated in steel industries and their sources of origin include [1,2]:

1. Blast furnace wastewater: Generated during the cleaning of blast furnace gas to remove impurities like sulfur compounds.
2. Coke oven wastewater: Generated during the heating and carbonization of coal in coke ovens at high temperatures to produce coke.
3. Pickling wastewater: Generated during the pickling process to remove scales and oxides from steel surfaces.
4. Rolling mill wastewater: Generated during the rolling of steel (hot rolling and cold rolling) into various shapes and sizes.
5. Quenching wastewater: Generated during the rapid cooling of hot steel products in a quenching bath.
6. Annealing wastewater: Generated during the annealing process, which is used to soften and improve the properties of steel.
7. Plating and coating wastewater: Generated during the application of protective coatings or plating to finished steel products.

#### *2.1.1.1 Biological oxidation treated (BOT) wastewater*

The coal is heated in a coke oven convertor to generate coke, which is then transferred to a blast furnace for smelting, leading to the production of pig iron. During this process, highly impure and contaminated effluent is generated, which undergoes subsequent biological treatment. Anaerobic and aerobic digestion, bio-filters and activated sludge process are some of the commonly utilized

biological methods in the steel industry. The water that is obtained after the biological oxidation treatment is known as the biological oxidation treated (BOT) wastewater. Although, biological treatments can be effective in reducing the organic loads and some inorganic components in steel industry wastewater; however, the presence of coloured compounds and recalcitrant pollutants, may require additional treatment methods, to be effectively removed from the wastewater. Therefore, the BOT wastewater with high concentrations of iron, colour, and ammonia-N was collected from Tata Steel Industry, India to conduct the experiments for the present study.

#### *2.1.1.2 Cold rolling mill (CRM) wastewater*

The coarse iron ore is converted into molten steel via basic oxygen furnace, which then undergoes continuous casting before being subjected to the rolling processes (hot and cold rolling). Cold rolling is a process by which the metal is passed through rollers at temperatures below its recrystallization temperatures. It is used in the manufacturing of metal sheets and strips, in which the metal is compressed and squeezed, thereby increasing its yield strength and hardness. These rolling mills use large amounts of water for cooling purposes. As hot metal passes through the rolling process, it is cooled with water to achieve the desired material properties. This cooling water becomes contaminated with metal fines, scales, and other impurities from the rolling process. The cold rolling mills also requires substantial amounts of lubricants and emulsions to reduce friction and ensure a smooth operation. These lubricants can mix with water and become a byproduct of the process, resulting in oily wastewater. These contaminated water generated during the cold rolling process is known as the cold rolling mill (CRM) wastewater. For the present study, highly contaminated CRM wastewater was collected from Tata Steel Industry, India to perform the experiments.

### 2.1.2 Chemicals

98% sulphuric acid ($H_2SO_4$) and 0.1 M sodium hydroxide (NaOH) were procured from Merck (Darmstadt, Germany) for pH adjustment of the wastewater sample and for washing the electrodes to retain its efficiency. High performance liquid chromatography (HPLC) grade methanol ($CH_3OH$) and acetic acid ($CH_3COOH$) were also procured from Merck (Darmstadt, Germany) for determining the phenol intermediates during HPLC analysis. These analytical reagent (AR) grade chemicals were used for all the experiments and analysis without any further purification.

### 2.1.3 Electrode materials

Electrode materials used for the electrocoagulation experiments were made of aluminum sheets. These aluminum sheets were bought from the local market of IIT, Guwahati. The electrodes were washed and gently scrubbed with the help of diluted $H_2SO_4$ (0.01 M) and 120–grit (28 cm × 22 cm) sandpapers to maintain their efficiency after each experiment. The electrode arrangement used for all the experiments was bipolar electrode connection, as it was found to be optimum during preliminary investigations.

## 2.2 Experimental methods

### 2.2.1 Ozonation

Ozonation is a water treatment process that involves the use of ozone gas ($O_3$) to treat and disinfect water. Ozone is a powerful oxidising agent consisting of one-strong double bond and one-week single bond. It may either react as a nucleophile or an electrophile, considering the presence of its two inter-convertible resonance structures. It can break down and remove a wide range of contaminants in both water and wastewater. It can also effectively reduce the color and odour in wastewater, thereby making it suitable for various reuse applications [3]. It is often used as a tertiary or advanced treatment step in wastewater treatment plants to address specific water quality concerns.

The corona discharge method is typically employed for the generation of ozone. It electrically charges the oxygen molecules to a higher energy state, thereby causing the molecules to break apart. The resultant free oxygen atoms then react with other available oxygen molecules to produce ozone [4]. During the ozonation process, the decomposition of ozone in water accompanies a chain mechanism, combined with initiation, propagation, and termination. Depending upon the pH, the dominant oxidants viz. molecular ozone (under acidic conditions) and hydroxyl radical (under alkaline conditions) are primarily responsible for the oxidation of various organic and inorganic compounds in the wastewater. Both molecular ozone and hydroxyl radical have significantly higher oxidation potential of 2.1 V and 2.8 V, respectively, compared to other oxidants [5]. Fig. 2.1 shows the schematic layout of the corona discharge method.

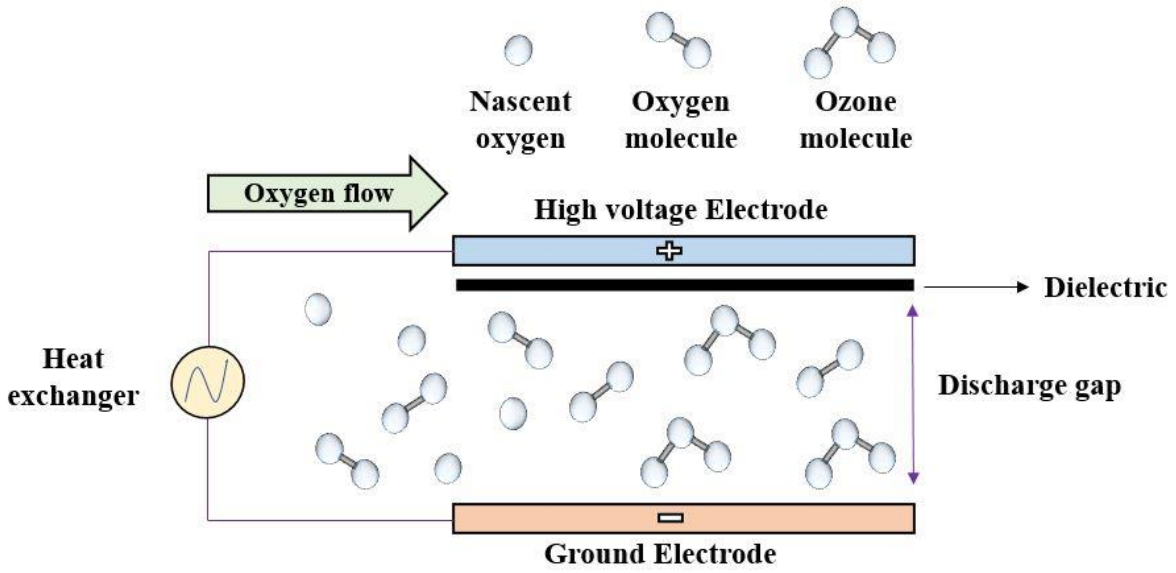


**Fig. 2.1:** Schematic diagram showing the corona discharge method for ozone formation

### *2.2.1.1 Mechanism of ozone oxidation*

There are two different mechanisms through which ozone reacts with the wastewater contaminants: (i) direct reaction mechanism via molecular ozone, and (ii) indirect reaction mechanism via $HO^{\bullet}$ free radicals [6]. Both these mechanisms result in the generation of various oxidation products and are governed by separate kinetic reactions.

#### *2.2.1.1.1 Direct reaction mechanism*

- Oxidation-reduction reaction

The high redox potential of ozone allows it to react with a broad range of contaminants via oxidation-reduction reactions viz. reaction of $O_3$ with $HO_2^-$ and $O_2^{\bullet -}$ (Eq. 1 and Eq. 2), in which the electron transfer mechanism plays a crucial role [7].

$$O_3 + HO_2^- \rightarrow O_3^{\bullet -} + HO_2^{\bullet} \quad (2.1)$$

$$O_3 + O_2^{\bullet -} \rightarrow O_3^{\bullet -} + O_2 \quad (2.2)$$

- Cycloaddition reaction

In general, the electrophilic species react with unsaturated molecules (π electrons) to produce a variety of compounds (Eq. 3). Cycloaddition reaction refers to the addition of two or more π electrons to produce a cyclic adduct, having a net reduction in bond multiplicity [8].

$$– C = C – + XY \rightarrow – XC – CY – \quad (2.3)$$

A three-step mechanism was proposed by Criegee (1975) for the cycloaddition reaction involving ozone and olefinic compounds: (i) production of ozonide compounds, (ii) formation of zwitterion molecules, and (iii) different chain reactions of zwitterion and formation of end products viz. ketones, aldehydes, and acids (in aqueous phase) [9].

- Electrophilic substitution reaction

Ozone has the potential to attack the nucleophilic site of organic compounds due to its electrophilic nature, thereby resulting in the replacement of one electron from the organic molecule. Moreover, $-NO_2^-$, -Cl, and $-OH^-$ groups of the aromatic compounds has a substantial effect on the ozone reactivity of the aromatic rings. Thus, different substitution reactions might take place depending upon the properties of the replacement groups. The triggering groups aids in the replacement of -H in the para- and ortho- positions, while the deactivating groups replaces -H at the meta- position [10].

- Nucleophilic reaction

The ozone molecule acquires a negative charge on one of the terminal oxygen atoms due to its resonance structure. Thus, it exhibits nucleophilic properties and may react with the electrophilic

compounds if they contain double, triple or carbonyl carbon-nitrogen linkages. However, only non-aqueous environments are suitable to validate such reactions [6].

*2.2.1.1.2 Indirect reaction mechanism*

The $OH^{\bullet}$ free radicals formed may participate in hydrolysis reactions (Eq. 4 and Eq. 5) [11].

$$O_3 + OH^- \rightarrow HO_4^- \quad (2.4)$$

$$HO_4^- \leftrightarrow HO_2^{\bullet} + O_2^{\bullet -} \quad (2.5)$$

The generated $O_2^{\bullet -}$ and $HO_2^{\bullet}$ radicals may disproportionate to $HO_2^-$ and $O_2$ in absence of ozone, which in turn protonate to $H_2O_2$. However, the presence of ozone can effectively produce $OH^{\bullet}$ radicals (Eqs. 6-8) [12].

$$O_2^{\bullet -} + O_3 \rightarrow O_2 + O_3^{\bullet -} \quad (2.6)$$

$$O_3^{\bullet -} \rightarrow O_2 + O^{\bullet -} \quad (2.7)$$

$$O^{\bullet -} + H_2O \rightarrow OH^{\bullet} + OH^- \quad (2.8)$$

The $OH^{\bullet}$ radicals have the potential to degrade both organic and inorganic contaminants due to its non-selective and strong oxidising properties. However, the production of $OH^{\bullet}$ radicals is severely restricted under acidic or neutral conditions because of the poor stability of ozone molecules. According to Eqs. 9-12, the formation of $OH^{\bullet}$ radicals is also constrained in the presence of scavengers such as $H_2PO_4^-$, $HPO_4^{2-}$, $CO_3^{2-}$ and $HCO_3^-$ [13].

$$OH^{\bullet} + HCO_3^- \rightarrow OH^- + HCO_3 . K_2 = 1.5 \times 10^7\ M^{-1}\ s^{-1} \quad (2.9)$$

$$OH^{\bullet} + CO_3^{2-} \rightarrow OH^- + CO_3^- . K_2 = 4.2 \times 10^8\ M^{-1}\ s^{-1} \quad (2.10)$$

$$OH^{\bullet} + H_2PO_4^- \rightarrow OH^- + H_2PO_4 . K_2 < 10^5\ M^{-1}\ s^{-1} \quad (2.11)$$

$$OH^{\bullet} + HPO_4^{2-} \rightarrow OH^- + H_2PO_4^- . K_2 < 107\ M^{-1}\ s^{-1} \quad (2.12)$$

#### *2.2.1.2 Ozonation set-up*

High purity oxygen was produced with the help of an oxygen concentrator (HG 03, Oz-Air, India), which works on the pressure swing adsorption technique. The oxygen produced was fed to the ozone generator (ISM 10 Oxy EC, Oz-Air, India), where it gets circulated through a rotameter. Typically, the rate of ozone generation varies from 0 to 3 mg $s^{-1}$. The corona discharge method converts the supplied oxygen into ozone inside the ozone generator. Ozone was then fed to the reactor via a sparger, which generates microbubbles. The excess ozone was transformed into oxygen with the help of an ozone destructor (Dest 50, Oz-Air, India). The volume of the glass reactor used for conducting the experiments was of 2 L capacity, and the amount of wastewater sample taken for each test was 1 L.

### 2.2.2 Electrocoagulation

Electrocoagulation is a wastewater treatment technique that has received significant attention for its effective degradation of organic and inorganic contaminants from different wastewater sources. It is a sustainable and low-cost treatment technique that breaks the stable emulsion and suspension in a solution using salt polymers or polyelectrolytes. The electrocoagulation process is based on the phenomenon of electrochemistry, in which oxidation or loss of electrons takes place at the anode, whereas reduction or gain of electrons occurs at the cathode surface [14]. The electrolysis effect is responsible for chemical and physiochemical phenomenon in electrocoagulation. This indicates that, electricity is required for in-situ coagulants (metal hydroxides) production, destabilization of particulate and pollutant suspension as well as floc formation due to aggregation of the destabilised phase. The metal hydroxides produced in-situ acts as an adsorbent, in which the

contaminants such as suspended solids, heavy metals, oils, and other compounds gets adsorbed on its surface [15]. Besides, the electrocoagulation process does not necessitate the use of added chemicals, as in-situ coagulants are formed during the treatment. Since no chemicals are added, electrocoagulation does not pose any risk of secondary contaminant generation unlike chemical coagulation. Also, the particle size of flocs produced during electrocoagulation are stable and large and can be easily separated via decantation or simple filtration. The flocs contain less water (acid resistant compound), thereby making it easier to remove via filtration [16].

#### *2.2.2.1 Mechanism of electrocoagulation*

The electrocoagulation process is widely used to destabilize the pollutants present in the form of dissolved or suspended particles in the electrolytic solution through the application of electric current. The electrocoagulation set up comprises of an electrolytic cell and a series of sacrificial metal electrodes (usually Fe or Al) coupled to a controlled DC power source. The cathodes and anodes used during the process can be made either from the same or different materials [17]. The pollutant removal mechanism via electrocoagulation process is shown in Fig. 2.2. There are seven important steps in electrocoagulation mechanism viz. (i) formation of metal cations due to the supply of electric current to the anodes; (ii) production of hydroxyl ions due to cathode hydrolysis; (iii) interaction of metal cations with hydroxyl ions to form metal hydroxides; (iv) oxidation of toxic contaminants into harmless intermediate products; (v) charge neutralization of contaminants due to its reaction with the metal hydroxides; (vi) adsorption of charge neutralized contaminants on metal hydroxides, followed by its removal via sweep coagulation and (vii) gas formation ($H_2$ gas) at the cathode lifts the generated flocs to the solution surface via sweep flotation [18,19].

Thus, the degradation of contaminants in EC process is primarily attributed to three phenomena viz. adsorption, coagulation, and floatation. In-situ coagulants are generated in the electrocoagulation chamber due to anodic dissolution, along with the formation of $H_2$ gas at the cathode and hydroxyl ions at the anode. These electrogenerated coagulants are accountable for the formation of floc encircled by metal hydroxides, which functions as an efficient adsorbent [20].

At anode:

$$M\,(s) \rightarrow M^{n+}\,(aq) + ne^{-} \qquad (2.13)$$

$$2H_2O \rightarrow O_2\,(g) + 4H^{+}\,(aq) + ne^{-} \qquad (2.14)$$

At cathode:

$$2H_2O + ne^{-} \rightarrow H_2\,(g) + 2OH^{-}\,(aq) \qquad (2.15)$$

Overall:

$$M^{n+}\,(aq) + nOH^{-} \rightarrow M(OH)_n\,(s) \qquad (2.16)$$

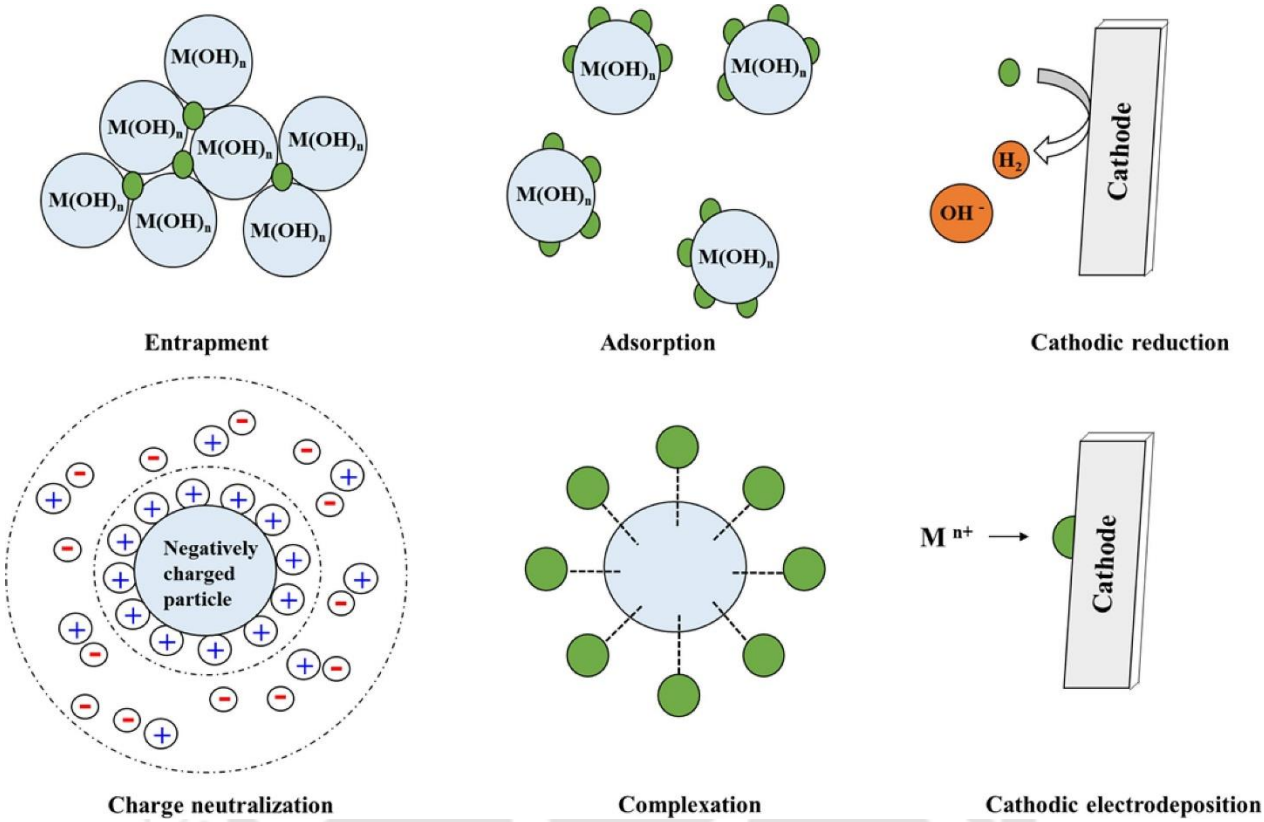


**Fig. 2.2:** Mechanism of pollutant degradation by electrocoagulation process

### *2.2.2.2 Electrocoagulation set-up*

An acrylic electrochemical reactor of 500 mL volume (semi-batch system) was used for conducting the experiments. Aluminum sheets having dimensions of 0.07 m × 0.035 m and an effective surface area of 0.00245 $m^2$ were used as electrode materials for both anode and cathode. The quantity of wastewater sample taken for each test was 300 mL. Four electrodes with bipolar arrangement were connected to a direct current (DC) power supply (Crown, DC regulated power supply, 0–30 V/10 A) with galvanostatic mode to provide constant current. On applying a potential to the end of the electrodes, induced polarization occurs, thus resulting in the bi-polarization of the

entire assembly. A distance of 0.005 m was maintained between the electrodes throughout the process, based on preliminary investigations. The laboratory scale electrocoagulation set-up is shown in Fig. 2.3.

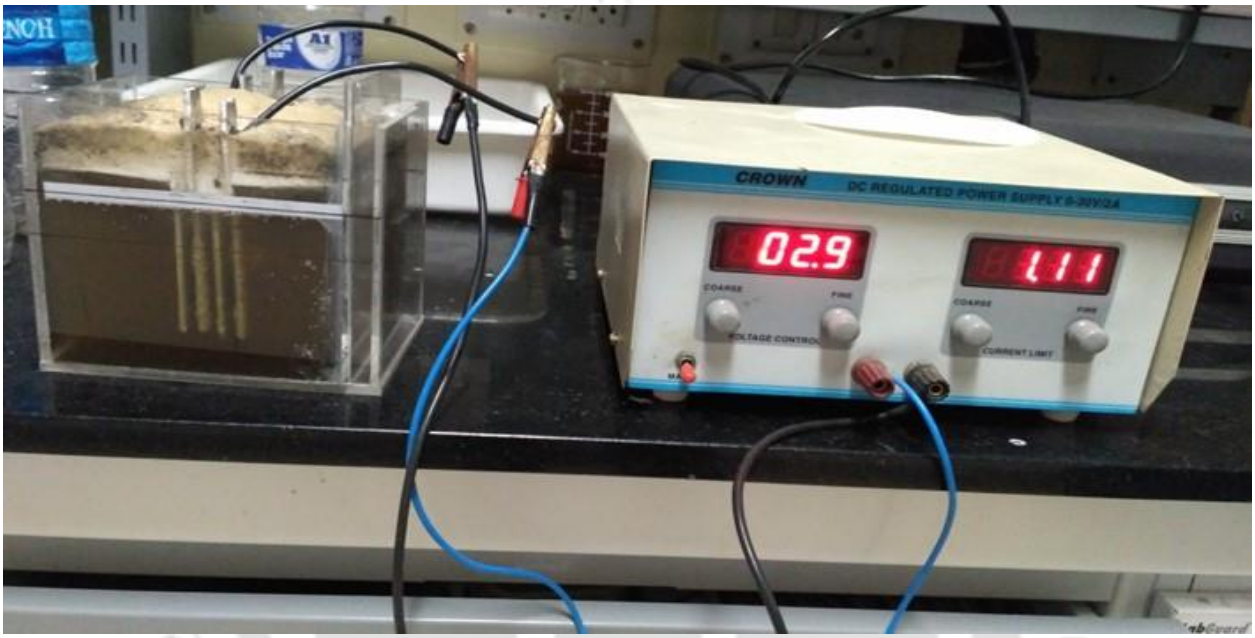


**Fig. 2.3:** Lab-scale set up of electrocoagulation process

### 2.2.3 Integrated ozone-electrocoagulation process

During the treatment of steel industry wastewater, the ozonation and electrocoagulation methods when performed individually failed to reduce the pollutants concentration below their assigned permissible limits. Therefore, both the methods were combined, and a hybrid approach viz. ozone assisted electrocoagulation was considered for carrying out further experiments.

The ozonation process has the potential to enhance the decolorization of the target wastewater. The decolorization process mainly involves dissociation of the chromophore groups (usually double bonds) present in the organic compounds and aromatic hydrocarbons (primarily responsible

for the brown color of the steel plant wastewater), which gets oxidized resulting in bond cleavage, thus losing the ability to absorb visible light. However, it was observed that after the completion of the ozonation process, if the treated sample is kept idle for a longer period (24 h or more) without any further treatment, it gradually starts to re-attain its color. This may be attributed to the re-association of bonds present in the chromophore groups, thereby regaining the potential to absorb visible light. Moreover, the ozonation process increases the dissolved oxygen concentration in the treated solution as all the ozone supplied to the solution did not take part in the reaction. In this context, the electric field generated during electrocoagulation can convert the dissolved ozone in the solution to reactive oxygen species, thereby enhancing the overall pollutant removal efficiency. Besides, preliminary investigations showed that when electrocoagulation was used as a post-treatment method to ozonation, the color reoccurrence phenomenon completely diminished. Further, the ozone assisted electrocoagulation process was found to be quite significant both in terms of performance and cost-effectiveness when compared to other hybrid treatment processes. As such, the hybrid approach of ozonation followed by electrocoagulation was adopted. The schematic diagram of ozonation assisted electrocoagulation process is shown in Fig. 2.4.

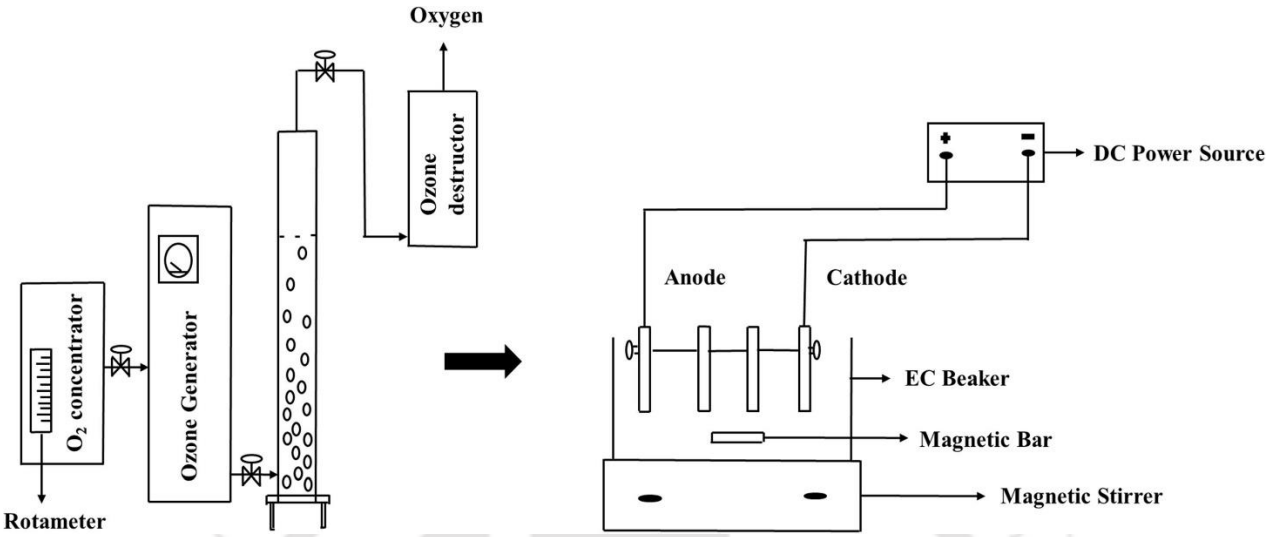


**Fig. 2.4:** Schematic diagram of ozone assisted electrocoagulation process

## 2.3 Analytical techniques

### 2.3.1 Atomic absorption spectrometry (AAS)

Atomic absorption spectrometry (AAS) is an analytical technique used to determine the concentration of specific chemical elements in a wide range of samples by measuring the absorption of characteristic wavelengths of light by atoms in their ground state. It is a widely used technique in analytical chemistry, particularly for trace metal analysis.

AAS relies on the fundamental principles of atomic spectroscopy. When a sample is atomized and introduced into a flame or furnace, the atoms absorb light at specific wavelengths that correspond to electronic transitions in the atom's structure. By measuring the decrease in the intensity of the emitted light at the characteristic absorption wavelength, the concentration (µg/L or mg/L) of the target element in the solution can be quantified. The variation in the pollutant concentration of all the wastewater samples during the standalone and hybrid processes were measured using an atomic

absorption spectrometer (Make: M/s Varian; Model: Spectra AA 220 FS). The instrument determines the metal ion concentration via flame mode and the burner used is either air-acetylene or nitrous oxide-acetylene. It is equipped with vapor generation accessory and electro thermal controller for carrying out flameless hydride vapor analysis.

### 2.3.2 Photometer

Photometers are analytical instruments used to measure the intensity of light, typically in the visible or ultraviolet spectrum, to quantify the concentration of substances, and monitor chemical reactions. Photometers often require calibration using standard solutions of known concentration to establish a linear relationship between absorbance and concentration.

Photometers rely on the Beer-Lambert law, that relates the concentration of a solute in a solution to the amount of light it absorbs. This law is used to relate the absorbance to the concentration of a solute in a solution, forming the basis for quantification. Transmittance measures the fraction of incident light that passes through the sample, while absorbance quantifies the amount of light absorbed by the sample. These values are inversely related; higher transmittance corresponds to lower absorbance and vice versa. The variation in the cyanide concentration of steel plant wastewater sample was determined using a photometer (Make: Palintest; Model: 7100) during both the standalone and hybrid processes. The instrument determines the light intensity as Transmittance (%T) or Absorbance (A) and subsequently compare these values to the calibration tables stored within the Photometer 7100. The stored calibration tables convert the transmittance or absorbance to concentration (μg/L or mg/L) for quantification.

## 2.4 Characterization techniques

### 2.4.1 Field emission scanning electron microscopy (FESEM)

Field Emission Scanning Electron Microscopy (FESEM), also known as Field Emission Electron Microscopy (FEEM), is an advanced and high-resolution imaging technique that uses electrons to visualize the surface morphology and ultrastructure of materials at a nanoscale level. The FESEM in contrary to conventional scanning electron microscopy (SEM), produces clearer, less electrostatically distorted images with high spatial resolution down to 1 nanometer. It employs a field emission electron source, consisting of a sharp, nanometer-sized tungsten or other refractory metal tip that emits electrons when subjected to a high electric field. The field-emission cathode in the electron gun of the instrument provides narrower probing beams at both low and high electron energy, resulting in an improved spatial resolution, minimized sample charging and less damage though the detectors viz. in-lens SE (in-lens secondary), SE (secondary electron) and BS (backscatter electron) detectors. The surface morphology of the electrode materials prior and after to the electrocoagulation treatment along with the electrocoagulated sludge was determined by a Field Emission Scanning Electron Microscope (Make: Zeiss; Model: Sigma 300).

### 2.4.2 Fourier transform infrared (FTIR) spectroscopy

Fourier Transform Infrared Spectroscopy (FTIR) is a widely used technique in analytical chemistry to study the interaction of matter with infrared (IR) radiation by identifying and analyzing the chemical composition of various substances. FTIR spectrometers consist of an IR light source, a sample holder, a beam splitter, a detector, and a computer with Fourier transform algorithms. The sample is exposed to broad spectrums of IR radiation, and the resulting transmitted

or reflected light is directed into an interferometer, which modulates the incoming IR beam using a movable mirror. The interferogram is generated by recording the intensity of the modulated beam as a function of the mirror's position. The interferogram is then subjected to a Fourier transform algorithm, which converts it into a spectrum of intensity versus frequency. This spectrum represents the unique IR absorption pattern of the sample. FTIR covers a broad spectral range, typically from 4000 $cm^{-1}$ to 400 $cm^{-1}$, which corresponds to the mid-infrared region. The wide range of chemical functional groups and molecular vibrations of the dried electrocoagulated sludge were determined by a FTIR spectrometer (Make: M/s Shimadzu; Model: IRAffinity-1).

### 2.4.3 Particle size analyzer

Particle size distribution analysis, also known as particle sizing, is an analytical technique used to measure and characterize the size and distribution of particles within a sample. A Particle size analyzer mainly uses three approaches to measure the particle size, viz. laser diffraction, dynamic light scattering, and image analysis. Amongst these, laser diffraction is one of the most common approach which involves passing a laser beam through a sample and measuring the angles and intensity of scattered light to determine the particle size of a sample. The system consists of detectors that capture the scattered light or diffracted light patterns produced by the particles in the sample and provides information in the form of a particle size distribution curve, which shows the frequency or percentage of particles at different size ranges. It can measure particle sizes over a wide range, from 0.6 nm to 7.0 micron with forward 15º & backscatter 165º. The particle size distribution of the electrocoagulated sludge at different treatment time was measured by a particle size analyzer (Make: M/s Beckman Coulter; Model: Delsa Nano C).

## References

[1] R. Garg, S.K. Singh, Treatment technologies for sustainable management of wastewater from iron and steel industry — a review, Environ. Sci. Pollut. Res. 29 (2022) 75203–75222. https://doi.org/10.1007/s11356-022-23051-3.

[2] W. Sun, X. Xu, Z. Lv, H. Mao, J. Wu, Environmental impact assessment of wastewater discharge with multi-pollutants from iron and steel industry, J. Environ. Manage. 245 (2019) 210–215. https://doi.org/10.1016/j.jenvman.2019.05.081.

[3] S. Lim, J.L. Shi, U. von Gunten, D.L. McCurry, Ozonation of organic compounds in water and wastewater: A critical review, Water Res. 213 (2022) 118053. https://doi.org/10.1016/j.watres.2022.118053.

[4] C. von Sonntag, U. von Gunten, Chemistry of Ozone in Water and Wastewater Treatment, 2012. https://iwaponline.com/ebooks/book-pdf/650791/wio9781780400839.pdf.

[5] C. V. Rekhate, J.K. Srivastava, Recent advances in ozone-based advanced oxidation processes for treatment of wastewater- A review, Chem. Eng. J. Adv. 3 (2020) 100031. https://doi.org/10.1016/j.ceja.2020.100031.

[6] Z. Liu, K. Demeestere, S. Van Hulle, Comparison and performance assessment of ozone-based AOPs in view of trace organic contaminants abatement in water and wastewater: A review, J. Environ. Chem. Eng. 9 (2021) 105599. https://doi.org/10.1016/j.jece.2021.105599.

[7] J. Hoigné, Chemistry of Aqueous Ozone and Transformation of Pollutants by Ozonation and Advanced Oxidation Processes, in: J. Hrubec (Ed.), Springer Berlin Heidelberg, Berlin, Heidelberg, 1998: pp. 83–141. https://doi.org/10.1007/978-3-540-68089-5_5.

[8] F.J. Beltrán, F.J. Rivas, R. Montero-de-Espinosa, Ozone-enhanced oxidation of oxalic acid in water with cobalt catalysts. 1. Homogeneous catalytic ozonation, Ind. Eng. Chem. Res. 42 (2003) 3210–3217. https://doi.org/10.1021/ie0209982.

[9] R. Criegee, Mechanism of Ozonolysis, Angew. Chemie Int. Ed. 14 (1975) 745–752. https://doi.org/https://doi.org/10.1002/anie.197507451.

[10] J. Wang, H. Chen, Catalytic ozonation for water and wastewater treatment: Recent advances and perspective, Sci. Total Environ. 704 (2020) 135249. https://doi.org/10.1016/j.scitotenv.2019.135249.

[11] G. Merényi, J. Lind, S. Naumov, C. von Sonntag, The Reaction of Ozone with the Hydroxide Ion: Mechanistic Considerations Based on Thermokinetic and Quantum Chemical Calculations and the Role of $HO_4^-$ in Superoxide Dismutation, Chem. – A Eur. J. 16 (2010) 1372–1377. https://doi.org/https://doi.org/10.1002/chem.200802539.

[12] B.H.J. Bielski, D.E. Cabelli, R.L. Arudi, A.B. Ross, Reactivity of $HO_2/O_2^-$ Radicals in Aqueous Solution, J. Phys. Chem. Ref. Data. 14 (1985) 1041–1100. https://doi.org/10.1063/1.555739.

[13] B. Kasprzyk-Hordern, M. Ziółek, J. Nawrocki, Catalytic ozonation and methods of enhancing molecular ozone reactions in water treatment, Appl. Catal. B Environ. 46 (2003) 639–669. https://doi.org/10.1016/S0926-3373(03)00326-6.

[14] A. Tahreen, M.S. Jami, F. Ali, Role of electrocoagulation in wastewater treatment: A developmental review, J. Water Process Eng. 37 (2020) 101440. https://doi.org/10.1016/j.jwpe.2020.101440.

[15] S. Garcia-Segura, M.M.S.G. Eiband, J.V. de Melo, C.A. Martínez-Huitle, Electrocoagulation and advanced electrocoagulation processes: A general review about the fundamentals, emerging applications and its association with other technologies, J. Electroanal. Chem. 801 (2017) 267–299. https://doi.org/10.1016/j.jelechem.2017.07.047.

[16] I.D. Tegladza, Q. Xu, K. Xu, G. Lv, J. Lu, Electrocoagulation processes: A general review about role of electro-generated flocs in pollutant removal, Process Saf. Environ. Prot. 146 (2021) 169–189. https://doi.org/10.1016/j.psep.2020.08.048.

[17] D. Syam Babu, T.S. Anantha Singh, P. V. Nidheesh, M. Suresh Kumar, Industrial wastewater treatment by electrocoagulation process, Sep. Sci. Technol. 55 (2020) 3195–3227. https://doi.org/10.1080/01496395.2019.1671866.

[18] G. Chen, Electrochemical technologies in wastewater treatment, Sep. Purif. Technol. 38 (2004) 11–41. https://doi.org/10.1016/j.seppur.2003.10.006.

[19] C. An, G. Huang, Y. Yao, S. Zhao, Emerging usage of electrocoagulation technology for oil removal from wastewater: A review, Sci. Total Environ. 579 (2017) 537–556. https://doi.org/10.1016/j.scitotenv.2016.11.062.

[20] P. V. Nidheesh, T.S.A. Singh, Arsenic removal by electrocoagulation process: Recent trends and removal mechanism, Chemosphere. 181 (2017) 418–432. https://doi.org/10.1016/j.chemosphere.2017.04.082.

# Chapter 3

# Hybrid ozone assisted electrocoagulation technique for the treatment of cyanide and phenol rich steel plant wastewater

# Chapter 3

# Hybrid ozone assisted electrocoagulation technique for the treatment of cyanide and phenol rich steel plant wastewater

*This work focuses on the treatment of cyanide and phenol rich steel plant wastewater from Tata Steel Industry, India by hybrid ozonation assisted electrocoagulation method. The steel plant wastewater consisted of high cyanide and phenol concentrations along with chlorides, COD and BOD. The removal efficiency of the pollutants was found to be inadequate when the electrocoagulation or ozonation process was performed separately. However, a combination of ozonation and electrocoagulation showed highly satisfactory results. The effects of operating variables viz. ozone generation rate, current density, and analysis time on pollutant removal were primarily analyzed for the hybrid process. The experimental operating condition was optimized and was seen that ozone generation rate of 1.33 mg $s^{-1}$, ozonation time of 40 min, a current density of 100 A $m^{-2}$, and electrolysis time of 30 min were sufficient for reducing the pollutant concentration below its permissible limits. The removal efficiencies of the combined process at optimum conditions were 99.8%, 99.5%, 94.7%, 95%, and 46.5% for cyanide, phenol, COD, BOD, and chloride, respectively. A kinetic study was performed for the degradation of the pollutants during ozonation. The pseudo first-order kinetic model was found to be best suited for the analysis with the highest $R^2$ value of 0.99 for cyanide, COD, BOD, and chloride, respectively. Further, the mass transfer study illustrates an increase in the dissolved ozone concentration in the solution for an increase in the volumetric mass transfer coefficient, $K_l a$. Finally, the cost estimation study of the hybrid process was carried out and compared with that of the other reported literature.*

# Chapter 3

## 3.1 Experimental

### 3.1.1 Measurement and analysis

Cyanide and phenol rich steel plant wastewater was collected from Tata Steel industry, India to carry out the experiments for the present study. The initial characteristics of the wastewater sample were measured. The concentration of the pollutants targeted in this work were: cyanide: 150 mg $L^{-1}$, phenol: 150 mg $L^{-1}$, COD: 2050 mg $L^{-1}$, chloride: 1820 mg $L^{-1}$, and pH: 7.72. An acrylic electrocoagulation reactor of 500 mL volume and an ozonation reactor of 2 L volume were used for conducting the experiments. All the experiments were performed at a constant temperature of 20°C. The sample analysis was done at an interval of 5 min, and the residual concentration of all the pollutants was measured using an atomic absorption spectrometry (Make: M/s Varian; Model: Spectra AA 220 FS) and a photometer (Make: Palintest; Model: 7100). The change in solution pH was determined using a benchtop pH Meter (Make: Eutech; Model: 700). The details of all the measurement and analysis have been elaborately reported in section 2.3 of chapter 2.

### 3.1.2 Operational parameters

Both the ozonation and electrocoagulation experiments were carried out at different operational parameters. In the ozonation process, the effect of ozone generation rates and reaction time on the pollutant removal efficiency was determined. Three different ozone generation rates viz. 1.00 mg $s^{-1}$, 1.11 mg $s^{-1}$ and 1.33 mg $s^{-1}$ were selected for carrying out the experiments and the reaction time was varied between 10-40 min. In the electrocoagulation process, the effect of current density and electrolysis time on the pollutant removal efficiency was measured. Three different current densities viz. 50 A $m^{-2}$, 100 A $m^{-2}$, and 150 A $m^{-2}$ were chosen for conducting the experiments and

the electrolysis time was varied between 10-30 min. The spacing between the electrodes was constantly maintained at 0.005 m during the process. During the application of three different ozone generation rates viz. 1.00, 1.11, and 1.33 mg $s^{-1}$, it was found that the experiments carried out beyond 1.33 mg $s^{-1}$ significantly increased the energy consumption of the entire hybrid process. Moreover, the permissible limits of all the target parameters were effectively reached at an ozone generation rate of 1.33 mg $s^{-1}$. Further, a marginal increase in the pollutant removal rate was observed on prolongation of the oxidation time beyond 40 min. Therefore, the optimum operating conditions were taken as 1.33 mg $s^{-1}$ and 40 min for the ozonation process. During the application of three different current densities viz. 50, 100, and 150 A $m^{-2}$, it was observed that the experiments conducted beyond 100 A $m^{-2}$ yielded similar results in terms of pollutant removal efficiency. Further, prolongation of the electrolysis time beyond 30 min significantly increased the operating cost of the entire hybrid process. Moreover, an electrolysis time of 30 min was sufficient to reduce the pollutant concentrations below their assigned permissible limits. Therefore, the optimum operating conditions were taken as 100 A $m^{-2}$ and 30 min for the electrocoagulation process.

## 3.2 Results and discussion

### 3.2.1 Variation in solution pH during hybrid ozone assisted electrocoagulation process

The change in solution pH with time was observed at 20°C (operating temperature) during the hybrid process. The pH rapidly decreases from 7.72 to 3.20 during the initial stage of the ozonation process, i.e., within 5–10 min of the experiment, followed by a further decrease in pH in the subsequent ozonation time until a steady-state condition is achieved at pH 3.0. This was since molecular ozone oxidation resulted in the formation of acidic by-products (such as organic anions

and inorganic acids) [1]. Since ozone reacts with both the degradation products produced during oxidation via hydroxyl radicals (usually carboxylic acids) as well as with the hydroxyl anions, the solution pH decreases during the experiment. Due to the higher consumption of ozone in the primary phase of the process, the reduction in the solution pH is very eminent (particularly for alkaline solutions) [2]. Besides, this study mainly concentrated on the influence of the operating parameters viz. ozone generation rate, current density, and analysis time on the removal of pollutants at pH 3.0. Thus, the operational parameters were controlled in such a way that the impact of different ozone generation rates (1.00-1.33 mg $s^{-1}$) and current densities (50-100 A $m^{-2}$) on the experimental results can be investigated. However, the effect of varying pH on pollutant removal is not the primary focus of this study. On the contrary, the solution pH during electrocoagulation increases from 3.0 to 8.30, where it reaches an equilibrium condition due to the buffering capacity of $Al(OH)_3/Al(OH)_4^-$. The evolution of $H_2$ at the cathode vicinity and the formation of ions at the cathode surface can be attributed to the increase in the solution pH [3]. Further, TDS and conductivity were found to decrease from an initial concentration of 2670-2050 mg $L^{-1}$ and 3.26-2.35 mS $cm^{-1}$, respectively, for an optimum operating condition of 1.33 mg $s^{-1}$ and 100 A $m^{-2}$.

### 3.2.2 Removal of cyanide by hybrid ozone assisted electrocoagulation process

Figure 3.1 shows the cyanide removal efficiency with ozone generation rate and ozonation time. It was observed that with an increase in ozone generation rate from 1.00 to 1.33 mg $s^{-1}$, the cyanide removal percentage also increases from 76.7% to 94.0%, respectively. Moreover, for an optimum ozone generation rate and operating time of 1.33 mg $s^{-1}$ and 40 min, respectively, cyanide decreases from an initial concentration of 150 mg $L^{-1}$ to a final concentration of 9 mg $L^{-1}$. Free

cyanide ion undergoes a rapid degradation when it comes in contact with ozone, as seen from Figure 3.1. In case of cyanide, oxidation of ozone follows a two-step reaction mechanism [4].

$$CN^- + O_3 \rightarrow CNO^- + O_2 \quad (3.1)$$

$$2CNO^- + 3O_3 + H_2O \rightarrow 2HCO_3^- + N_2 + O_2 \quad (3.2)$$

It is well established that the first reaction occurs rapidly, while the oxidation of cyanate by ozone is the slow and rate-determining step. The ozone is one of the most powerful oxidizing agents, oxidizes the cyanide ions to cyanate, and releases oxygen gas in the process. Continued ozonation converts cyanate ions to carbonate ions and nitrogen gas. The rate of ozonation of the cyanate ion is approximately one-fifth that of cyanide ozonation [5].

$$CNO^- + 2H_2O \rightarrow NH_3 + CO_2 + OH^- \quad (3.3)$$

At low pH, the cyanate ion rapidly undergoes acid hydrolysis to form carbon dioxide and ammonia. During the ozonation process, the pH of the effluent remained in the acidic range and attained a minimum value of 3.0, which favored the formation of gaseous products. The evolution of nitrogen and carbon dioxide gases during the reaction makes the liquid phase to swell exponentially [6]. Nearly three-fourths of the initial cyanide content is oxidized (at an optimum ozone generation rate of 1.33 mg $s^{-1}$) within the first 15 min of treatment time. Besides, an increase in the ozone generation rate increases the percentage removal of cyanide. However, there is a decline in the rate of cyanide removal with further progress of the experiment, and eventually, after 40 min of reaction time, no significant reduction in cyanide concentration was observed. This trend was independent of the ozone generation rates. It was found that ozonation alone was insufficient to reduce the contamination below its permissible limit of 0.2 mg $L^{-1}$, for safe surface discharge. In

addition, ammonia produced during the hydrolysis reaction of cyanate at acidic pH further reacts with ozone, leading to ammonia oxidation and the formation of nitrates and nitrogen gas as the final product. As a result of this, ammonia decreases from a concentration of 130 mg $L^{-1}$ to 48.5 mg $L^{-1}$, which is well below its permissible limit of 50 mg $L^{-1}$.

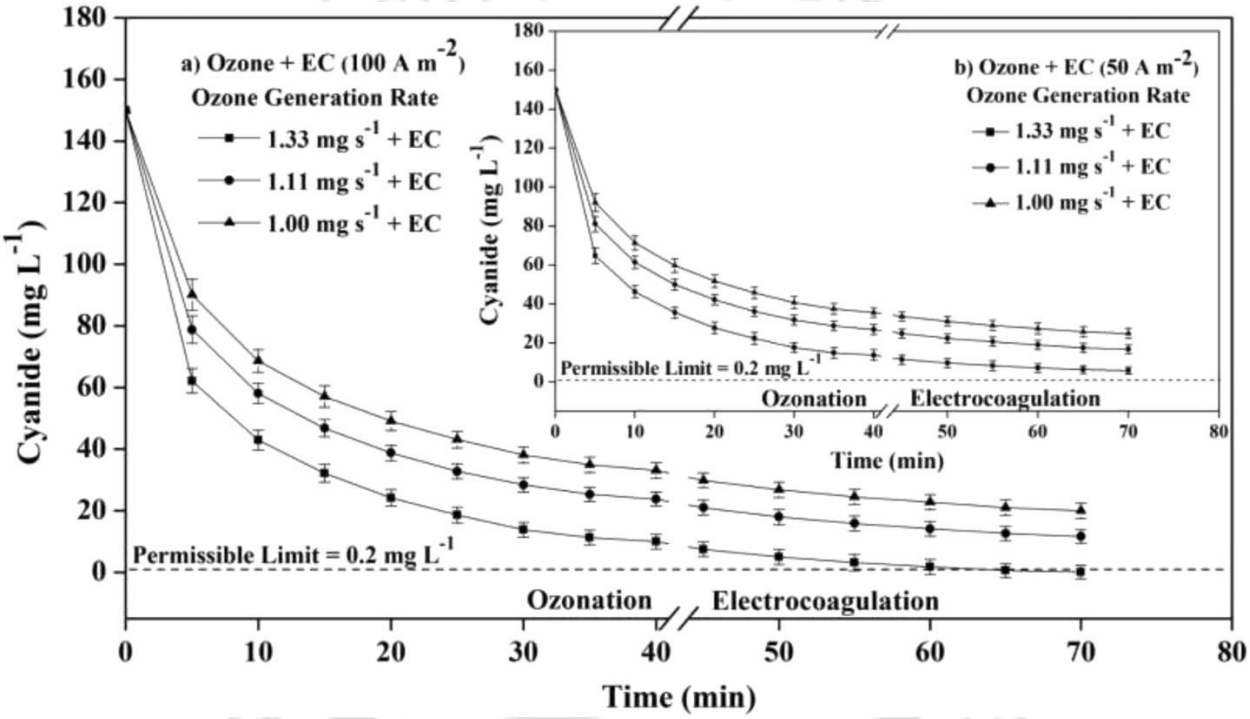


**Fig. 3.1:** Effect of ozone generation rates on cyanide removal with treatment time. Outset: 100 A $m^{-2}$ current density, Inset: 50 A $m^{-2}$ current density

The electrocoagulation process with Al-Al electrodes removed the remaining cyanide via surface adsorption and or sweep coagulation mechanism. As a result, during the electrocoagulation process, the cyanide concentration further decreases from 9 mg $L^{-1}$ (obtained at 1.33 mg $s^{-1}$) to 0.1 mg $L^{-1}$ for an optimum current density of 100 A $m^{-2}$ and electrolysis time of 30 min, as shown

in Figure 3.1. The surface of aluminum hydroxyl flocs, which is formed during electrocoagulation, traps and removes soluble and colloidal contaminants from aqueous environments through a deposition. Anodic oxidation of aluminum electrodes releases trivalent aluminum ions ($Al^{3+}$) and produces a plethora of various monomeric and polymeric species like $Al(OH)_2^+$, $Al(OH)^{2+}$, $Al(OH)^{4-}$, $Al_2(OH)_2^{4+}$, $Al_6(OH)_{15}^{3+}$, $Al_7(OH)_{17}^{4+}$, $Al_8(OH)_{20}^{4+}$, $Al_{13}(OH)_{34}^{5+}$ [7,8]. The produced hydroxyl species and hydroxyl ions are proficient in removing ionic contaminants. Thus, the electrocoagulation process further reduced the remaining concentration of cyanide ions after the ozonation process. The cyanide concentration declines linearly with electrocoagulation time, and this trend remains invariant of the change in current density [9]. However, a high current density yields a high removal efficiency. The maximum removal efficiency attained during the electrocoagulation process was 98.8% for a current density and electrolysis time of 100 A $m^{-2}$ and 30 min, respectively.

### 3.2.3 Removal of phenol by hybrid ozone assisted electrocoagulation process

The $HO^{\bullet}$ radicals are formed during the ozonation of phenol. The reason may be due to the transfer of an electron from phenolate/phenol to ozone ($E^7$ phenol = 0.86 V; $E^7$ ozone = 1.03 V) [10].

$$PhO^-/PhOH + O_3 \rightarrow PhO^{\bullet}/PhOH^{\bullet+} + O_3^{\bullet-} \quad (3.4)$$

In Eq. (3.4), the reaction of ozone with phenol occurs through direct transfer of an electron, which leads to the formation of an ozonide radical and a phenoxyl radical. Ozone oxidizes inorganic compounds to their higher oxidation states while oxidizing organic compounds into carbon dioxide and water. The higher the amount of dissolved ozone present in the effluent, the higher will be the rate of phenol oxidation. Degradation of phenol occurs through its oxidation which results in the

formation of catechol as well as hydroquinone at para-position, which then rapidly transforms to p-benzoquinone and o-benzoquinone [11]. Further reports suggest that the formation of benzoquinone is due to hydroquinone oxidation which is attributed either due to the direct ozone attack at the para-position and successive $H_2O_2$ loss or via the attack of $HO_2^{\bullet}$ at the para-position of the phenoxyl radical, with successive water loss. During the ozonation process, the system pH reduces (pH 3 was attained in our study), which facilitates oxidation of benzoquinone to organic acids as well as a reduction in benzoquinone yield i.e., the aromatic rings are opened, resulting in the decomposition of p-benzoquinone and o-benzoquinone to organic acids. Oxidation of these organic acids finally produces carbon dioxide and water as the end products [12]. The formation and subsequent oxidation of various phenolic by-products into $CO_2$ and $H_2O$ signify the reduction in phenol concentration. Thus, it can be concluded that the phenol concentration decreases drastically with the progress of the ozonation experiment. As a result, for an optimum ozone generation rate and operating time of 1.33 mg $s^{-1}$ and 40 min, respectively, phenol decreases from an initial concentration of 150 mg $L^{-1}$ to a final concentration of 11 mg $L^{-1}$. Figure 3.2 shows the phenol removal efficiency with respect to ozone generation rate and reaction time. It was observed that, with an increase in ozone generation rate from 1.00 mg $s^{-1}$ to 1.33 mg $s^{-1}$, the phenol degradation rate also increases from 79.5% to 92.6%.

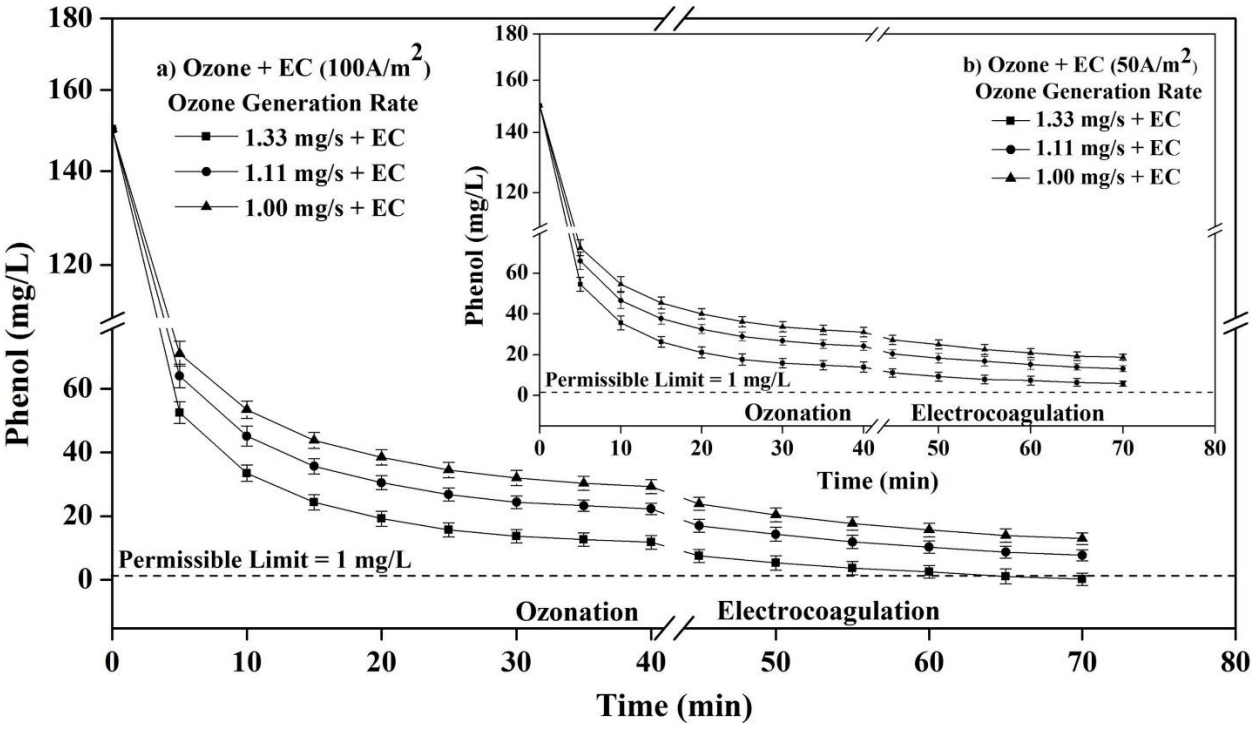


**Fig. 3.2:** Effect of ozone generation rates on phenol removal with treatment time. Outset: 100 A $m^{-2}$ current density, Inset: 50 A $m^{-2}$ current density

Moreover, during the electrocoagulation process, phenol concentration further decreases from 11 mg $L^{-1}$ (obtained at 1.33 mg $s^{-1}$) to 0.5 mg $L^{-1}$ for an optimum current density of 100 A $m^{-2}$ and electrolysis time of 30 min, as seen in Figure 3.2. Using the Al electrodes, it is seen that the phenol removal increases with electrolysis time and current density. The chemical interaction of phenol and organic acids with trivalent cations, results in the formation of insoluble species by integrated complexation, precipitation, and/or coagulation processes. Besides, phenol, as well as similar organic compounds, inclines to shift towards the aqueous solution. They are thought to get adsorbed onto the surface of the hydrolyzed products formed during electrocoagulation, which can then be simultaneously trapped within the forming hydroxides (coagulation process), and then the

resulting particulate compounds can interact physically to form flocs (flocculation process) [13]. Also, adequate current density leads to a reduction of phenol (like other organic compounds) to smaller molecules at the cathode. $Al(OH)_3$, as well as other monomeric and polymeric hydroxides formed during the process, adsorbs these small organic molecules and the suspended solids, followed by subsequent removal as a result of sedimentation or $H_2$ flotation. Thus, it can be ascertained that an increase in current density leads to an increase in bubble density and a decrease in its size, thereby intensifying the removal efficiency by creating a greater upward flux as well as the sludge flotation [14]. This corresponds to the fact that the amount of aluminum dissolution increases with higher current density, resulting in a greater amount of precipitation, thus assisting in the phenol removal. The maximum removal efficiency attained during the electrocoagulation process was 95.4% for the current density and electrolysis time of 100 A $m^{-2}$ and 30 min, respectively.

### 3.2.4 Removal of COD by hybrid ozone assisted electrocoagulation process

During ozonation, the reduction in COD and BOD can be attributed to the fact that ozone oxidizes the pollutants present in the sample, leading to a decrease in COD and BOD concentration. The pathways for ozonation involves either direct oxidation by ozone or radical oxidation by OH. radical. Direct oxidation is more selective and predominates under acidic conditions, while radical oxidation is less selective and predominates under alkaline conditions [15]. At high pH, there is a possibility of substantial ozone wastage via scavenging reactions with both organic and inorganic substances present in the solution, due to the predomination of indirect hydroxyl–radical-mediated reactions. However, at low pH, ozone wastage is less through the scavenging reactions in solution

as compared to hydroxyl radicals, due to the predomination of molecular ozone ($O_3$) [16]. As such, the COD and BOD removal efficiency increase under acidic conditions. Figure 3.3 shows the COD removal efficiency with respect to ozone generation rate and reaction time. It was observed that at pH of 3.2-3.0, the percentage of COD reduction increases from 58.5% to 72.2% when the ozone generation rate increases from 1.00 to 1.33 mg $s^{-1}$ at the end of 40 min of ozonation time. However, no noticeable increase in COD removal was found beyond 40 min. Therefore, an ozone generation rate of 1.33 mg $s^{-1}$ and an operating time of 40 min were considered to be the optimum operating conditions. The initial concentration of COD was found to decrease from 2050 mg $L^{-1}$ to a final concentration of 570 mg $L^{-1}$.

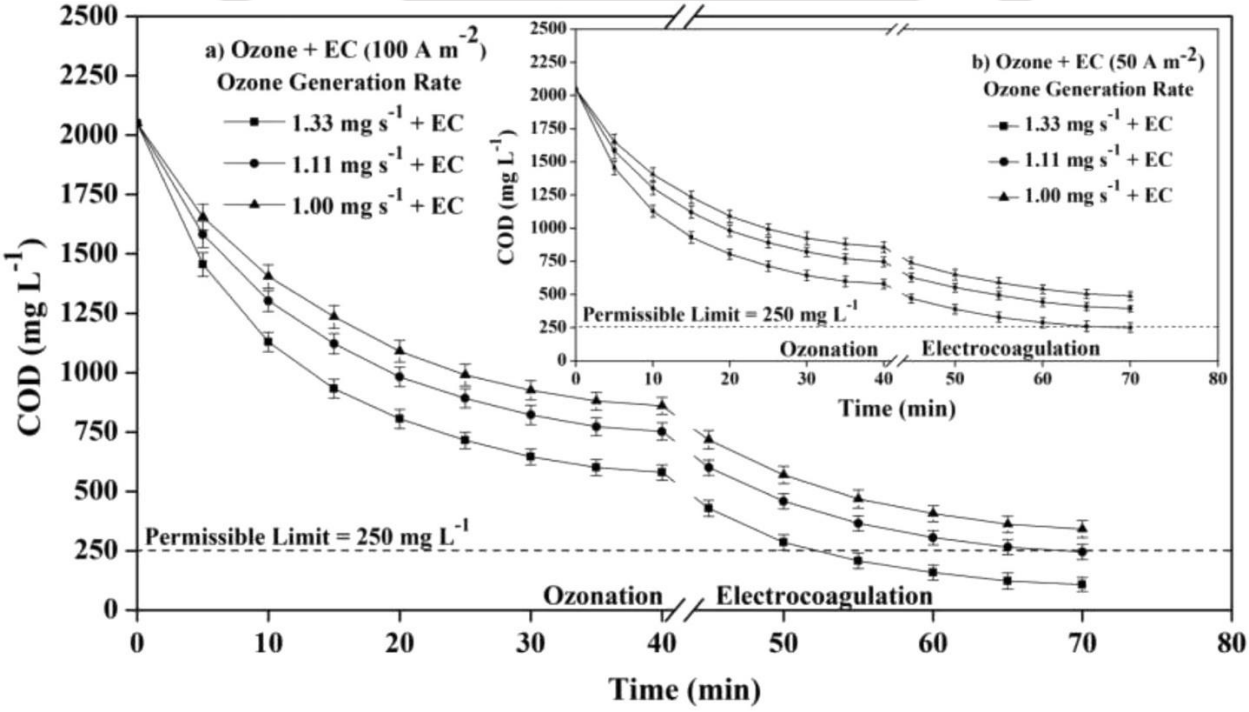


**Fig. 3.3:** Effect of ozone generation rates on COD removal with treatment time. Outset: 100 A $m^{-2}$ current density, Inset: 50 A $m^{-2}$ current density

Moreover, during the electrocoagulation process, the COD concentration further decreases from 570 (obtained at 1.33 mg $s^{-1}$) to 110 mg $L^{-1}$ for an optimum current density and electrolysis time of 100 A $m^{-2}$ and 30 min, respectively as shown in Figure 3.3. The production of $OH^-$ ions at the cathode having outstanding absorptive behavior played a significant role in reducing COD content from the solution. Free cation i.e. $Al^{3+}$ is the predominant form under acidic condition. Charge neutralization of colloids in the solution and adsorption of pollutants to the insoluble metal species due to electrostatic forces reduces the COD content during electrocoagulation. An increase in the cationic metal ion concentration with electrolysis time helps in removing the pollutants [17]. It can be concluded that the increasing rate of reaction time and current density is directly proportional to the pollutant removal. The maximum removal efficiency attained during the electrocoagulation process was 80.8% for a current density and electrolysis time of 100 A $m^{-2}$ and 30 min, respectively.

Furthermore, the BOD reduction efficiency also showed a similar decreasing trend, as shown in Figure 3.4. For the optimum operating conditions viz. ozone generation rate of 1.33 mg $s^{-1}$ and current density of 100 A $m^{-2}$ of the hybrid process (ozonation assisted electrocoagulation), it was found that BOD decreases from an initial concentration of 490 mg $L^{-1}$ to a final concentration of 24 mg $L^{-1}$. Like COD, the decreasing trend of BOD was also observed to reduce at a current density of 50 A $m^{-2}$ (inset of Figure 3.4). The decreasing trend of BOD could be attributed to the phenomenon of oxidation (ozonation) followed by flocculation (electrocoagulation) during the ozone assisted electrocoagulation process [18,19].

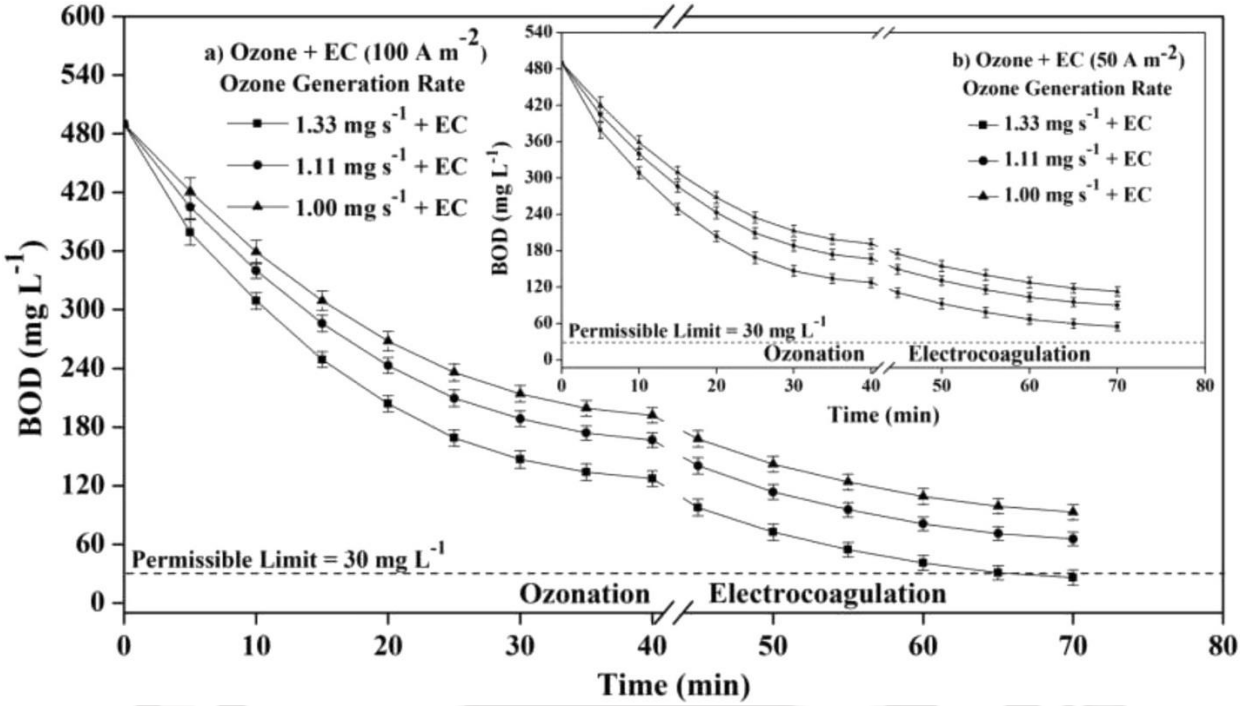


**Fig. 3.4:** Effect of ozone generation rates on BOD removal with treatment time. Outset: 100 A $m^{-2}$ current density, Inset: 50 A $m^{-2}$ current density

### 3.2.5 Removal of chloride by hybrid ozone assisted electrocoagulation process

Ozone participates in the reaction with chloride ions to produce $Cl_2$ and $H_2O$ as the end product. In highly acidic media, the rate of the reaction $O_3 + Cl^-$ considerably increases. Hence, it can be assumed that $H^+$ ions are the catalyst of the reaction i.e. $O_3$ reaction with $Cl^-$(aq) proceeds rapidly due to catalysis by $H^+$ ions [20]. The final product of the reaction between $O_3$ and $Cl^-$(aq) is the formation and subsequent release of molecular chlorine ($Cl_2$) into the gaseous phase, leading to a decrease in the chloride content [21]. Thus, it was found that the chloride concentration decreases from 1820 mg $L^{-1}$ to 1260 mg $L^{-1}$ for the optimum operating condition of 1.33 mg $s^{-1}$ and 40 min, respectively. Figure 3.5 shows the chloride removal efficiency with respect to the ozone generation

rates and reaction time. It was observed that the chloride removal efficiency increases from 22.0% to 30.5% with an increase in the ozone generation rate from 1.00-1.33 mg $s^{-1}$, respectively.

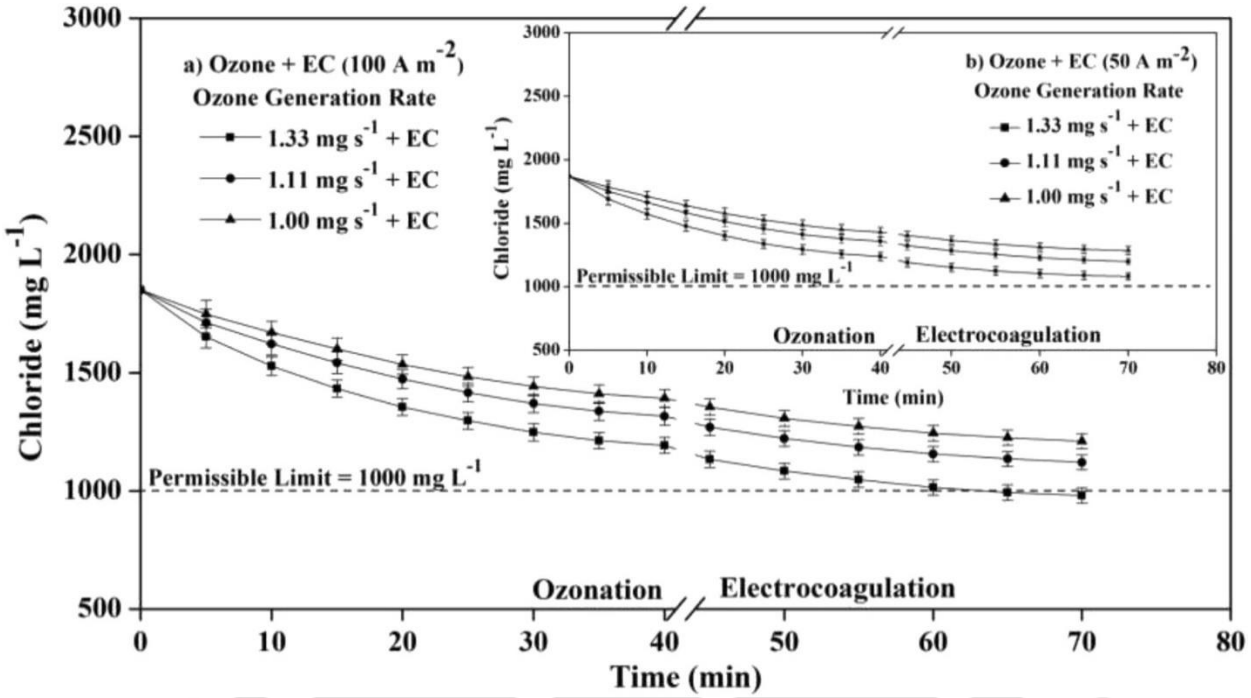


**Fig. 3.5:** Effect of ozone generation rates on chloride removal with treatment time. Outset: 100 A $m^{-2}$ current density, Inset: 50 A $m^{-2}$ current density

Besides, during the electrocoagulation process, the chloride concentration further decreases from 1260 (obtained at 1.33 mg $s^{-1}$) to 975 mg $L^{-1}$ for an optimum current density and electrolysis time of 100 A $m^{-2}$ and 30 min, respectively, as shown in Figure 3.5. It was found that even with an increase in electrolysis time (30 min) and current density (100 A $m^{-2}$), the highest removal rate obtained was just 22.5%, indicating that modifications in the electrocoagulation technique may be required to increase the removal percentage of chloride. The reduction in pollutant concentrations viz. cyanide, phenol, COD, BOD, and chloride via the ozone assisted electrocoagulation process

is shown in Table 3.1. Further, Table 3.2 provides a comparative analysis of the ozone assisted electrocoagulation process with other reported hybrid treatment techniques for industrial wastewater. The present study resulted in a much effective removal of the target pollutants compared to other hybrid techniques reported in the literature.

**Table 3.1:** Removal rate of pollutants (cyanide, phenol, COD, BOD, and chloride) during ozone assisted electrocoagulation process

| Parameters | Feed ($mg\ L^{-1}$) | Final concentration (mg/L) | | | | | | | | Permissible limit ($mg\ L^{-1}$) [WHO] |
|---|---|---|---|---|---|---|---|---|---|---|
| | | Current density 50 A $m^{-2}$ | | | Percentage removal* (%) | Current density 100 A $m^{-2}$ | | | Percentage removal* (%) | |
| | | 1.00 $mg\ s^{-1}$ | 1.11 $mg\ s^{-1}$ | 1.33 $mg\ s^{-1}$ | | 1.00 $mg\ s^{-1}$ | 1.11 $mg\ s^{-1}$ | 1.33 $mg\ s^{-1}$ | | |
| Cyanide | 150 | 23 ± 2 | 16.5 ± 3 | 6.0 ± 1 | 96.0 | 20 ± 2 | 12.5 ± 2 | 0.1 ± 0.05 | 99.8 | 0.2 |
| Phenol | 150 | 18.0 ± 0.5 | 13.5 ± 0.3 | 6.0 ± 0.2 | 96.0 | 15.0 ± 0.4 | 9.5 ± 0.2 | 0.5 ± 0.1 | 99.5 | 1.0 |
| COD | 2050 | 445 ± 5 | 370 ± 3 | 250 ± 4 | 87.7 | 340 ± 4 | 250 ± 5 | 110 ± 3 | 94.7 | 250 |
| BOD | 490 | 108 ± 5 | 88 ± 2 | 57 ± 3 | 88.4 | 96 ± 3 | 68 ± 4 | 24 ± 2 | 95.0 | 30 |
| Chloride | 1820 | 1250 ± 5 | 1185 ± 3 | 1085 ± 4 | 40.5 | 1180 ± 4 | 1100 ± 5 | 975 ± 4 | 46.5 | 1000 |

***** At the optimum ozone generation rate of 1.33 $mg\ s^{-1}$ for both current densities 50 and 100 A $m^{-2}$.

**Table 3.2:** Comparison of performance efficiency in terms of pollutant removal with other hybrid treatment processes

| Ozone-based hybrid process | Types of wastewater | Pollutant removal | References |
|---|---|---|---|
| Ozone-UV | Jewellery manufacturing effluent | 98% cyanide removal | [22] |
| Ozone-$H_2O_2$ and $H_2O_2$-Ozone | Synthetic wastewater | $O_3/H_2O_2$ process 73% cyanide removal $H_2O_2/O_3$ process 99.5% cyanide removal | [23] |
| UV/Ozone/$H_2O_2$ | Plating wastewater | 99% cyanide removal | [24] |
| Ozone-EC | Olive mill wastewater | 87.5% phenol removal | [25] |
| EC-Ozone | Industrial wastewater | 67.3% COD and 57% BOD | [26] |
| UV/Ozone/$H_2O_2$ | Engine manufacturing wastewater | 76.6% cyanide removal | [27] |
| Ozone-Biological treatment | Textile wastewater | 82.8% COD | [2] |
| Ozone-EC | Steel plant wastewater | 99.8% cyanide, 99.5% phenol, 94.7% COD and 95% BOD removal | **Present Work** |

## 3.3 Kinetic modelling of cyanide, phenol, chloride and COD reduction

Various kinetic models were investigated to analyze the kinetics of pollutant removal. Here, the pseudo first-order kinetic model was fitted well to explain pollutant degradation [28].

$$\frac{dC_p}{dt} = -k_{obs}\, C_p \qquad (3.5)$$

Integration of Eq. (5) gives:

$$C_p = C_p^0\, e^{-k_{obs}t} \qquad (3.6)$$

where, $C_p$ = pollutant concentration (mg $L^{-1}$), $C_p^0$ = Initial pollutant concentration (mg $L^{-1}$), t = residence time (min) and $k_{obs}$ = observed first-order rate constant ($min^{-1}$). The $k_{obs}$ ($min^{-1}$) was determined from the regression of ln $C_p$ versus residence time (t) of the well-known pseudo first-order reaction. The values of $R^2$ and $k_{obs}$ for cyanide, phenol, COD, BOD, and chloride at three different ozone generation rate is shown in Table 3.3. It was found from the regression line of ln $C_p$ versus t that for cyanide and phenol, the rate constants ($k_{obs}$ = 0.1208 $min^{-1}$ and $k_{obs}$ = 0.1401 $min^{-1}$) were highest at an ozone generation rate of 1.33 mg $s^{-1}$, whereas it decreases for 1.11 mg $s^{-1}$, ($k_{obs}$ = 0.1030 $min^{-1}$ and $k_{obs}$ = 0.1305 $min^{-1}$) and 1.00 mg $s^{-1}$ ($k_{obs}$ = 0.0908 $min^{-1}$ and $k_{obs}$ = 0.1229 $min^{-1}$) respectively. Similarly, highest rate constants were also observed for COD ($k_{obs}$ = 0.0309 $min^{-1}$), BOD ($k_{obs}$ = 0.0338 $min^{-1}$) and chloride ($k_{obs}$ = 0.0125 $min^{-1}$) at an ozone generation rate of 1.33 mg $s^{-1}$.

The results from Table 3.3 depict that the pollutant removal obeyed pseudo first-order kinetics quite well with the highest $R^2$ value of 0.99 for cyanide, phenol, COD, BOD, and chloride respectively. With increasing, ozone generation rate from 1.00 to 1.33 mg $s^{-1}$, the $k_{obs}$ values for

cyanide and phenol removal increases from 0.0908 to 0.1208 $min^{-1}$ and 0.1229 to 0.1401 $min^{-1}$, respectively. A similar trend was observed during the removal of COD, BOD, and chloride. It was hence concluded that with increasing ozone generation rate, the rate of reaction for the removal of pollutants increased. As such, the generation of more ozone molecules paved the way for enhanced pollutant reduction in the wastewater.

**Table 3.3:** Observed reaction rate and $R^2$ values for the removal of target pollutants during the ozonation process

| Pollutants | Kinetic model | Model equation | Ozone Generation Rate (mg $s^{-1}$) | $R^2$ | $K_{obs}$ |
|---|---|---|---|---|---|
| Cyanide | Pseudo First-order | $\ln C_p = k_{obs} \times t + \ln C_{p0}$ | 1.33 | 0.99 | 0.1208 |
| | | | 1.11 | 0.99 | 0.1030 |
| | | | 1.00 | 0.98 | 0.0908 |
| Phenol | Pseudo First-order | $\ln C_p = k_{obs} \times t + \ln C_{p0}$ | 1.33 | 0.981 | 0.1401 |
| | | | 1.11 | 0.972 | 0.1305 |
| | | | 1.00 | 0.978 | 0.1229 |
| COD | Pseudo First-order | $\ln C_p = k_{obs} \times t + \ln C_{p0}$ | 1.33 | 0.99 | 0.0309 |
| | | | 1.11 | 0.98 | 0.0252 |
| | | | 1.00 | 0.99 | 0.0219 |
| BOD | Pseudo First-order | $\ln C_p = k_{obs} \times t + \ln C_{p0}$ | 1.33 | 0.99 | 0.0338 |
| | | | 1.11 | 0.99 | 0.0301 |
| | | | 1.00 | 0.98 | 0.0240 |
| Chloride | Pseudo First-order | $\ln C_p = k_{obs} \times t + \ln C_{p0}$ | 1.33 | 0.99 | 0.0125 |
| | | | 1.11 | 0.99 | 0.0104 |
| | | | 1.00 | 0.98 | 0.0088 |

## 3.4 Mass transfer study of ozone

A mass balance equation results from the simultaneous absorption of gaseous ozone into the aqueous solution and its self-decomposition reaction; which typically determines the phenomenon of volumetric mass transfer coefficient of ozone [29].

$$\frac{dX_t}{dt} = K_l\, a\, (X_t^* - X_t) - K\, dX_t^* \quad (3.7)$$

The concentration of ozone diffused in the solution intensifies with the increase in operating time and reaches a steady-state, which correlates to the equilibrium concentration of dissolved ozone in the solution ($X_e$). The following equation represents the ozone equilibrium concentration in the solution:

$$X_e = \left(\frac{K_l\, a}{K_l\, a + K_d}\right) X_t^* \quad (3.8)$$

The mass balance equation may be given as [30]:

$$\frac{dX_t}{dt} = (K_l\, a + K_d) \times (X_e - X_t) \quad (3.9)$$

The above equation can be integrated to:

$$X_t = X_e\, [1 - \exp\{-(K_l\, a + K_d) \times t\}] \quad (3.10)$$

$$\ln\left(\frac{X_e}{X_e - X_t}\right) = (K_l\, a + K_d) \times t \quad (3.11)$$

Figure 3.6 (inset) shows the plot of $\ln\left(\frac{X_e}{X_e - X_t}\right)$ vs t, which results in a straight line with slope ($K_l$ a + $K_d$). The values of the diffusion coefficient, $K_d$ at different pH can be evaluated from the correlation given by Sotelo et al. (1987) [31]. For $K_d$ value of $2.6 \times 10^4$ $s^{-1}$ (at pH 3), the values of $K_l$ a were found to be $0.43 \times 10^3$, $0.55 \times 10^3$, and $0.74 \times 10^3$ $s^{-1}$ for an ozone generation rate of

1.00, 1.11, and 1.33 mg $s^{-1}$, respectively. Thus, the volumetric mass transfer coefficient ($K_l$ a) increases with an increase in the ozone generation rate as shown in Table 3.4. This enhances the mass transfer from the gaseous phase to the aqueous phase. As such, the concentration of the dissolved ozone in the solution increases with an increase in the ozone generation rate.

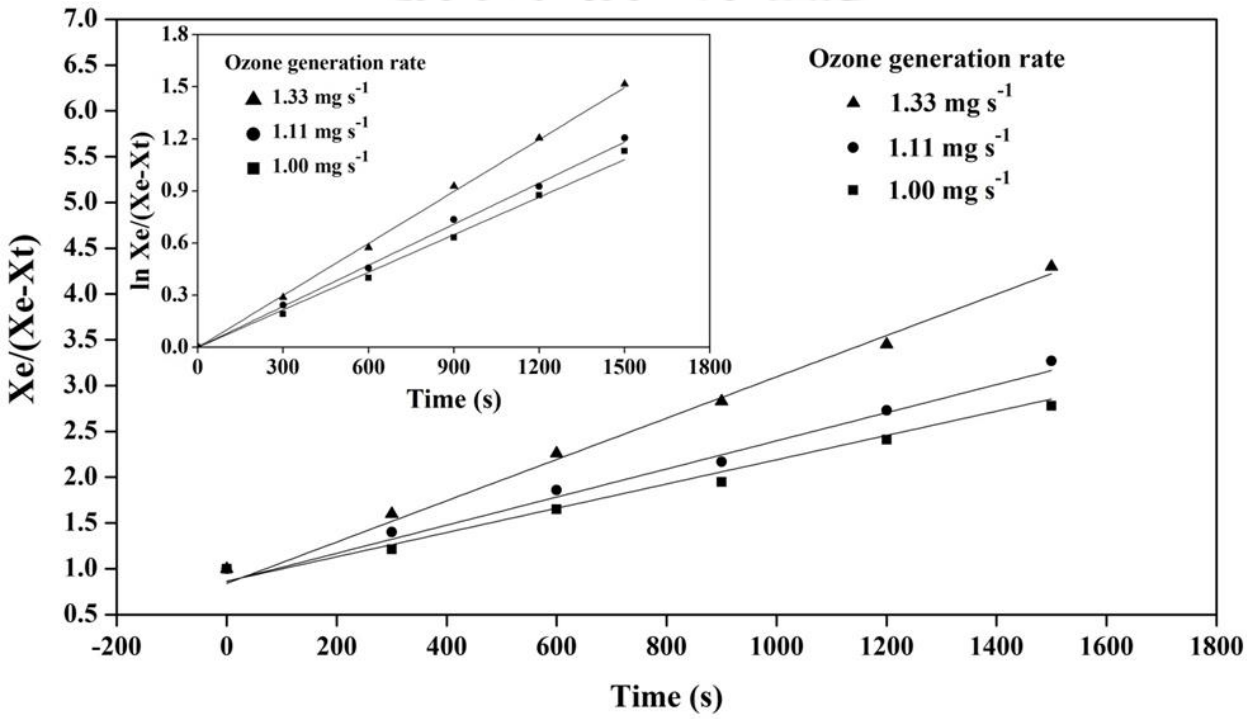


**Fig. 3.6:** Plot of ($\frac{Xe}{Xe-Xt}$) vs t at different ozonation rates. Inset: Plot of ln ($\frac{Xe}{Xe-Xt}$) vs t for the determination of volumetric mass transfer coefficient ($K_l$ a).

**Table 3.4.** Volumetric mass transfer coefficient ($k_l$ a) at different ozone generation rates

| pH | $K_d \times 10^4$ ($s^{-1}$) (Sotelo et al., 1987) | Ozone generation rate (mg $s^{-1}$) | $K_l$ a $\times 10^3$ ($s^{-1}$) |
|---|---|---|---|
| 3 | 2.6 | 1.33 | 0.74 |
| | | 1.11 | 0.55 |
| | | 1.00 | 0.43 |

## 3.5 Evaluation of operating cost and energy consumption of the hybrid process

The energy cost of the entire operation was mainly considered during the preliminary cost estimate of the ozonation process (US$ $m^{-3}$ of solution). For the ozonation process, Figure 3.7 (inset, top) shows the change in operating cost with a change in ozone generation rate (1.00 - 1.33 mg $s^{-1}$). The cost of operation was determined by the following equation:

$$\text{Operating cost}_{(\text{ozonation})} = b \times E_{\text{energy}} \quad (3.12)$$

where $E_{\text{energy}}$ represents the consumption of electricity required for pollutant removal, and ‘‘b” represents the rate of electrical energy. The consumption of electrical energy can be given as [32]:

$$E_{\text{energy}} = \frac{V \times I \times t}{V_L} \quad (3.13)$$

Here I represent the current (A), V represents the voltage (V), t represents the analysis time (s), and $V_L$ represents the effluent volume ($m^3$). The electricity cost was taken as per its price for the state of Assam (India) in the year 2019 (0.0924 US$ $kWh^{-1}$). The experiments establish that for an optimum ozone generation rate of 1.33 mg $s^{-1}$, the power consumption of the ozonation process

estimates to be 105.2 W. This leads to an increase in the energy cost from 14.64 to 58.53 US$ $m^{-3}$ as the ozonation time increases from 10 to 40 min, respectively. Therefore, the operating cost was increased from 1.30 US$ $m^{-3}$ after 10 min of analysis time to 5.37 US$ $m^{-3}$ at the end of the ozonation process.

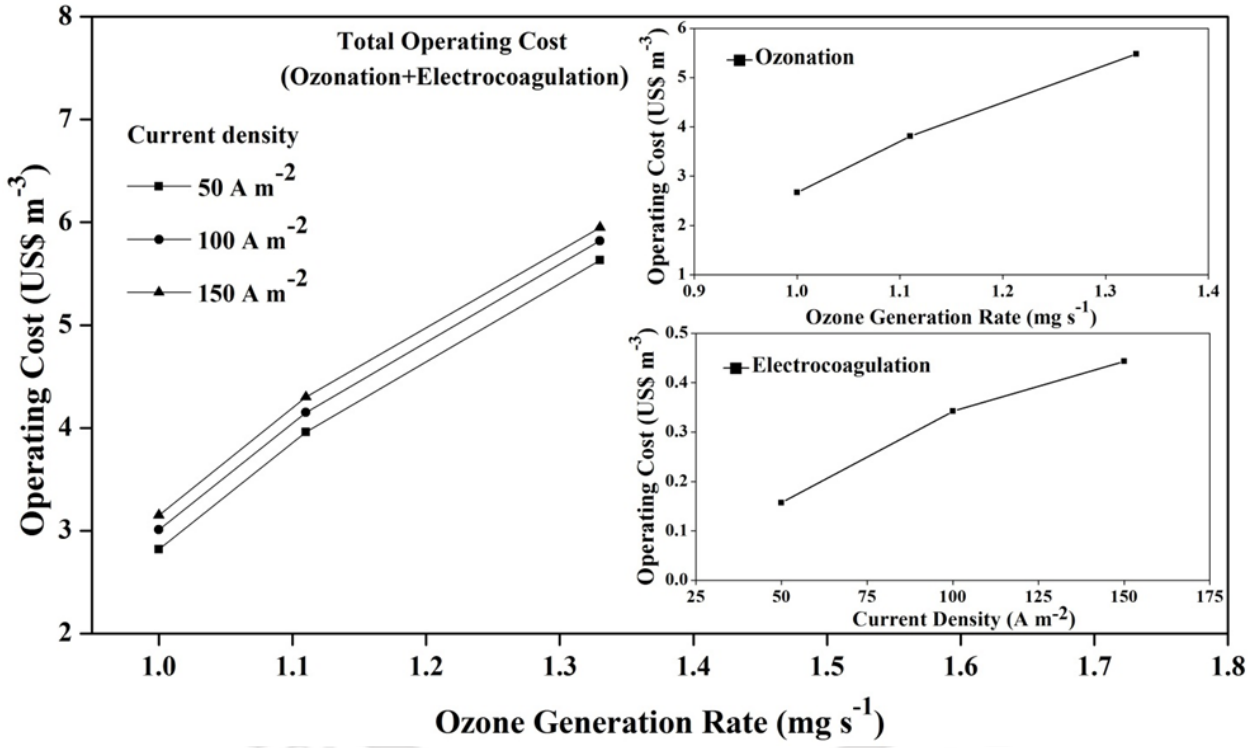


**Fig. 3.7:** Variation in operating cost during the ozone assisted electrocoagulation process. Inset (top): Operating cost with ozonation process, Inset (bottom): Operating cost with electrocoagulation process

During electrocoagulation, the operating cost includes electricity, chemical, sludge disposal, electrode cost, and fixed cost. However, for simplicity, the determination of the operating cost for

the electrocoagulation process involves only the electricity rate and the cost of electrodes. The cost of operation was calculated from the following equation [33]:

$$\text{Operating cost}_{(\text{electrocoagulation})} = a \times E_{\text{electrode}} + b \times E_{\text{energy}} \quad (3.14)$$

where, $E_{\text{electrode}}$ and $E_{\text{energy}}$ represent the consumption of electrode materials and electrical energy, respectively. ''a" represents the cost of electrode materials (2.0436 US$ $kg^{-1}$ of aluminum) and ''b" represents the cost of electricity consumption (0.0924 US$ $kWh^{-1}$). Consumption of electrode material was determined from the following Faraday's law [34]:

$$E_{\text{electrode}} = \frac{I \times t \times M.W}{F \times z \times V_L} \quad (3.15)$$

Here M.W represents the molar mass of aluminum (26.98 g $mol^{-1}$), I represent the current (A), t represents the electrocoagulation time (s), VL represents the effluent volume ($m^3$), F represents the Faraday's constant (96,487 C $mol^{-1}$) and z represents the number of electrons transferred (z = 3). For the electrocoagulation process, Figure 3.7 (inset, bottom) shows the change in operating cost with a change in current density (50 - 150 A $m^{-2}$). From the experiments conducted, it was found that for an optimum current density of 100 A $m^{-2}$, the electrode, and the energy cost were found to increase from 0.000353 to 0.00106 US$ $m^{-3}$ and from 1.04 to 3.12 US$ $m^{-3}$, respectively, as the electrocoagulation time increases from 10 to 30 min. As such, the operating cost was increased from 0.113 US$ $m^{-3}$ after 10 min of operation to 0.340 US$ $m^{-3}$ at the end of the electrocoagulation process. Therefore, by combining the operating cost of both the processes, the total cost of operation for the ozone assisted electrocoagulation process was found to be 5.801 US$ $m^{-3}$. The operating cost of the entire hybrid process is shown in Figure 3.7.

## 3.6 Summary of work

For the hybrid ozone assisted electrocoagulation process, ozone generation rate and current density played a significant role in pollutant removal as the percentage removal increases with both the parameters. During ozonation, the pH of the effluent rapidly decreases from an initial pH of 7.72 to 3.0. However, the pH later increases up to 8.30 after electrocoagulation, owing to the generation of $OH^-$ ions at the cathode surface. The combined process of ozonation and electrocoagulation was very effective in reducing the concentration of cyanide, phenol, COD, BOD, and chloride below their respective permissible limit of surface water quality. The kinetic study performed indicates that the degradation of all the target contaminants can be well explained by the pseudo first-order kinetic model. Both the removal efficiency and rate constant ($k_{obs}$) of the target contaminants were found to be highest at an ozone generation rate of 1.33 mg $s^{-1}$. On the other hand, with a decrease in the ozone generation rate to 1.11 and 1.00 mg $s^{-1}$, the percentage removal of the contaminants was also decreased. The mass transfer study showed that an increase in the ozone generation rate increases the volumetric mass transfer coefficient ($K_l$ a), which leads to an increase in the ozone concentration in the solution. The efficiency of the hybrid process was compared with that of other reported literature, and the performance was found to be satisfactory. The preliminary cost for the hybrid ozone assisted electrocoagulation process was found to be 5.801 US$ $m^{-3}$. The treatment cost of this hybrid process is comparably lower than the reported literature.

## References:

[1] S. Venkatesh, N.D. Pandey, A.R. Quoff, Decolorization of synthetic dye solution containing congo red by Advanced Oxidation Process (AOP), Int. J. Adv. Res. Civil,Structural,Environment Infrastruct. Eng. Dev. 2 (2014) 49–55. https://doi.org/10.1016/ijarcsei.2014.106115.

[2] S.M. de A.G.U. de Souza, K.A.S. Bonilla, A.A.U. de Souza, Removal of COD and color from hydrolyzed textile azo dye by combined ozonation and biological treatment, J. Hazard. Mater. 179 (2010) 35–42. https://doi.org/10.1016/j.jhazmat.2010.02.053.

[3] D. Ghosh, C.R. Medhi, M.K. Purkait, Treatment of fluoride containing drinking water by electrocoagulation using monopolar and bipolar electrode connections, Chemosphere. 73 (2008) 1393–1400. https://doi.org/10.1016/j.chemosphere.2008.08.041.

[4] F. Barriga-Ordonez, F. Nava-Alonso, A. Uribe-Salas, Cyanide oxidation by ozone in a steady-state flow bubble column, Miner. Eng. 19 (2006) 117–122. https://doi.org/10.1016/j.mineng.2005.09.001.

[5] F.R. Carrillo-Pedroza, F. Nava-Alonso, A. Uribe-Salas, Cyanide oxidation by ozone in cyanidation tailings: Reaction kinetics, Miner. Eng. 13 (2000) 541–548. https://doi.org/10.1016/S0892-6875(00)00034-0.

[6] W.J. Rowley, F.D. Otto, Ozonation of cyanide with emphasis on gold mill wastewaters, Can. J. Chem. Eng. 58 (1980) 646–653. https://doi.org/https://doi.org/10.1002/cjce.5450580516.

[7] G. Moussavi, F. Majidi, M. Farzadkia, The influence of operational parameters on elimination of cyanide from wastewater using the electrocoagulation process, Desalination. 280 (2011) 127–133. https://doi.org/10.1016/j.desal.2011.06.052.

[8] M. Changmai, P.P. Das, P. Mondal, M. Pasawan, A. Sinha, P. Biswas, S. Sarkar, M.K. Purkait, Hybrid electrocoagulation–microfiltration technique for treatment of nanofiltration rejected steel industry effluent, Int. J. Environ. Anal. Chem. 102 (2022) 62–83. https://doi.org/10.1080/03067319.2020.1715381.

[9] M.K. Chegeni, A. Shahedi, A.K. Darban, A. Jamshidi-Zanjani, M. Homaee, Simultaneous removal of lead and cyanide from the synthetic solution and effluents of gold processing plants using electrochemical method, J. Water Process Eng. 43 (2021) 102284. https://doi.org/10.1016/j.jwpe.2021.102284.

[10] S. Enami, M.R. Hoffmann, A.J. Colussi, How phenol and a-tocopherol react with ambient ozone at gas/liquid interfaces, J. Phys. Chem. A. 113 (2009) 7002–7010. https://doi.org/10.1021/jp901712k.

[11] M.K. Ramseier, U. von Gunten, Mechanisms of phenol ozonation-kinetics of formation of primary and secondary reaction products, Ozone Sci. Eng. 31 (2009) 201–215. https://doi.org/10.1080/01919510902740477.

[12] L.P. Yang, W.Y. Hu, H.M. Huang, B. Yan, Degradation of high concentration phenol by ozonation in combination with ultrasonic irradiation, Desalin. Water Treat. 21 (2010) 87–95. https://doi.org/10.5004/dwt.2010.1233.

[13] A.S. Fajardo, R.C. Martins, R.M. Quinta-Ferreira, Treatment of a synthetic phenolic mixture by electrocoagulation using Al, Cu, Fe, Pb, and Zn as anode materials, Ind. Eng. Chem. Res. 53 (2014) 18339–18345. https://doi.org/10.1021/ie502575d.

[14] M. Uğurlu, A. Gürses, Ç. Doğar, M. Yalçin, The removal of lignin and phenol from paper mill effluents by electrocoagulation, J. Environ. Manage. 87 (2008) 420–428. https://doi.org/10.1016/j.jenvman.2007.01.007.

[15] D. Yang, J. Yuan, COD and Color Removal from Real Dyeing Wastewater by Ozonation, Water Environ. Res. 88 (2016) 403–407. https://doi.org/https://doi.org/10.1002/j.1554-7531.2016.tb00145.x.

[16] C.D. Adams, S. Gorg, Effect of pH and Gas-Phase Ozone Concentration on the Decolorization of Common Textile Dyes, J. Environ. Eng. 128 (2002) 293–298. https://doi.org/10.1061/(asce)0733-9372(2002)128:3(293).

[17] C.E. Barrera Díaz, N. González-Rivas, The Use of Al, Cu, and Fe in an Integrated Electrocoagulation-Ozonation Process, J. Chem. 2015 (2015) 1–7. https://doi.org/10.1155/2015/158675.

[18] S. Baig, P.A. Liechti, Ozone treatment for biorefractory COD removal, Water Sci. Technol. 43 (2001) 197–204. https://doi.org/10.2166/wst.2001.0090.

[19] Q.H. Nguyen, T. Watari, T. Yamaguchi, Y. Takimoto, K. Niihara, J.P. Wiff, T. Nakayama, COD removal from wastewater by electrocoagulation using aluminum electrodes, Int. J. Electrochem. Sci. 15 (2020) 39–51. https://doi.org/10.20964/2020.01.42.

[20] A. V. Levanov, I. V. Kuskov, A. V. Zosimov, E.E. Antipenko, V. V. Lunin, Acid Catalysis in Reaction of Ozone with Chloride Ions, Kinet. Catal. 44 (2003) 740–746. https://doi.org/10.1023/B:KICA.0000009047.90252.2d.

[21] A. V. Levanov, I. V. Kuskov, E.E. Antipenko, V. V. Lunin, Stoichiometry and products of ozone reaction with chloride ion in an acidic medium, Russ. J. Phys. Chem. A. 86 (2012) 757–762. https://doi.org/10.1134/S0036024412050202.

[22] B.K. Mert, Ö. Sivrioğlu, T. Yonar, S. Özçiftçi, Treatment of Jewelry Manufacturing Effluent Containing Cyanide Using Ozone-Based Photochemical Advanced Oxidation Processes, Ozone Sci. Eng. 36 (2014) 196–205. https://doi.org/10.1080/01919512.2013.860354.

[23] U. Kepa, E. Stanczyk-Mazanek, L. Stepniak, The use of the advanced oxidation process in the ozone + hydrogen peroxide system for the removal of cyanide from water, Desalination. 223 (2008) 187–193. https://doi.org/10.1016/j.desal.2007.01.215.

[24] Y.J. Kim, T.I. Qureshi, K.S. Min, Application of advanced oxidation processes for the treatement of cyanide containing effluent, Environ. Technol. (United Kingdom). 24 (2003) 1269–1276. https://doi.org/10.1080/09593330309385669.

[25] P. García-García, F.N. Arroyo-López, F. Rodríguez-Gómez, Partial purification of iron solutions from ripe table olive processing using ozone and electro-coagulation, Sep. Purif. Technol. 133 (2014) 227–235. https://doi.org/10.1016/j.seppur.2014.06.011.

[26] M. Hernández-Ortega, T. Ponziak, C. Barrera-Díaz, M.A. Rodrigo, G. Roa-Morales, B. Bilyeu, Use of a combined electrocoagulation-ozone process as a pre-treatment for industrial wastewater, Desalination. 250 (2010) 144–149. https://doi.org/10.1016/j.desal.2008.11.021.

[27] J. Ford, R. Hernandez, M. Zappi, Bench-scale evaluation of advanced oxidation processes for treatment of a cyanide-contaminated wastewater from an engine manufacturing facility, Environ. Prog. 25 (2006) 32–38. https://doi.org/https://doi.org/10.1002/ep.10098.

[28] P. Mondal, M.K. Purkait, Green synthesized iron nanoparticles supported on pH responsive polymeric membrane for nitrobenzene reduction and fluoride rejection study: Optimization approach, J. Clean. Prod. 170 (2018) 1111–1123. https://doi.org/10.1016/j.jclepro.2017.09.222.

[29] S. Khuntia, S.K. Majumder, P. Ghosh, Removal of ammonia from water by ozone microbubbles, Ind. Eng. Chem. Res. 52 (2013) 318–326. https://doi.org/10.1021/ie302212p.

[30] S. Patel, R. Agarwal, S.K. Majumder, P. Das, P. Ghosh, Kinetics of ozonation and mass transfer of pharmaceuticals degraded by ozone fine bubbles in a plant prototype, Heat Mass Transf. Und Stoffuebertragung. 56 (2020) 385–397. https://doi.org/10.1007/s00231-019-02718-7.

[31] J.L. Sotelo, F.J. Beltran, F.J. Benitez, J. Beltran-heredia, Ozone Decomposition: Kinetic Study, Ind. Eng. Chem. Res. 26 (1987) 39–43. https://doi.org/10.1021/ie00061a008.

[32] D. Ghosh, C.R. Medhi, H. Solanki, M.K. Purkait, Decolorization of Crystal Violet Solution by Electrocoagulation, J. Environ. Prot. Sci. 2 (2008) 25–35. https://doi.org/10.1016/j.eps.2008.11.035.

[33] D. Ghosh, C.R. Medhi, M.K. Purkait, Techno-economic analysis for the electrocoagulation of fluoride-contaminated drinking water, Toxicol. Environ. Chem. 93 (2011) 424–437. https://doi.org/10.1080/02772248.2010.542158.

[34] M. Changmai, M. Pasawan, M.K. Purkait, A hybrid method for the removal of fluoride from drinking water: Parametric study and cost estimation, Sep. Purif. Technol. 206 (2018) 140–148. https://doi.org/10.1016/j.seppur.2018.05.061.

# Chapter 4

# Removal of ammonia-N, iron and colour from steel plant generated biological oxidation treated (BOT) wastewater via hybrid ozone assisted electrocoagulation

# Chapter 4

# Removal of ammonia-N, iron and colour from steel plant generated biological oxidation treated (BOT) wastewater via hybrid ozone assisted electrocoagulation

*This chapter describes the combined effect of ozonation and electrocoagulation for the treatment of steel industry wastewater since only ozonation or electrocoagulation is incompetent to reduce the pollutant concentrations below the assigned permissible limits. Biological oxidation treated (BOT) wastewater consisting of coloured compounds, iron, and ammonia-N from Tata Steel Industry, India was considered here. The effects of operating variables like ozone generation rate, current density and treatment time on pollutant removal were analyzed for the hybrid process. The experimental conditions such as 1.33 mg $s^{-1}$ (ozone generation rate), 40 min (ozonation time), 100 A $m^{-2}$ (current density), and 30 min (electrolysis time) were found to be optimum for reducing all the pollutant concentrations (iron, ammonia-N, and colour) below their respective permissible limits of surface water quality. The removal capacity of the hybrid process was found to be 98.2%, 90.6%, and 62.8% for colour, iron, and ammonia-N, respectively. A kinetic study was performed for the degradation of the pollutants during the hybrid process. The pseudo-first-order kinetic model was found to be best suited for the analysis with the $R^2$ value of about 0.99 for iron, ammonia, and colour, respectively, for an optimum ozone generation rate of 1.33 mg $s^{-1}$. Further, an image processing software (Image J Software, 9.0) was used for analyzing the bubble size in which the sauter mean diameter of the microbubble was found to be 425 µm, and the range of the microbubble size varied from 20 µm to 650 µm. Finally, the cost analysis showed that the proposed hybrid process was economical compared to other reported literature.*

# Chapter 4

## 4.1 Experimental

### 4.1.1 Measurement and analysis

Biological Oxidation Treated (BOT) wastewater was obtained from Tata Steel Industry, India to carry out the experiments for the present study. The initial characteristics of the wastewater sample were measured. The concentration of the pollutants targeted in this work were: colour (dark brown): 2450 hazen, ammonia-N: 130 mg $L^{-1}$, iron: 7.3 mg $L^{-1}$, conductivity: 3.26 mS $cm^{-1}$, TDS: 2670 mg $L^{-1}$ and pH: 7.72. An acrylic electrocoagulation reactor of 500 mL volume and an ozonation reactor of 2 L volume were used for conducting the experiments. All the experiments were performed at a constant temperature of 20°C. The sample analysis was done at an interval of 5 min, and the residual concentration of the pollutants was measured using an atomic absorption spectrometry (Make: M/s Varian; Model: Spectra AA 220 FS) and a photometer (Make: Palintest; Model: 7100). The quality of the untreated and treated water such as pH, conductivity, and total dissolved solids were determined using a microprocessor based water analyzer kit (Make: VSI electronics; Model: VSI-302). The details of all the measurement and analysis have been elaborately reported in section 2.3 of chapter 2.

### 4.1.2 Operational parameters

The experiments involving ozonation and electrocoagulation were conducted using varying operational conditions. The study aimed to investigate the impact of ozone generation rates and reaction time on the efficiency of pollutant removal during ozonation. Three distinct ozone generation rates, specifically 1.00 mg $s^{-1}$, 1.11 mg $s^{-1}$, and 1.33 mg $s^{-1}$, were chosen to conduct the experiments. The reaction time was varied within the range of 10-40 min. The study also evaluated

the impact of current density and electrolysis time on the efficiency of pollutant removal during electrocoagulation. Three distinct current densities, viz. 50 A $m^{-2}$, 100 A $m^{-2}$, and 150 A $m^{-2}$, were selected for the experiments. The electrolysis time was varied within the range of 10-30 min and the inter-electrode distance was maintained at 0.005 m throughout the process.

During the application of three different ozone generation rates viz. 1.00 mg $s^{-1}$, 1.11 mg $s^{-1}$ and 1.33 mg $s^{-1}$, it was observed that an ozone generation rate of 1.33 mg $s^{-1}$ was sufficient to effectively reduce all the target parameters below their assigned permissible limits. Further, continuation of the experiments beyond 1.33 mg $s^{-1}$ substantially increased the operating cost of the hybrid process. Moreover, the removal rate of the pollutants remained constant on prolongation of the oxidation time beyond 40 min. Therefore, the optimum operating conditions were taken as 1.33 mg $s^{-1}$ and 40 min for the ozonation process. During the application of three different current densities viz. 50, 100, and 150 A $m^{-2}$, it was found that the experiments conducted at current density higher than 100 A $m^{-2}$, showed only a marginal increase in the pollutant removal rate. Further, prolongation of the electrolysis time beyond 30 min resulted in negligible removal of the pollutants as the process efficiency reaches saturation. Moreover, the energy consumption of the hybrid process was substantially increased beyond 30 min of electrolysis time. Therefore, the optimum operating conditions were taken as 100 A $m^{-2}$ and 30 min for the electrocoagulation process.

## 4.2 Results and discussion

### 4.2.1 Variation in solution pH during hybrid ozone assisted electrocoagulation process

Figure 4.1 shows the change in pH at 20 °C (operating temperature) with ozonation assisted electrocoagulation process, indicating that the initial pH value decreases rapidly from 7.72 ± 0.1

to 3.2 during the first 5-10 min of the experiment and from 3.2 to 3.0 in the subsequent period of ozonation time. It was observed from Figure 4.1 that the initial pH of the effluent decreases from 7.72 as the ozonation process continues until a steady-state condition is achieved at pH 3. This shows that ozone oxidation leads to the production of by-products of acidic nature (organic anions along with inorganic acids). During the experiment, the pH of the effluent tends to decrease as ozone reacts with both the degradation products produced during oxidation via hydroxyl radicals (usually carboxylic acids) as well as with the hydroxyl anions. During the initial stage of the process, pH reduction is very prominent (particularly for alkaline solutions) due to higher ozone consumption [1].

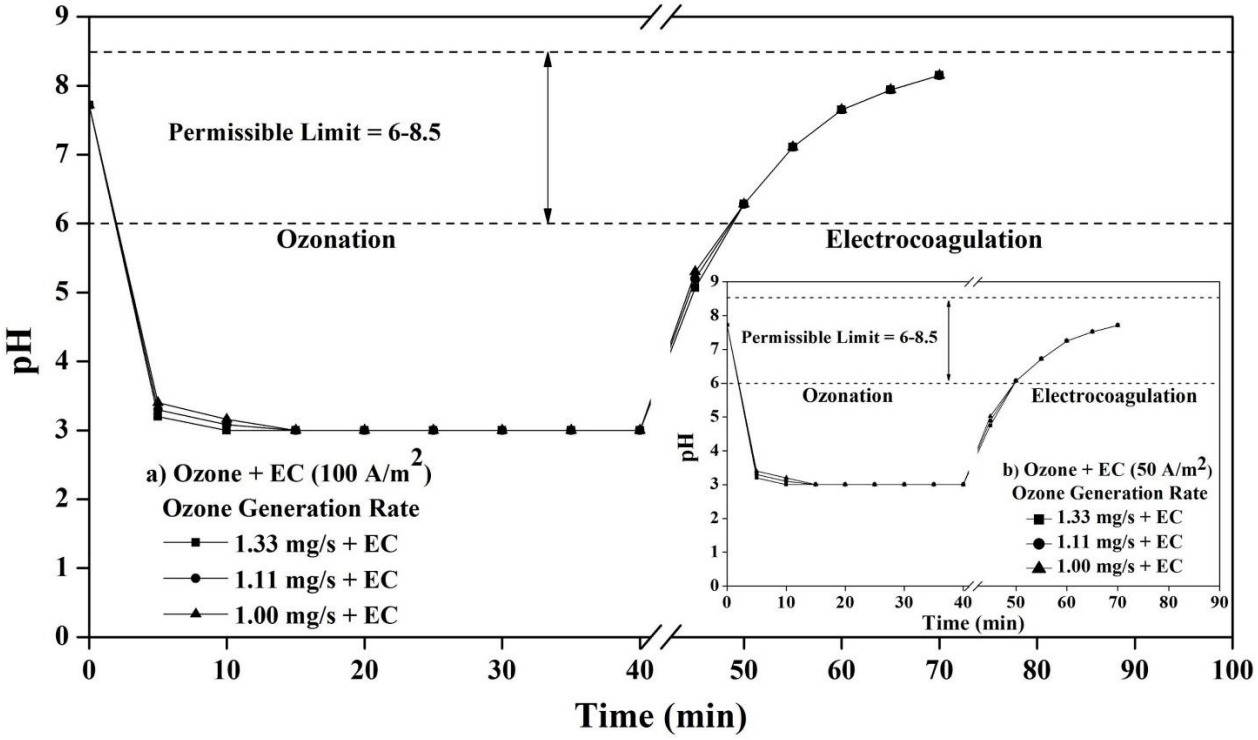


**Fig. 4.1:** Variation in solution pH with treatment time at different ozone generation rates. Outset: 100 A $m^{-2}$ current density, Inset: 50 A $m^{-2}$ current density.

During electrocoagulation, the pH gradually increases from 3.0 until it reaches a plateau at around a pH of 8.2, where it attains a steady state due to the buffering capacity of $Al(OH)_3/Al(OH)_4^-$. This increase in pH is due to the evolution of $H_2$ at the cathode vicinity as well as the formation of $OH^-$ ions at the cathode surface [2]. Thus, from Figure 4.1, it can be ascertained that as electrocoagulation time increases, the pH of the solution also increases. Further, the TDS and conductivity of the treated solution were determined at the end of each experiment. For the optimum operating conditions (ozone generation rate: 1.33 mg $s^{-1}$, reaction time: 40 min and current density: 100 A $m^{-2}$, electrolysis time: 30 min), the TDS and conductivity were found to decrease from an initial concentration of 2670 to 1850 mg $L^{-1}$ and 3.26 to 2.35 mS $cm^{-1}$, respectively, for the hybrid ozone assisted electrocoagulation process.

Further, the experiments carried out in this study primarily focused on the impact of ozone generation rate, current density, and analysis time on the pollutant removal efficiency under highly acidic condition. Thus, the study was conducted at a constant acidic pH of 3 to support the feasibility of the operating parameters used for the removal of the target pollutants.

### 4.2.2 Removal of colour by hybrid ozone assisted electrocoagulation process

The pH of the effluent directly affects the decomposition of ozone. As already discussed, at higher pH, the decomposition of ozone leads to the formation of hydroxyl radicals, while at low pH values, the main oxidant being the molecular ozone. The extent of decolourization at low pH value is favored by direct ozone attack. At low pH, molecular ozone ($O_3$) predominates, and as such less ozone is wasted on scavenging reactions in solution compared to hydroxyl radicals, which are more effective at higher pH [3]. At high pH, indirect hydroxyl–radical-mediated reactions

predominate, leading to ozone wastage through scavenging reactions with non-colored saturated bonds, as well as inorganic and organic compounds in solution. Therefore, under acidic conditions, the decolorization efficiency of the solution increases [4]. Furthermore, the chromophore groups present in lignin are mainly responsible for the brownish color of the BOT wastewater. By increasing the ozone generation rate, a higher amount of molecular ozone can be formed under acidic conditions. As such, the molecular ozone leads to the destruction of the chromophore groups (usually double bonds), which gets oxidized to single bonds resulting in a bond cleavage, thus losing the ability to absorb visible light, leading to decolorization of the sample [5]. As a result, for an optimum ozone generation rate and operating time of 1.33 mg $s^{-1}$ and 40 min, respectively, the color decreases from an initial concentration of 2450 hazen to a final concentration of 250 hazen. Figure 4.2 depicts a decreasing trend for color removal with ozone generation rate and operating time. From Figure 4.2, it was observed that with increasing ozone generation rate from 1.0 to 1.33 mg $s^{-1}$, the decolorization percentage also increases from 75.3% to 90%, respectively. Also, at the initial stage of the experiment, decolorization efficiency was found to be higher, as molecular ozone attributes to the destruction of most of the chromophore groups within the first 5-15 min of the ozonation process. However, due to higher oxidation potential and less selectivity of hydroxyl radicals compared to molecular ozone, decolorization efficiency decreases at higher pH.

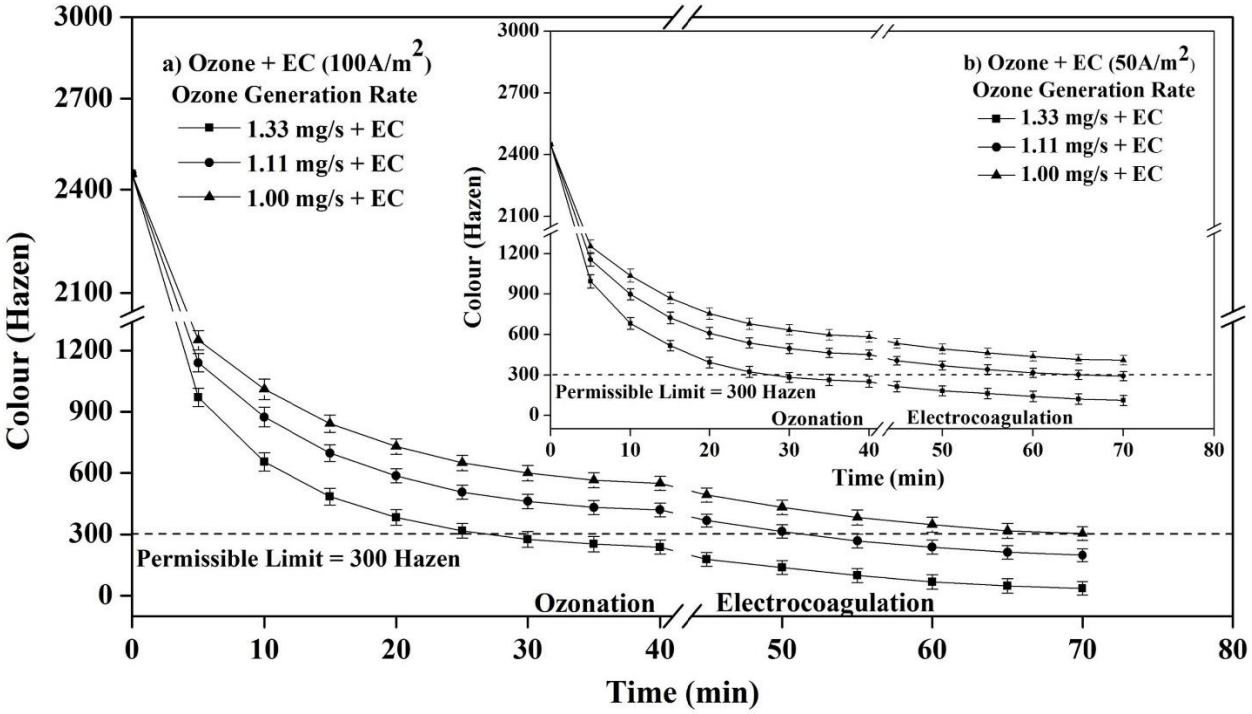


**Fig. 4.2:** Effect of ozone generation rates on colour removal with treatment time. Outset: 100 A $m^{-2}$ current density, Inset: 50 A $m^{-2}$ current density.

During electrocoagulation, the color concentration further decreases from 250 hazen (obtained at 1.33 mg $s^{-1}$) to 45 hazen for an optimum current density of 100 A $m^{-2}$ and electrolysis time of 30 min as seen in Figure 4.2. The quantity of electricity consumed as well as the initial pH of the solution is important parameters that affect the decolorization efficiency of the process during electrocoagulation. Another important parameter in the decolorization process is the role of different species generated during the experiment. Lower initial pH is responsible for stimulating hydroxy polymeric species and retarding the formation of $Al(OH)_3$ flocs [6]. The efficient precipitation of the colored compounds is responsible for higher reduction efficiencies even at a low pH value of 3. Two important interaction mechanisms are responsible for color removal, viz.

adsorption and precipitation, each one being suggested for a different range of pH. Higher decolorization efficiency is primarily caused by the precipitation process, while adsorption of the polymeric species colloidal precipitates by $Al(OH)_3$ flocs have a more secondary effect. Flocculation in the high pH range of >6.5 can be described as adsorption, while that in the lower pH range of 3-6 can be described as precipitation. Cationic monomers such as $A1^{3+}$ and $Al(OH)_2^+$ are the dominant species, during the application of low initial pH along with aluminum as a sacrificial anode [7]. Double-layer compression is the main mechanism for the coagulation of the organic molecules containing the chromophore group. In such instance, coagulant ($A1^{3+}$) at a high concentration is required for effective removal of the colored compounds present in the sample. Polymeric species ($Al_{13}O_4(OH)_{24}^{7+}$) and precipitate such as $Al(OH)_3$(s) was formed in the pH range of 4-9. As such, the mechanisms of adsorption, charge neutralization, and enmeshment are responsible for effective coagulation and precipitation of the organic molecules (having the chromophore groups). Besides, with the increase in the electrocoagulation time decolorization capacity increases, indicating the continuous generation of surplus flocs formed due to the application of current density to the aqueous solution [8]. As such, due to the analogy between the effects of current density as well as operating time, these two variables can be combined into one variable viz. the quantity of electricity consumed per cubic meter of effluent, which can be indicated as faradays per cubic meter. The maximum removal efficiency attained during the electrocoagulation process was 82% for the current density and electrolysis time of 100 A $m^{-2}$ and 30 min, respectively. The schematic diagram of color change during the integrated process is shown in Figure 4.3.

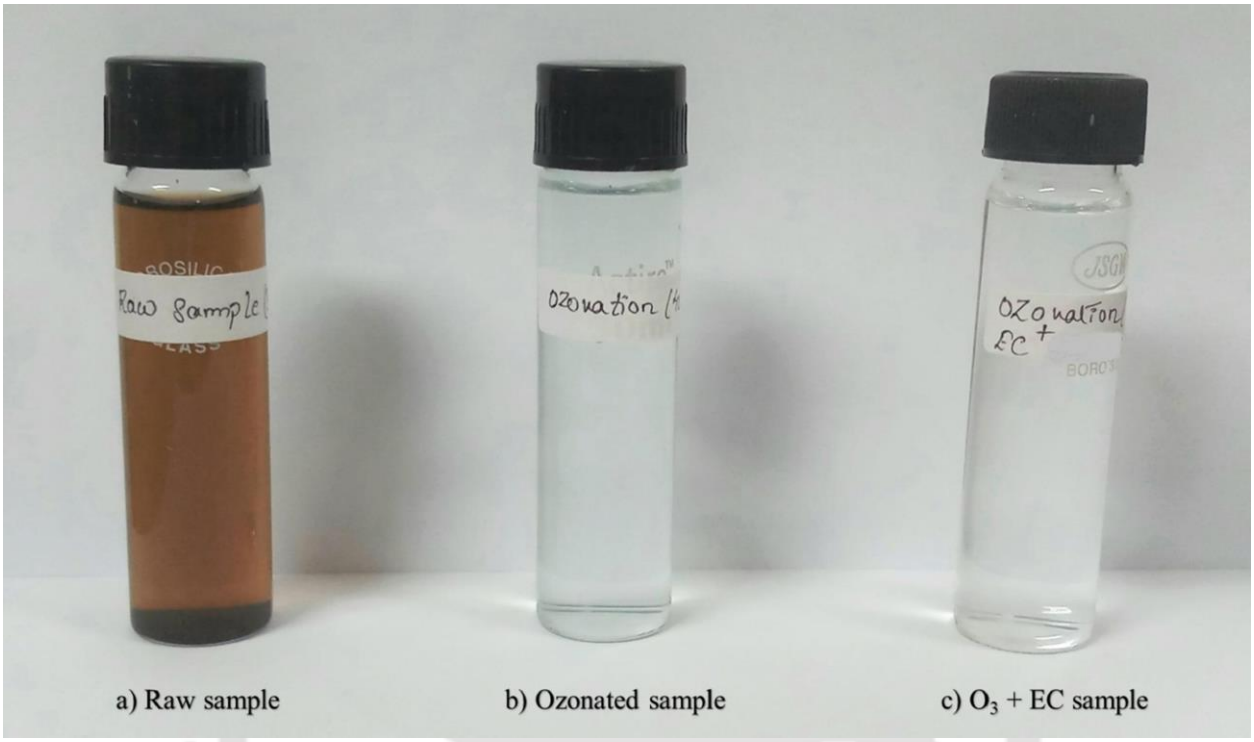


**Fig. 4.3:** Schematic diagram of colour change. a) raw sample, b) ozonated sample and c) $O_3$ assisted EC sample

### 4.2.3 Removal of ammonia-N by hybrid ozone assisted electrocoagulation process

Depending upon temperature and, most importantly the pH, ammonia exists in two forms in the aqueous solution viz. ionized form ($NH_4^+$) and/or un-ionized form ($NH_3$). The proportion of $NH_3$ and $NH_4^+$ in the solution is mainly determined by the solution pH. From the literature, it can be ascertained that $NH_4^+$ is found mostly at initial pH < 7.0, while $NH_3$ content increases at initial pH > 7.0. Since the initial pH of BOT wastewater is 7.72, most of the ammonia exist as molecular $NH_3$ and not as $NH_4^+$ (Eq. (1) [9].

$$NH_4^+ + OH^- \leftrightarrow NH_3 + H_2O \quad (4.1)$$

The reaction of molecular ozone (Eqs. 4.2 - 4.5) during the ozonation process leads to the oxidative decomposition of ammonia in water. Ammonia, on direct reaction with $O_3$, oxidizes to nitrite, nitrate as well as nitrogen gas. Nitrite on further oxidation by $O_3$ gets converted to nitrate (Eq. 4.3). As such, nitrite in the solution can hardly be estimated. Moreover, at higher pH, the decomposition of ozone leads to the formation of hydroxyl radicals ($HO^{\bullet}$), while at low pH values, the main oxidant being the molecular ozone ($O_3$) [10]. Since the pH value of the solution rapidly decreases to 3 (highly acidic pH) during the very initial period of the experiments conducted, as such only molecular ozone was involved in the oxidation of ammonia during ozonation. The following are the reactions of ammonia with $O_3$ (produced via the chain of reactions of $O_3$ decomposition) [11].

$$NH_3\,(aq) + 3O_3\,(aq) \rightarrow H^+\,(aq) + NO_2^-\,(aq) + H_2O\,(l) + 3O_2\,(g) \quad (4.2)$$

$$NO_2^-\,(aq) + O_3\,(aq) \rightarrow NO_3^-\,(aq) + O_2\,(g) \quad (4.3)$$

$$NH_3\,(aq) + 4O_3\,(aq) \rightarrow H^+\,(aq) + NO_3^-\,(aq) + H_2O\,(l) + 4O_2\,(g) \quad (4.4)$$

$$4NH_3\,(aq) + O_3\,(aq) \rightarrow 2N_2\,(g) + 3H_2O\,(l) + 6H^+\,(aq) \quad (4.5)$$

Eq. (4.2) to Eq. (4.5) explains the major pathway of $NH_3$ reduction. This attributes to the reaction of molecular ozone with ammonia upon ozone decomposition, with $NO_3^-$ being the end product. Thus, the formation and increase in the nitrate ($NO_3^-$) concentration in the BOT wastewater, as shown in the above-mentioned reactions, corresponds to the decrease in the concentration of ammonia, indicating that ammonia was oxidized by ozone. The reactions have also elucidated the lowering of solution pH due to the formation of hydrogen ions ($H^+$) during ammonia oxidation, i.e., the decrease in solution pH is directly associated with the extent of ammonia decomposition. Also, the decomposition of ammonia was found to be much more at higher initial pH compared to

a lower one, resulting in the production of more $H^+$ ions, and as such, the pH decreased more [12]. As a result, for an optimum ozone generation rate and operating time of 1.33 mg $s^{-1}$ and 40 min, respectively, the initial concentration of ammonia decreases from 130 mg $L^{-1}$ to a final concentration of 72 mg $L^{-1}$. Figure 4.4 shows the ammonia removal efficiency with ozone generation rate and ozonation time. It was observed from Figure 4.4 that the ammonia decomposition increases from 20.2% to 44.7%, with an increase in ozone generation rate from 1.00 mg $s^{-1}$ to 1.33 mg $s^{-1}$. Moreover, an increase in nitrate concentration with the decomposition of ammonia for the optimum ozone generation rate of 1.33 mg $s^{-1}$ and treatment time of 40 min is shown in Figure 4.5. In Figure 4.5 at time (t) = 0, the nitrate concentration of 12 mg $L^{-1}$ corresponds to the initial concentration of nitrate present in the feed, which eventually increases during the oxidation of ammonia with analysis time. Although the nitrate formation intensifies with the continuation of ammonia decomposition, it was observed that the concentration of $NO_3^-$ increases from 12 mg $L^{-1}$ and reaches a maximum concentration of 31 mg $L^{-1}$ at the optimum operating condition, which is well below its permissible limit (45 mg $L^{-1}$).

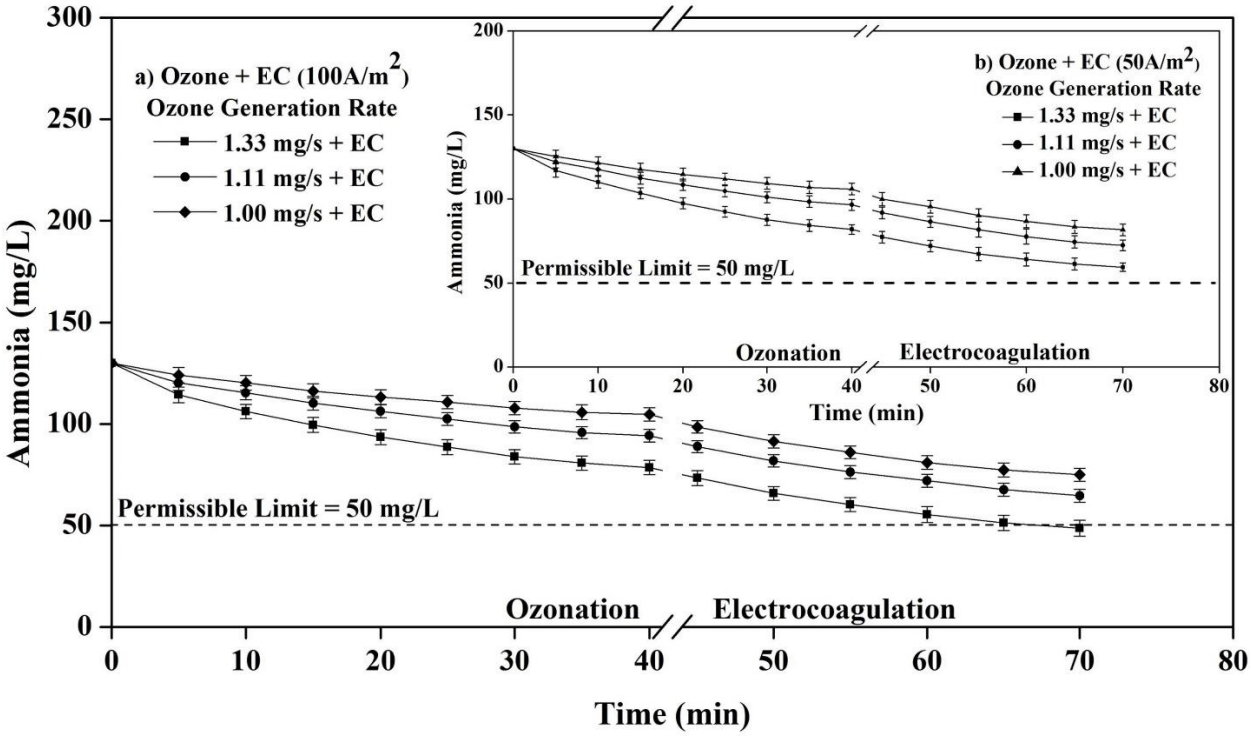


**Fig. 4.4:** Effect of ozone generation rates on ammonia-N removal with treatment time. Outset: 100 A $m^{-2}$ current density, Inset: 50 A $m^{-2}$ current density

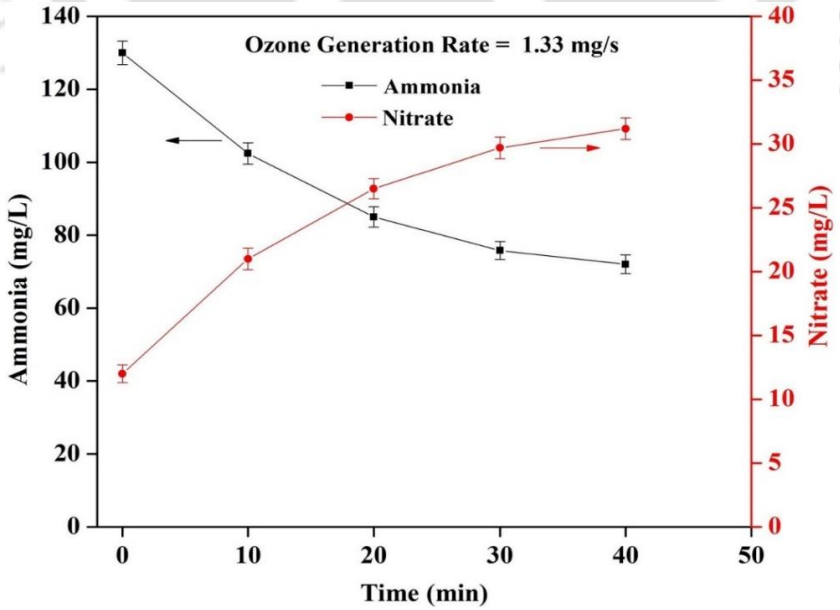


**Fig. 4.5:** Effect of ammonia oxidation on nitrate formation at optimum ozone generation rate

During electrocoagulation, the concentration of ammonia further decreases from 72 mg $L^{-1}$ (obtained at 1.33 mg $s^{-1}$) to 48.5 mg $L^{-1}$ for an optimum current density of 100 A $m^{-2}$ and electrolysis time of 30 min as seen in Figure 4.4. It was seen during electrocoagulation that the corresponding elimination rate was only 32.5%, even though a higher current density (100 A $m^{-2}$) was applied. Electrocoagulation contributes less significantly to the reduction of $NH_3$, suggesting a weaker affinity of ammonia towards the electrogenerated coagulants. However, ammonia stripping due to an increase in pH to alkaline values as well as an increase in temperature (Joule effect) may be responsible for the reduction in ammonia concentration during the process. The process, as such, is intensified under alkaline conditions as the evolution of hydrogen on cathode enhances the reduction of ammonia by stripping [13]. The generation of $OH^-$ ions during oxygen evolution partly decomposes ammonia into nitrogen under neutral and acidic conditions and not by direct electrode reaction. Besides, reduction in ammonia concentration could also be due to the chlorides already present in the wastewater, which plays an important role in indirect oxidation of ammonia during the electrochemical reaction as well as due to the generation of molecular chlorine, i.e., at the anode, chloride ($Cl^-$) is oxidized to chlorine during electrolysis [14]. A protective oxide film is formed on the electrode surface as the electrodes used in the experiment are reactive, causing erosion of the metal. Chlorine ions are discharged due to the increased potential caused by the film, resulting in the generation of chlorine gas during electrolysis. Hypochlorous acid is formed from the hydrolyzes of molecular chlorine, which depending upon the pH, consecutively changes to hypochlorite ion. Ammonia could be easily decomposed into by-products, presumably to nitrogen gas by both hypochlorite ion and hypochlorous acid due to their high oxidative potentials. Thus the presence of chlorides showed significant improvement in terms

of capacity and selectivity for the transformation of ammonia into $N_2$ gas during the electrochemical process as shown in the reactions below [15]:

$$2Cl^- \rightarrow Cl_2 + 2e^- \quad (4.6)$$

$$Cl_2 + H_2O \rightarrow HOCl + H^+ + Cl^- \quad (4.7)$$

$$HOCl \rightarrow OCl^- + H^+ \quad (4.8)$$

$$2NH_3 + 3HOCl \rightarrow N_2 + 3H^+ + 3Cl^- + 3H_2O \quad (4.9)$$

$$2NH_3 + 2OCl^- \rightarrow N_2 + 2H^+ + 2Cl^- + 2H_2O + 2e^- \quad (4.10)$$

In addition, the amount of nitrates formed during ozonation was found to decrease from 31 mg $L^{-1}$ to 7.8 ± 0.5 mg $L^{-1}$ at the end of the electrocoagulation process. The phenomenon for nitrate degradation can be attributed to the adsorption of nitrate ions onto the surface of the growing aluminum hydroxide flocs, followed by its removal via sedimentation or flotation from the treated water.

### 4.2.4 Removal of iron by hybrid ozone assisted electrocoagulation process

During the oxidation of iron by $O_3$, ferrous ions ($Fe^{2+}$) gets converted to ferric state ($Fe^{3+}$), followed by precipitation of the oxidized salts as ferric hydroxide ($Fe(OH)_3$). The clear solution is analysed for residual ($Fe^{2+}$). Under acidic condition, ozone oxidizes $Fe^{2+}$ rapidly into $Fe^{3+}$ as suggested by the Eq. (12) and Eq. (13). For the generation of $HO^{\bullet}$ radicals, $Fe^{2+}$ acts as a catalyst during the decomposition of ozone. Meanwhile, an intermediate species $FeO^{2+}$ is formed which rapidly evolves to $HO^{\bullet}$ radical during the reaction of $O_3$ with $Fe^{2+}$ [16]. Several runs were performed to validate the effect of the operating parameters such as ozone generation rate and ozone reaction time on the removal efficiency of $Fe^{2+}$ ions. Thus, iron removal involves transformation of the

soluble form into insoluble oxides, which can be filtered out of water. $Fe^{2+}$ can therefore be easily oxidized by $O_3$ as shown in the reactions below [17]:

$$Fe \rightarrow Fe^{2+}(aq) + 2e^{-} \quad (4.11)$$

$$Fe^{2+} + O_3 \rightarrow FeO^{2+} + O_2 \quad (4.12)$$

$$FeO^{2+} + H_2O \rightarrow HO^{\bullet} + Fe^{3+} + OH^{-} \quad (4.13)$$

$$Fe^{3+} + 3OH^{-} \rightarrow Fe(OH)_3 \quad (4.14)$$

$$2Fe^{2+} + O_3 + 5H_2O \rightarrow 2Fe(OH)_3 + O_2 + 4H^{+} \quad (4.15)$$

Ferric ions ($Fe^{3+}$), depending upon the pH range, transform into $Fe(OH)_3$ and precipitates. Thus, the formation of $Fe(OH)_3$ precipitates due to the oxidation of $Fe^{2+}$ to $Fe^{3+}$ is responsible for the reduction of $Fe^{2+}$. Since the oxidation of $Fe^{2+}$ is faster, less oxidation power is required for the conversion of $Fe^{2+}$ to $Fe(OH)_3$. Since $Fe(OH)_3$ is not soluble in water, it is assumed that under equilibrium, it will have gradually descended to the bottom of the container and will not contribute further to any kind of reaction in the solution and can be easily filtered out of the water [18]. Ozone solubility in water is higher at low temperatures (in this study, the operating temperature is 20 °C). Therefore, the oxidation reaction of soluble iron salts is increased as long as the solubility of ozone is increased, resulting in higher percent removal of $Fe^{2+}$ from the solution. During ozonation, the direct reaction between $Fe^{2+}$ and $O_3$ predominates at lower pH resulting in efficient iron oxidation. As a result, for an optimum ozone generation rate and operating time of 1.33 mg $s^{-1}$ and 40 min, respectively, the initial concentration of iron decreases from 7.3 mg $L^{-1}$ to a final concentration of 2.6 mg $L^{-1}$. Figure 4.6 shows the iron removal efficiency with ozone generation rate and ozonation time. It was observed that with an increase in ozone generation rate from 1.00 mg $s^{-1}$ to 1.33 mg $s^{-1}$, the iron removal percentage also increases from 51.4% to 64.5%, as shown in Figure 4.6.

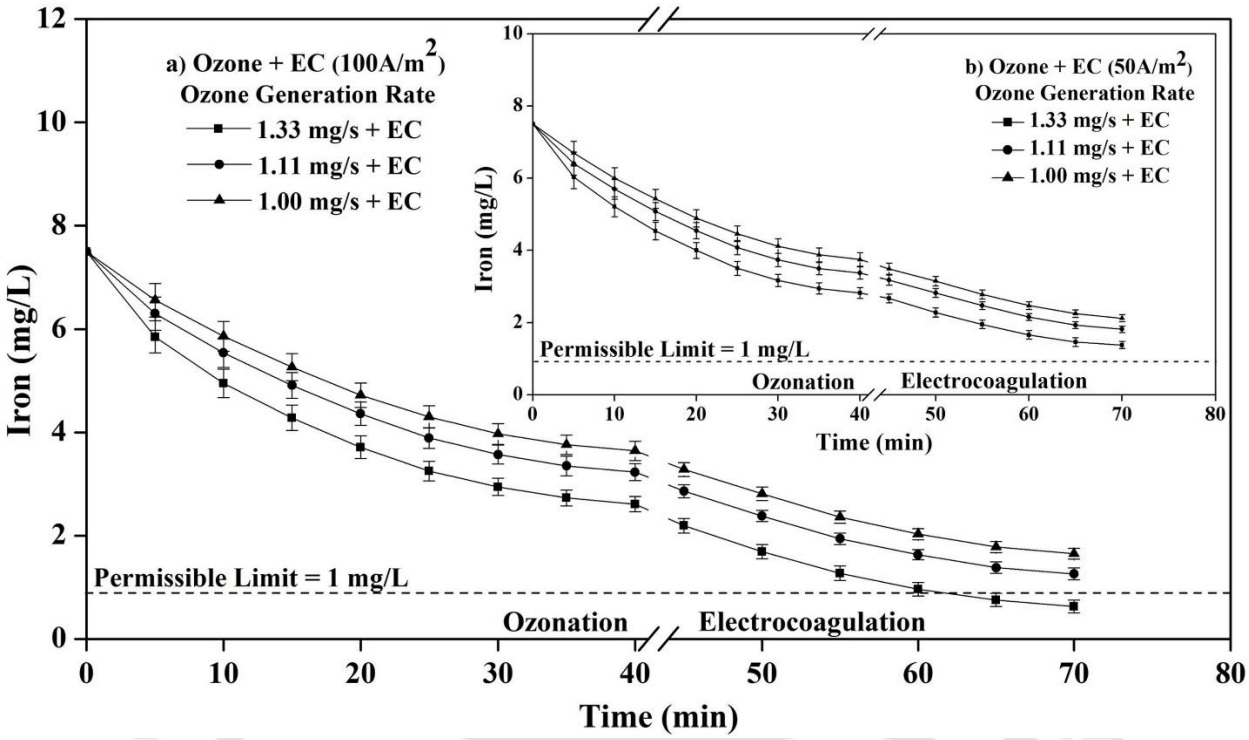


**Fig. 4.6:** Effect of ozone generation rates on iron removal with treatment time. Outset: 100 A $m^{-2}$ current density, Inset: 50 A $m^{-2}$ current density

Moreover, during the electrocoagulation process, the iron concentration further decreases from 2.6 mg $L^{-1}$ (obtained at 1.33 mg $s^{-1}$) to 0.6 mg $L^{-1}$ for an optimum current density of 100 A $m^{-2}$ and electrolysis time of 30 min, as seen in Figure 4.6. The phenomenon for iron removal by electrocoagulation can be explained by the formation of aluminum hydroxide flocs and the simultaneous adsorption of $Fe^{2+}$ on its surface. The pH and the redox potential determines the state of iron in the solution. When the pH of the solution is above 4, the dissolved iron species are mostly divalent as very little soluble $Fe(OH)_3$ are formed by $Fe^{3+}$ ions. Even though the bulk pH remains well below the value corresponding to the solubility product, the formed $Fe(OH)_2$ particles remain insoluble even after their transport to the liquid bulk [19]. As such, improvement in removal

efficiency is mainly due to the local formation of Fe(II) hydroxide and its subsequent oxidation on the surface of the Al flocs. As per Faraday's law, the amount of adsorbent ($Al(OH)_3$) generated is directly proportional to the applied current density. Thus, an increase in the concentration of the adsorbent (with an increase in current density) increases the amount of iron adsorption on its surface. This indicates the dependency of the adsorption process upon the available binding sites for iron. Aluminum hydroxide generated upon hydrolysis reaction results in the formation of reactive Al(III) – Fe(II) complexes, which enhances $Fe^{2+}$ oxidation as well as adsorption of $Fe^{2+}$ on the surface of $Al(OH)_3$ flocs [20]. With the increase in solution pH, the dissolved iron, i.e., $Fe^{2+}$ hydrolyzes and forms precipitates. The shape and size of the particles formed after coagulation and its subsequent adsorption on the active sites of the generated $Al(OH)_3$ flocs mainly determines the precipitation process. An adequate amount of coagulants in the medium leads to the adsorption of iron hydroxide (in the form of brown flocks), which determines the removal of iron at higher pH. As such larger flocs were formed that settled down as precipitates at the bottom of the reactor and can be observed in the form of a reddish-brown sludge after the completion of the experiment. The reason may be due to the production of more amount of $Al(OH)_3$ which in turn results in increased adsorption of $Fe(OH)_2$ from the solution and subsequent precipitation at the bottom [21]. The maximum removal efficiency attained during the electrocoagulation process was 77.0% for the current density and electrolysis time of 100 A $m^{-2}$ and 30 min, respectively. The mechanism of iron removal by ozone assisted electrocoagulation process is shown in Figure 4.7.

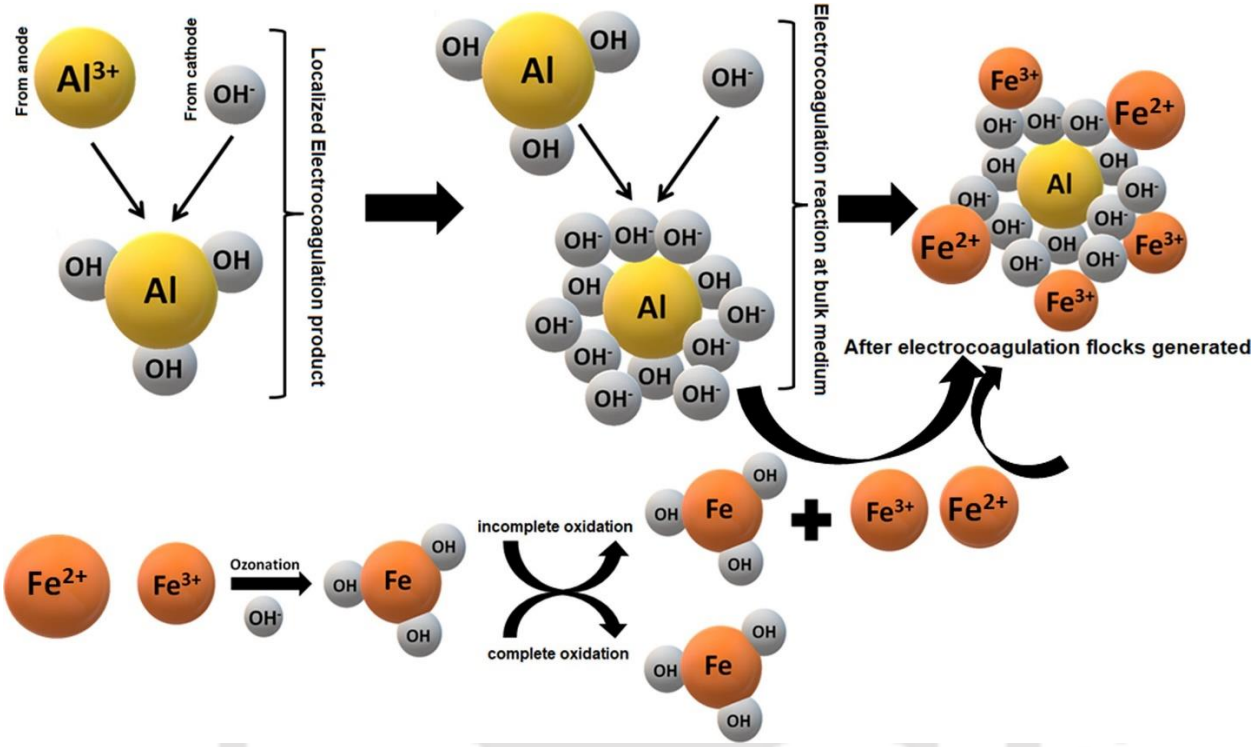


**Fig. 4.7:** Iron removal mechanism via ozone assisted electrocoagulation process

Furthermore, Table 4.1 depicts the feed/initial composition and the percentage reduction in pollutant concentration viz. color, ammonia, and iron using ozone assisted electrocoagulation process. Table 4.2 provides a comparative analysis of the ozone assisted electrocoagulation process with other reported hybrid water treatment techniques for industrial wastewater. It was found that the present study resulted in a much effective degradation of the target pollutants as compared to other hybrid techniques reported in the literature.

**Table 4.1:** Removal rate of pollutants (color, ammonia-N, and iron) during ozone assisted electrocoagulation process

| Parameters | Feed ($mg\ L^{-1}$) | Final concentration (mg/L) | | | | | | | | Permissible limit ($mg\ L^{-1}$) [WHO] |
|---|---|---|---|---|---|---|---|---|---|---|
| | | Current density 50 A $m^{-2}$ | | | Percentage removal* (%) | Current density 100 A $m^{-2}$ | | | Percentage removal* (%) | |
| | | 1.00 $mg\ s^{-1}$ | 1.11 $mg\ s^{-1}$ | 1.33 $mg\ s^{-1}$ | | 1.00 $mg\ s^{-1}$ | 1.11 $mg\ s^{-1}$ | 1.33 $mg\ s^{-1}$ | | |
| Color (Hazen) | 2450 | 370 ± 5 | 285 ± 5 | 140 ± 3 | 94.2 | 300 ± 4 | 205 ± 5 | 45 ± 2 | 98.2 | 300 |
| Ammonia-N | 130 | 92 ± 3 | 80.5 ± 2 | 63 ± 3 | 51.4 | 84 ± 2 | 70 ± 2 | 48.5 ± 1 | 62.8 | 50 |
| Iron | 7.3 | 2.4 ± 0.4 | 2.0 ± 0.2 | 1.4 ± 0.3 | 79.5 | 1.9 ± 0.2 | 1.4 ± 0.2 | 0.6 ± 0.1 | 90.6 | 1.0 |

***** At the optimum ozone generation rate of 1.33 $mg\ s^{-1}$ for both current densities 50 and 100 A $m^{-2}$.

**Table 4.2:** Comparison of performance efficiency in terms of color degradation with other hybrid treatment processes

| **Ozone-based hybrid process** | **Type of wastewater** | **Pollutant removal** | **Reference** |
|---|---|---|---|
| Ozone-UV | Synthetic samples of citrus wastewater | 68.4% color removal | [22] |
| Ozone-UV | Polyester and acetate fiber dyeing effluent | 93% color removal | [23] |
| Ozone-UV | Azo dyes | 95% color removal | [24] |
| Ozone-$H_2O_2$ | Textile industry wastewater | 60–63% color removal | [25] |
| Ozone-EC | C.I. reactive blue 19 in synthetic water | 96% color removal | [26] |
| Ozone-EC | Industrial wastewater | 90% color removal | [27] |
| Ozone-EC | Azo dyes | 94% color removal | [28] |
| Heterogeneous catalytic ozonation | Textile dyeing wastewater | 85% color removal | [29] |
| Ozone-EC | Steel plant wastewater | 98.2% color removal and 90.6% iron removal | **Present Work** |

## 4.3 Kinetic modelling of colour, ammonia-N and iron reduction

Degradation of the pollutants can be described with the help of the pseudo first-order kinetic model as [30]:

$$\frac{dC_p}{dt} = -k_{obs}\, C_p \qquad (4.16)$$

where, $C_p$ is the concentration of the pollutant and $k_{obs}$ ($min^{-1}$) is the observed first order rate constant. Integrated form of the above equation is as below:

$$C_p = C_p^0\, e^{-k_{obs}t} \qquad (4.17)$$

where, $C_p^0$ is the initial concentration of the pollutant (mg $L^{-1}$) and t is the residence time (min). Therefore, $k_{obs}$ ($min^{-1}$) was evaluated from the residence time versus regression of ln $C_p$. In this study, it was observed that the highest pollutant reduction was obtained at an ozone generation rate of 1.33 mg $s^{-1}$, whereas with a decrease in the ozone generation rate up to 1 mg $s^{-1}$, the reduction percentage decreases. The increase in pollutant reduction at an $O_3$ generation rate of 1.33 mg $s^{-1}$ was attributed to the higher oxidation of the pollutants. Hence with the increasing generation rate of $O_3$, the percentage reduction of pollutants also increases.

Table 4.3 represents the values of $k_{obs}$ and $R^2$ at different ozone generation rates for colour, iron, and ammonia-N, respectively. The regression line of ln $C_p$ versus t for ammonia-N showed that the rate constant ($k_{obs}$ = 0.0107 $min^{-1}$) is highest at ozone generation rate of 1.33 mg $s^{-1}$ whereas it decreases for 1.11 mg $s^{-1}$, ($k_{obs}$ = 0.0073 $min^{-1}$) and 1.0 mg $s^{-1}$ ($k_{obs}$ = 0.0051 $min^{-1}$), respectively. Similarly, the rate constants of color, and iron were $k_{obs}$ = 0.0951 and 0.0229 $min^{-1}$, respectively, for an ozone generation rate of 1.33 mg $s^{-1}$. However, at a lower ozone generation

rate of 1.11 mg $s^{-1}$, the rate constants were found to decrease ($k_{obs}$ = 0.0927 and 0.0203 $min^{-1}$, respectively). Similar trend was also observed for an ozone generation rate of 1.0 mg $s^{-1}$ ($k_{obs}$ = 0.0915 and 0.0175 $min^{-1}$, respectively). The results obtained from Table 4.3 depicted that for cation (e.g. iron) the pseudo first-order kinetics fitted the reaction quite well $R^2$ = 0.988, 0.981, 0.973 for increasing $O_3$ generation rate of 1.33, 1.11 and 1.0 mg $s^{-1}$, respectively. It can also be observed that for an ozone generation rate of 1.33 mg $s^{-1}$, the highest $R^2$ of 0.985 and 0.977 were obtained for ammonia and color, respectively. The fitting of reaction kinetics, according to pseudo first-order reaction, revealed that the cations responded well to the reaction. The results depicted that the nascent oxygen of the $O_3$ had a greater affinity towards cations compared to other compounds. However, it can be concluded that the cations, as well as the other compounds, responded quite well to the pseudo first-order reaction kinetic.

**Table 4.3:** Observed reaction rate and $R^2$ values at different ozone generation rates

| **Parameters** | **1.33 mg $s^{-1}$** | | **1.11 mg $s^{-1}$** | | **1.0 mg $s^{-1}$** | |
|---|---|---|---|---|---|---|
| | **$k_{obs}$ ($min^{-1}$)** | **$R^2$** | **$k_{obs}$ ($min^{-1}$)** | **$R^2$** | **$k_{obs}$ ($min^{-1}$)** | **$R^2$** |
| Colour | 0.0951 | 0.977 | 0.0927 | 0.973 | 0.0915 | 0.968 |
| Ammonia | 0.0107 | 0.985 | 0.0073 | 0.977 | 0.0051 | 0.974 |
| Iron | 0.0229 | 0.988 | 0.0203 | 0.981 | 0.0175 | 0.973 |

## 4.4 Size determination of ozone microbubbles

The photographic technique was utilized for measuring the size of the microbubble, whereas the sauter mean diameter of the bubble was calculated from Eq. (18). A digital camera (D5300 24

M P, Nikon, India) was used to capture the images of the microbubble. An image processing software (Image J Software, 9.0) was utilized for analyzing the bubble size. A total of 3–4 images were taken for each ozone generation rate, and the best quality image was chosen for the analysis. The sauter mean bubble diameter ($d_{32}$) can be calculated from the following equation [31]:

$$d_{32} = \frac{\sum_{i=1}^{n} n_i d_{bi}^3}{\sum_{i=1}^{n} n_i d_{bi}^2} \quad (4.18)$$

The sauter mean diameter of the microbubble was found to be 425 µm, and the range of the microbubble size varied between 20 µm and 650 µm. The bubble size increases as it rises upward and hence larger bubbles were obtained at the top of the reactor. The sauter mean diameter and the range of microbubble size were found to be in accordance with the study carried out by Patel et al. (2019) [32].

## 4.5 Electrode corrosion and variation in film thickness

The electrode corrosion study provides an overview on the sustainability of the EC process. This phenomenon is typically measured in terms of electrode weight reduction during the experiment. Corrosion is often accelerated by higher current densities and high pollutant concentrations in the target water; nevertheless, as the electrode distance increases, corrosion decreases. Also, higher dissolution of metal ions at elevated current densities increases the electrode corrosion [33]. It was found that the corrosion increased from 27.2 to 45.1 mg with an increase in the current density from 50 to 150 A $m^{-2}$. Nonetheless, with an increase in the electrode distance from 0.005 to 0.02 m, the extent of corrosion decreases from 45.1 to 33.3 mg. The reason may be attributed to the change in the production of aluminium hydroxide flocs during the process. As electrocoagulation

continues, a gelatinous hydroxide layer gradually forms around the electrodes. With prolonged electrolysis time, more amount of hydroxides are formed, which in turn adheres to the electrode surface and produces an extra blockade for anodic dissolution, thus lowering the process performance. The film thickness can be calculated from the equation below [34]:

$$\delta \approx \frac{(m_1 - m_2) \times 10^{-6}}{\rho \times A} \quad (4.19)$$

Here, δ is the film-thickness (μm), $m_1$ is the weight of the electrodes (mg) after the experiment without cleaning, $m_2$ is the weight of the electrodes (mg) after the experiment with cleaning, ρ is the density of the film (g $L^{-1}$) and A is the area of the electrodes ($m^2$). Increase in film thickness was observed from 6.1 to 8.8 μm as current density proceeds from 50 to 150 A $m^{-2}$. The increase in current density favoured the anodic oxidation that leads to the rise in the generation of gelatinous hydroxide. This hydroxide in turn adheres itself to the surface of the electrode (cathode) in the form of a film which increases with the increase in the EC time. On the other hand, at higher electrode distance it was found that lesser gelatin hydroxide was produced. As such, the film thickness increases from 6.7 to 7.6 μm over the electrode surface, when the inter-electrode distance decreased from 0.02 to 0.005 m at the optimum current density of 100 A $m^{-2}$ for 30 min.

## 4.6 Estimation of energy consumption and operating cost of the hybrid process

During ozonation, a primary cost analysis was conducted which mainly considers the energy cost of the whole operation (US$ $m^{-3}$ of solution). Figure 4.8 (a) depicts the change in operating cost and energy cost with ozonation time, for an optimum ozone generation rate of 1.33 mg $s^{-1}$. Estimation of the operating cost was carried out as per the following:

$$\text{Operating cost}_{(\text{ozonation})} = q \times Q_{\text{energy}} \quad (4.20)$$

where, $Q_{\text{energy}}$ is the electricity consumption needed for the removal of pollutants. ‘‘q” is the rate of electrical energy. The cost of electricity consumption was taken as per its price in the year 2019 (0.0936 US$ $kWh^{-1}$), for the state of Assam (India). The electrical energy consumption can be expressed as [35]:

$$Q_{\text{energy}} = \frac{\eta_G \times G_{O_3} \times C \times t}{V_L} \quad (4.21)$$

Here, $\eta_G$ represents the specific energy consumption of ozone generation (21.97 kWh $kg^{-1}$), $G_{O_3}$ is the ozone generation rate (mg $s^{-1}$), C is the unit conversion factor, t represents the ozonation time (min), and $V_L$ represents the effluent volume ($m^3$). Considering the power consumption of the ozonation process to be 51 W for an ozone generation rate of 1.00 mg $s^{-1}$, the energy cost was found to increase from 7.13 to 27.53 US$ $m^{-3}$, with an increase in the operating time. Thus, the operating cost increases from 0.667 US$ $m^{-3}$ for 10 min of operating time to 2.67 US$ $m^{-3}$ after 40 min. Likewise, for an ozone generation rate of 1.33 mg $s^{-1}$ with a power consumption of 105.2 W, the energy cost was found to increase from 14.71 to 58.61 US$ $m^{-3}$, as the operating time increases. As such, the operating cost increases from 1.37 US$ $m^{-3}$ for 10 min of operating time to 5.48 US$ $m^{-3}$ at the end of 40 min.

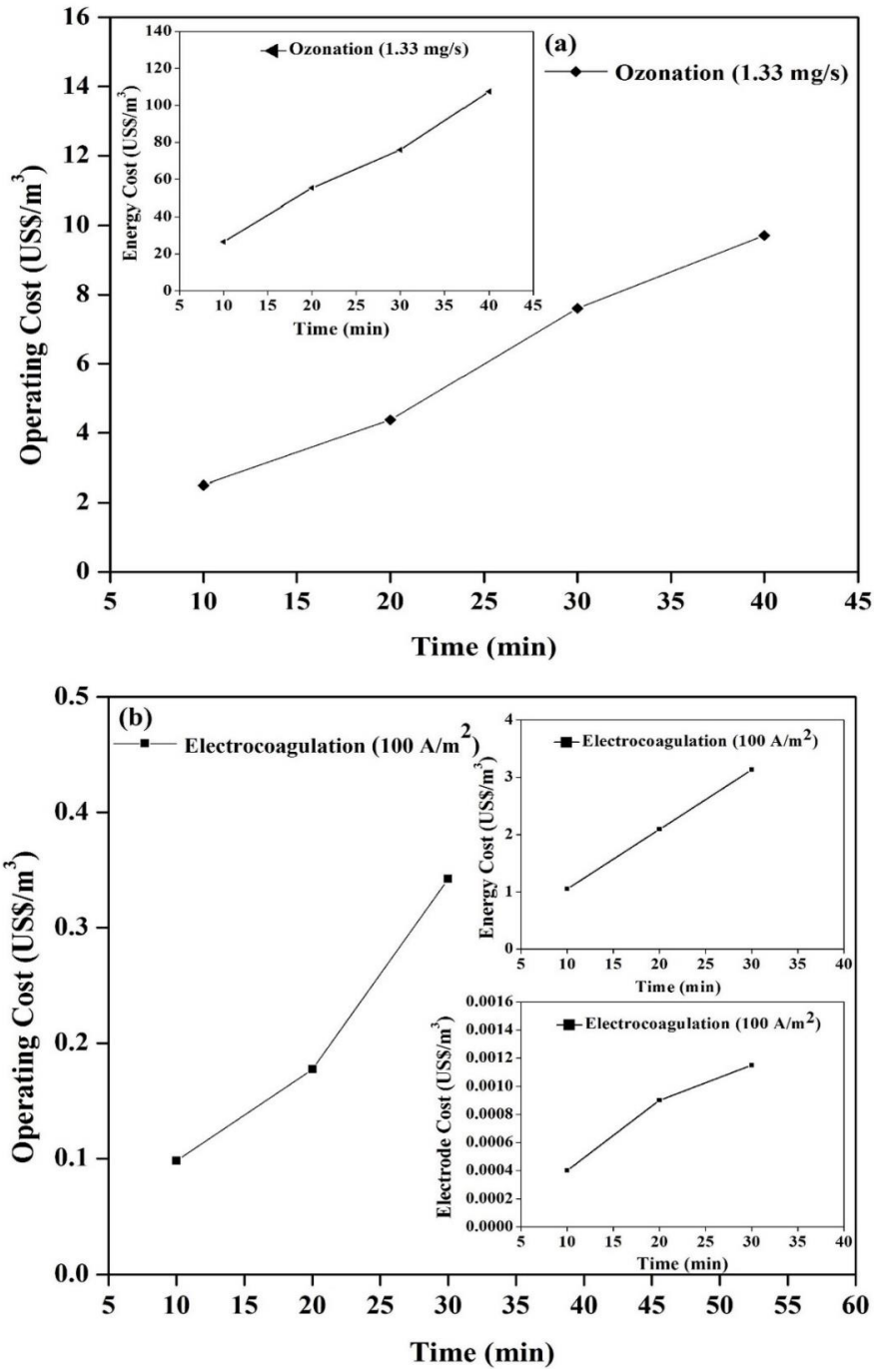


**Fig. 4.8:** At optimal operating condition: (a) Change in operating cost with ozonation time. Inset: energy cost with ozonation time, and (b) Change in operating cost with electrolysis time. Inset (top): energy cost with electrolysis time, Inset (bottom): electrode cost with electrolysis time.

Similarly, the total cost sustained during the treatment determines the feasibility of the electrocoagulation process. In this case, the cost of operation involves electricity, chemical, sludge disposal, electrode cost, and fixed cost. For simplicity, the determination of the operating cost for the electrocoagulation process involves only the electricity rate and the cost of electrodes. The operating cost was calculated as follows [36]:

$$\text{Operating cost}_{(\text{electrocoagulation})} = p \times Q_{\text{electrode}} + q \times Q_{\text{energy}} \quad (4.22)$$

where, $Q_{\text{energy}}$ and $Q_{\text{electrode}}$ are the consumption of electrical energy and electrode materials respectively. ‘‘p” represents the electrode cost (2.0462 US$ $kg^{-1}$ of aluminum) and ‘‘q” represents the electricity cost (0.0936 US$ $kWh^{-1}$) for the state of Assam (India) in the year 2019. The electrical energy consumption can be expressed as:

$$Q_{\text{energy}} = \frac{I \times V \times t}{V_L} \quad (4.23)$$

Here I represent the current (A), V represents the voltage (V), t represents the electrocoagulation time (s), and $V_L$ represents the effluent volume ($m^3$). Electrode consumption was estimated from Faraday’s law as follows [37]:

$$Q_{\text{electrode}} = \frac{I \times t \times M.W}{F \times z \times V_L} \quad (4.24)$$

Here M.W represents the molar mass of aluminum (26.98 g $mol^{-1}$), I represent the current (A), t represents the electrocoagulation time (s), VL represents the effluent volume (m3), F represents the Faraday’s constant (96,487 C $mol^{-1}$) and z represents the number of electrons transferred (z = 3). Figure 4.8 (b) depicts the change in energy cost, electrode cost, as well as an operating cost,

with electrocoagulation time, for an optimum current density of 100 A $m^{-2}$. The energy cost and the electrode cost increase as the current density increases due to high energy consumption and enhanced anodic oxidation, respectively. As such, the electrode cost is increased from 0.00061 to 0.0018 US$ $m^{-3}$, and the energy cost is increased from 1.57 to 4.70 US$ $m^{-3}$. The total cost of operation was thus increased to 0.157, 0.342, and 0.443 US$ $m^{-3}$ with increasing current densities of 50, 100, and 150 A $m^{-2}$, respectively, at the end of 30 min of analysis time. Hence, the overall operating cost of the combined process after 70 min of total treatment time ($O_3$ + EC) is given as:

$$\text{Operating cost}_{(\text{Total})} = \text{Operating cost}_{(\text{ozonation})} + \text{Operating cost}_{(\text{electrocoagulation})} \quad (4.25)$$

$$= 5.822 \text{ US\$ } m^{-3}$$

The operating cost for the present study was found to be economical when compared with other hybrid techniques utilized for treating industrial wastewater, as shown in Table 4.4.

**Table 4.4:** Comparison of cost estimation for the ozone assisted electrocoagulation process with other hybrid treatment methods

| Methods used | Types of wastewater | Operating cost | References |
|---|---|---|---|
| Electrocoagulation-Microfiltration (EC-MF) | Synthetic wastewater | 7.91 US$ $m^{-3}$ | [38] |
| Electrocoagulation-Ozonation (EC-$O_3$) | Textile wastewater | 11.86 US$ $m^{-3}$ | [39] |
| Ion Exchange-Reverse Osmosis (IE-RO) | Potato processing wastewater | 1.8 US$ $m^{-3}$ | [40] |
| Electrocoagulation-Microfiltration (EC-MF) | Synthetic wastewater | 197 US$ $m^{-2}$ | [41] |
| Electrochemical Oxidation-Ozonation (EO-$O_3$) | Synthetic wastewater (SW) and Olive mill wastewater (OW) | 12.4 US$ $m^{-3}$ (OW)<br>80.8 US$ $m^{-3}$ (SW) | [42] |
| Hydrogen Peroxide-Ultraviolet lamp ($H_2O_2$/UV) and Ozonation ($O_3$) | Textile dye wastewater | $H_2O_2$/UV lamp<br>74 € $m^{-3}$ ≅ 83 US$ $m^{-3}$<br>Ozonation<br>54 € $m^{-3}$ ≅ 60.6 US$ $m^{-3}$ | [43] |
| Ultrasonication-Ozonation (US-$O_3$) | Bore well water | Ultrasonication-Ozonation<br>8.0 US$ $m^{-3}$ | [44] |
| Ozonation-Electrocoagulation ($O_3$-EC) | Steel plant wastewater | 5. 822 US$ $m^{-3}$ | **Present Work** |

## 4.7 Summary of work

This work established the use of a hybrid ozone assisted electrocoagulation process for the treatment of color, iron, and ammonia from real BOT wastewater of the steel industry. A decrease of initial pH was observed from 7.72 to 3.0 during the ozonation process, owing to the formation of by-products (organic anions along with inorganic acids) of acidic nature. On the other hand, the pH increased to 8.2 after the subsequent electrocoagulation process. For an optimum ozone generation rate of 1.33 mg $s^{-1}$, the ozonation process alone was sufficient for the reduction of colour below its permissible limit. However, the combined process of ozone assisted electrocoagulation was required for other parameters viz. iron, and ammonia to ensure compliance with the water quality standards and regulatory requirements. The kinetic study performed indicated that the degradation of the pollutants followed the pseudo first-order kinetic model. The highest rate constant ($k_{obs}$) and pollutant reduction were obtained at the optimum ozone generation rate of 1.33 mg $s^{-1}$ for all the contaminants viz. iron, ammonia, and color. Size determination study of the ozone microbubbles showed that the bubble size varied between 20 µm and 650 µm, with the sauter mean diameter of 425 µm. The combined effect of ozone and electrocoagulation process was found to be very efficient not only in terms of pollutant removal, but also from the economic perspective. The hybrid ozone assisted electrocoagulation process showed a much lower operating cost of 5.822 US$ $m^{-3}$. Hence, this combined method could be efficient and useful for the treatment of different industrial effluents. However, a pilot plant study might be needed before an industrial-scale implementation.

## References

[1] S.M. de A.G.U. de Souza, K.A.S. Bonilla, A.A.U. de Souza, Removal of COD and color from hydrolyzed textile azo dye by combined ozonation and biological treatment, J. Hazard. Mater. 179 (2010) 35–42. https://doi.org/10.1016/j.jhazmat.2010.02.053.

[2] S.F. Weiss, M.L. Christensen, M.K. Jørgensen, Mechanisms behind pH changes during electrocoagulation, AIChE J. 67 (2021) e17384. https://doi.org/doi.org/10.1002/aic.17384.

[3] C.D. Adams, S. Gorg, Effect of pH and Gas-Phase Ozone Concentration on the Decolorization of Common Textile Dyes, J. Environ. Eng. 128 (2002) 293–298. https://doi.org/10.1061/(asce)0733-9372(2002)128:3(293).

[4] V. Preethi, K.S. Parama Kalyani, K. Iyappan, C. Srinivasakannan, N. Balasubramaniam, N. Vedaraman, Ozonation of tannery effluent for removal of cod and color, J. Hazard. Mater. 166 (2009) 150–154. https://doi.org/10.1016/j.jhazmat.2008.11.035.

[5] K. Turhan, I. Durukan, S.A. Ozturkcan, Z. Turgut, Decolorization of textile basic dye in aqueous solution by ozone, Dye. Pigment. 92 (2012) 897–901. https://doi.org/10.1016/j.dyepig.2011.07.012.

[6] N. Daneshvar, A. Oladegaragoze, N. Djafarzadeh, Decolorization of basic dye solutions by electrocoagulation: An investigation of the effect of operational parameters, J. Hazard. Mater. 129 (2006) 116–122. https://doi.org/10.1016/j.jhazmat.2005.08.033.

[7] J.S. Do, M.L. Chen, Decolourization of dye-containing solutions by electrocoagulation, J. Appl. Electrochem. 24 (1994) 785–790. https://doi.org/10.1007/BF00578095.

[8] D. Ghosh, C.R. Medhi, H. Solanki, M.K. Purkait, Decolorization of Crystal Violet Solution by Electrocoagulation, J. Environ. Prot. Sci. 2 (2008) 25–35. https://doi.org/10.1016/j.eps.2008.11.035.

[9] S.H. Lin, C.L. Wu, Removal of nitrogenous compounds from aqueous solution by ozonation and ion exchange, Water Res. 30 (1996) 1851–1857. https://doi.org/10.1016/0043-1354(95)00329-0.

[10] J. Hoigne, H. Bader, Ozonation of Water: Kinetics of Oxidation of Ammonia by Ozone and Hydroxyl Radicals, Environ. Sci. Technol. 12 (1978) 79–84. https://doi.org/10.1021/es60137a005.

[11] H. Liu, L. Chen, L. Ji, Ozonation of ammonia at low temperature in the absence and presence of MgO, J. Hazard. Mater. 376 (2019) 125–132. https://doi.org/10.1016/j.jhazmat.2019.05.034.

[12] S. Khuntia, S.K. Majumder, P. Ghosh, Removal of ammonia from water by ozone microbubbles, Ind. Eng. Chem. Res. 52 (2013) 318–326. https://doi.org/10.1021/ie302212p.

[13] S. Aoudj, A. Khelifa, N. Drouiche, Removal of fluoride, SDS, ammonia and turbidity from semiconductor wastewater by combined electrocoagulation–electroflotation, Chemosphere. 180 (2017) 379–387. https://doi.org/10.1016/j.chemosphere.2017.04.045.

[14] N.M. Niza, M.S. Yusoff, M.A.A.M. Zainuri, M.I. Emmanuel, A.M.H. Shadi, M.H.M. Hanif, M.A. Kamaruddin, Removal of ammoniacal nitrogen from old leachate using batch electrocoagulation with vibration-induced electrode plate, J. Environ. Chem. Eng. 9 (2021) 105064. https://doi.org/10.1016/j.jece.2021.105064.

[15] J. wei Feng, Y. bing Sun, Z. Zheng, J. biao Zhang, S. Li, Y. chun Tian, Treatment of tannery wastewater by electrocoagulation, J. Environ. Sci. 19 (2007) 1409–1415. https://doi.org/10.1016/S1001-0742(07)60230-7.

[16] N. Kishimoto, S. Ueno, Catalytic Effect of Several Iron Species on Ozonation, J. Water Environ. Technol. 10 (2012) 205–215. https://doi.org/10.2965/jwet.2012.205.

[17] R. El Araby, S. Hawash, G. El Diwani, Treatment of iron and manganese in simulated groundwater via ozone technology, Desalination. 249 (2009) 1345–1349. https://doi.org/10.1016/j.desal.2009.05.006.

[18] J. Sallanko, E. Lakso, J. Röpelinen, Iron behavior in the ozonation and filtration of groundwater, Ozone Sci. Eng. 28 (2006) 269–273. https://doi.org/10.1080/01919510600721795.

[19] D. Ghosh, C.R. Medhi, M.K. Purkait, Treatment of drinking water containing iron using Electrocoagulation, Int. J. Environ. Eng. 2 (2009) 212–227. https://doi.org/10.1504/IJEE.2010.029829.

[20] S. Vasudevan, J. Jayaraj, J. Lakshmi, G. Sozhan, Removal of iron from drinking water by electrocoagulation: Adsorption and kinetics studies, Korean J. Chem. Eng. 26 (2009) 1058–1064. https://doi.org/10.1007/s11814-009-0176-9.

[21] D. Ghosh, H. Solanki, M.K. Purkait, Removal of Fe(II) from tap water by electrocoagulation technique, J. Hazard. Mater. 155 (2008) 135–143. https://doi.org/10.1016/j.jhazmat.2007.11.042.

[22] J. Guzmán, R. Mosteo, J. Sarasa, J.A. Alba, J.L. Ovelleiro, Evaluation of solar photo-Fenton and ozone based processes as citrus wastewater pre-treatments, Sep. Purif. Technol. 164 (2016) 155–162. https://doi.org/10.1016/j.seppur.2016.03.025.

[23] N. Azbar, T. Yonar, K. Kestioglu, Comparison of various advanced oxidation processes and chemical treatment methods for COD and color removal from a polyester and acetate fiber dyeing effluent, Chemosphere. 55 (2004) 35–43. https://doi.org/10.1016/j.chemosphere.2003.10.046.

[24] H.Y. Shu, M.C. Chang, Decolorization effects of six azo dyes by O3, UV/O3 and UV/H2O2 processes, Dye. Pigment. 65 (2005) 25–31. https://doi.org/10.1016/j.dyepig.2004.06.014.

[25] C. Zaharia, D. Suteu, A. Muresan, R. Muresan, A. Popescu, Textile wastewater treatment by homogeneous oxidation with hydrogen peroxide, Environ. Eng. Manag. J. 8 (2009) 1359–1369. https://doi.org/10.30638/eemj.2009.199.

[26] S. Song, J. Yao, Z. He, J. Qiu, J. Chen, Effect of operational parameters on the decolorization of C.I. Reactive Blue 19 in aqueous solution by ozone-enhanced electrocoagulation, J. Hazard. Mater. 152 (2008) 204–210. https://doi.org/10.1016/j.jhazmat.2007.06.104.

[27] M. Hernández-Ortega, T. Ponziak, C. Barrera-Díaz, M.A. Rodrigo, G. Roa-Morales, B. Bilyeu, Use of a combined electrocoagulation-ozone process as a pre-treatment for industrial wastewater, Desalination. 250 (2010) 144–149. https://doi.org/10.1016/j.desal.2008.11.021.

[28] S. Song, Z. He, J. Qiu, L. Xu, J. Chen, Ozone assisted electrocoagulation for decolorization of C.I. Reactive Black 5 in aqueous solution: An investigation of the effect of operational parameters, Sep. Purif. Technol. 55 (2007) 238–245. https://doi.org/10.1016/j.seppur.2006.12.013.

[29] E. Hu, X. Wu, S. Shang, X.M. Tao, S.X. Jiang, L. Gan, Catalytic ozonation of simulated textile dyeing wastewater using mesoporous carbon aerogel supported copper oxide catalyst, J. Clean. Prod. 112 (2016) 4710–4718. https://doi.org/10.1016/j.jclepro.2015.06.127.

[30] P. Mondal, M.K. Purkait, Green synthesized iron nanoparticles supported on pH responsive polymeric membrane for nitrobenzene reduction and fluoride rejection study: Optimization approach, J. Clean. Prod. 170 (2018) 1111–1123. https://doi.org/10.1016/j.jclepro.2017.09.222.

[31] A. Gordiychuk, M. Svanera, S. Benini, P. Poesio, Size distribution and Sauter mean diameter of micro bubbles for a Venturi type bubble generator, Exp. Therm. Fluid Sci. 70 (2016) 51–60. https://doi.org/10.1016/j.expthermflusci.2015.08.014.

[32] S. Patel, S.K. Majumder, P. Das, P. Ghosh, Ozone microbubble-aided intensification of degradation of naproxen in a plant prototype, J. Environ. Chem. Eng. 7 (2019) 103102. https://doi.org/10.1016/j.jece.2019.103102.

[33] M. Changmai, P.P. Das, P. Mondal, M. Pasawan, A. Sinha, P. Biswas, S. Sarkar, M.K. Purkait, Hybrid electrocoagulation–microfiltration technique for treatment of nanofiltration rejected steel industry effluent, Int. J. Environ. Anal. Chem. 102 (2022) 62–83. https://doi.org/10.1080/03067319.2020.1715381.

[34] D. Ghosh, C.R. Medhi, M.K. Purkait, Treatment of fluoride containing drinking water by electrocoagulation using monopolar and bipolar electrode connections, Chemosphere. 73 (2008) 1393–1400. https://doi.org/10.1016/j.chemosphere.2008.08.041.

[35] I. Kim, H. Tanaka, Energy consumption for ppcps removal by o3 and o3/uv, Ozone Sci. Eng. 33 (2011) 150–157. https://doi.org/10.1080/01919512.2011.549427.

[36] M. Changmai, M. Pasawan, M.K. Purkait, A hybrid method for the removal of fluoride from drinking water: Parametric study and cost estimation, Sep. Purif. Technol. 206 (2018) 140–148. https://doi.org/10.1016/j.seppur.2018.05.061.

[37] D. Ghosh, C.R. Medhi, M.K. Purkait, Techno-economic analysis for the electrocoagulation of fluoride-contaminated drinking water, Toxicol. Environ. Chem. 93 (2011) 424–437. https://doi.org/10.1080/02772248.2010.542158.

[38] V.L. Dhadge, C.R. Medhi, M. Changmai, M.K. Purkait, House hold unit for the treatment of fluoride, iron, arsenic and microorganism contaminated drinking water, Chemosphere. 199 (2018) 728–736. https://doi.org/10.1016/j.chemosphere.2018.02.087.

[39] L. Bilińska, K. Blus, M. Gmurek, S. Ledakowicz, Coupling of electrocoagulation and ozone treatment for textile wastewater reuse, Chem. Eng. J. 358 (2019) 992–1001. https://doi.org/10.1016/j.cej.2018.10.093.

[40] M. Vanoppen, G. Stoffels, C. Demuytere, W. Bleyaert, A.R.D. Verliefde, Increasing RO efficiency by chemical-free ion-exchange and Donnan dialysis: Principles and practical implications, Water Res. 80 (2015) 59–70. https://doi.org/10.1016/j.watres.2015.04.030.

[41] D. Ghosh, M.K. Sinha, M.K. Purkait, A comparative analysis of low-cost ceramic membrane preparation for effective fluoride removal using hybrid technique, Desalination. 327 (2013) 2–13. https://doi.org/10.1016/j.desal.2013.08.003.

[42] P. Cañizares, R. Paz, C. Sáez, M.A. Rodrigo, Costs of the electrochemical oxidation of wastewaters: A comparison with ozonation and Fenton oxidation processes, J. Environ. Manage. 90 (2009) 410–420. https://doi.org/10.1016/j.jenvman.2007.10.010.

[43] A.M. El-Dein, J. Libra, U. Wiesmann, Cost analysis for the degradation of highly concentrated textile dye wastewater with chemical oxidation H2O2/UV and biological treatment, J. Chem. Technol. Biotechnol. 81 (2006) 1239–1245. https://doi.org/https://doi.org/10.1002/jctb.1531.

[44] K.K. Jyoti, A.B. Pandit, Ozone and cavitation for water disinfection, Biochem. Eng. J. 18 (2004) 9–19. https://doi.org/10.1016/S1369-703X(03)00116-5.

# Chapter 5

# Treatment of oil, phenol, and iron rich cold rolling mill (CRM) wastewater of steel plant by standalone electrocoagulation and ozonation techniques

# Chapter 5

# Treatment of oil, phenol, and iron rich cold rolling mill (CRM) wastewater of steel plant by standalone electrocoagulation and ozonation techniques

*The present chapter establishes the performance of standalone ozonation and electrocoagulation processes for the treatment of Cold Rolling Mill (CRM) wastewater consisting of phenol, COD, BOD, iron, and oil content from Tata Steel Industry, India. The operational variables of both the standalone processes, viz. current density, ozone generation rate, and treatment time, were addressed to analyse its effect on the removal efficiency of each process separately. Optimum experimental conditions of 200 A $m^{-2}$ (current density), 1.12 mg $s^{-1}$ (ozone generation rate), and 30 min (treatment time) were adequate in lowering the amount of all the target pollutants below their respective discharge limits. The electrocoagulation process proved to be more efficient (98% phenol, 97.5% iron, 90.5% COD, 85.7% BOD, and 88% oil & grease) compared to ozonation (93.5% phenol, 86.5% iron, 70% COD, 74.3% BOD, and 62% oil & grease) in terms of pollutant removal rate for the target wastewater. The electrocoagulated flocs were then characterized to analyse its particle size and confirm the presence of pollutants removed during the process. The kinetic study conducted showed that pseudo first-order reaction fitted best with the highest $R^2$ of 0.99 for phenol, COD, BOD, iron, and 0.98 for oil & grease. Moreover, mass transfer analysis for ozonation indicates an increase in the volumetric mass transfer coefficient ($K_l a$) with an increase in the ozone generation rate. The cost of ozonation process was found to be about six times than that of electrocoagulation. However, the efficiencies and operating costs for both the standalone processes were found to be satisfactory compared to other methods reported in the literature.*

# Chapter 5

## 5.1 Experimental

### 5.1.1 Measurement and analysis

Cold rolling mill (CRM) wastewater was collected from Tata Steel Industry, India to carry out the experiments for the present study. The initial characteristics of the wastewater sample were measured. The concentration of the pollutants targeted in this work were: phenol: 15 mg $L^{-1}$, COD: 750 mg $L^{-1}$, BOD: 105 mg $L^{-1}$, iron: 6 mg $L^{-1}$, oil & grease: 25 mg $L^{-1}$, and pH: 7.8. An acrylic electrocoagulation reactor of 500 mL volume and an ozonation reactor of 2 L volume were used for conducting the experiments. All the experiments were performed at a constant temperature of 20°C. The sample analysis was done at an interval of 5 min, and the residual concentration of the pollutants was measured using an atomic absorption spectrometry (Make: M/s Varian; Model: Spectra AA 220 FS) and a photometer (Make: Palintest; Model: 7100). The change in solution pH was determined using a benchtop pH Meter (Make: Eutech; Model: 700). The details of all the measurement and analysis have been elaborately reported in section 2.3 of chapter 2.

### 4.1.2 Operational parameters

The study on electrocoagulation and ozonation were carried out under diverse operational conditions. The objective was to examine the correlation between the operational parameters of both the processes and the efficiency of pollutant removal. During ozonation, the experiments were conducted at three discrete ozone generation rates, such as 0.85 mg $s^{-1}$, 1.00 mg $s^{-1}$, and 1.12 mg $s^{-1}$. The reaction time was altered between 10 and 30 min. During electrocoagulation, three discrete current densities were selected for the experiments such as 100 A $m^{-2}$, 150 A $m^{-2}$, and 200 A $m^{-2}$.

The electrolysis time was regulated between 10 and 30 min, while the inter-electrode spacing was kept constant at 0.005 m during the process.

During the application of three discrete ozone generation rates viz. 0.85 mg $s^{-1}$, 1.00 mg $s^{-1}$, and 1.12 mg $s^{-1}$, it was found that the experiments conducted at an ozone generation rate higher than 1.12 mg $s^{-1}$ yielded similar results in terms of pollutant removal efficiency. Further, the energy consumption of the ozonation process was significantly increased beyond an ozone generation rate of 1.12 mg $s^{-1}$. Moreover, an oxidation time of 30 min was sufficient to effectively reduce all the target parameters below their assigned permissible limits. Therefore, the optimum operating conditions were taken as 1.12 mg $s^{-1}$ and 30 min for the ozonation process. During the application of three discrete current densities viz. 100, 150, and 200 A $m^{-2}$, it was observed that the experiments carried out beyond 200 A $m^{-2}$ significantly increased the operating cost of the electrocoagulation process. Further, the permissible limits of all the target parameters were effectively reached at a current density of 200 A $m^{-2}$. Moreover, the pollutant removal rate was only marginally improved on prolongation of the electrolysis time beyond 30 min. Therefore, the optimum operating conditions were taken as 200 A $m^{-2}$ and 30 min for the electrocoagulation process.

## 5.2 Results and discussion

### 5.2.1 Performance of ozonation and electrocoagulation processes on pH variation

In ozonation processes, the initial pH of the solution was reduced from 7.8 ± 0.1 to a final pH of 3.5 at 20 °C. The pH remains unchanged thereafter. The reason for the decrease in solution pH was because of the oxidation by ozone, which resulted in derivatives of acidic character such as

inorganic acids and organic anions [1]. Also, the reaction of ozone both with hydroxyl anions and the degradation products formed by oxidation via hydroxyl radicals (usually carboxylic acids) tends to decrease the pH of the solution during treatment. Further, the decrease in solution pH was observed due to higher ozone consumption at the beginning of the experiment [2]. Furthermore, the principal focus during ozonation process was to validate the impact of experimental variables viz. ozone generation rate (0.85–1.12 mg $s^{-1}$) and treatment time (30 min) on the reduction efficiency of the pollutants, at a constant pH of 3.5.

However, in the electrocoagulation process, the solution pH steadily increased from 7.8 ± 0.1 until an equilibrium condition was achieved around a pH of 8.5. The equilibrium state was reached owing to the buffer capability of $Al(OH)_3/Al(OH)_4^-$ formed during the experiment. The pH was increased because of the generation of $OH^-$ ions at the cathode surface as well as $H_2$ evolution at the cathode vicinity. Moreover, as the current density and the analysis time was increased, more amount $OH^-$ ions and $H_2$ gas get generated during the experiment [3]. Thus, the solution pH gets enhanced with the progress of the electrocoagulation process.

### 5.2.2 Effect of ozonation and electrocoagulation processes on phenol degradation

Figure 5.1 (inset) depicts the change in the reduction of phenol concentration with varying ozone generation rates. From Figure 5.1 (inset), it is observed that, phenol reduction percentage increases from 63.5% to 93.5% as the ozone generation rate is increased from 0.85 to 1.12 mg $s^{-1}$, respectively, after 30 min of operation. During ozonation, phenol oxidation leads to the production of $HO^{\bullet}$ radicals. This was because of the shifting of an electron from phenol/phenolate ion to ozone, as shown in the equation below [4]:

$PhO^{-}/PhOH + O_3 \rightarrow PhO^{\bullet}/PhOH^{\bullet+} + O_3^{\bullet-}$ (5.1)

The generation of a phenoxyl radical and an ozonide radical may be attributed to the direct electron transfer during the ozone oxidation of phenol. The phenol decomposition rate increased as the dissolved quantity of ozone was increased in the solution. Oxidation of phenol resulted in the generation of hydroquinone at para-position, which immediately oxidized to o-benzoquinone and p-benzoquinone. Hydroquinone formation was attributed to the addition of $HO^{\bullet}$ to phenol, which resulted in the generation of di-hydroxycyclohexadienyl radicals that eventually led to the addition and elimination of dioxygen ($O_2^{\bullet-}$) and $HO_2^{\bullet}$ radicals, respectively [5]. Moreover, $HO_2^{\bullet}$ attack at the para-position of the phenoxyl radical with consecutive loss of $H_2O$ or direct attack by ozone at the para-position followed by the successive $H_2O_2$ loss was considered to be the reason behind benzoquinone formation. When benzoquinone was further oxidized under acidic conditions (pH ≈ 4), its aromatic rings were unfolded. As such, p-benzoquinone and o-benzoquinone get decomposed, resulting in the generation of various organic acids. These organic acids were finally converted into $CO_2$ and $H_2O$ as the end products during subsequent ozone oxidation. HPLC analysis was conducted to identify the phenolic intermediates formed during ozonation [6]. Figure 5.2 displays the HPLC chromatogram of phenol degradation. It could be seen that oxidation of phenol resulted in the formation of aromatic compounds, viz. hydroquinone and benzoquinone. The retention times of hydroquinone and benzoquinone were 4.42 and 7.92 min, respectively. The formed intermediates were coincident with those reported in the literature [7]. In addition, the formation of catechol was found to be insignificant at acidic pH of 3, whereas it is formed as an essential primary product during the oxidation of phenol at pH 7. As such, no peaks for catechol were observed during the analysis of the intermediate compound. Thus, the intermediates formed

during phenol degradation are hydroquinone, benzoquinone as well as organic acids. These intermediates do not remain in their present form for a more extended period as they get quickly oxidized into $CO_2$ and $H_2O$ as the final product, i.e., lowering of the phenol content may be denoted by the production of different phenolic by-products and its successive oxidation into carbon dioxide and water [8]. As such, it was inferred that with an increase in ozone oxidation, the phenol content decreases in the solution. Thus, at an optimum treatment time of 30 min and an ozone generation rate of 1.12 mg $s^{-1}$, the phenol content reduces from 15 mg $L^{-1}$ (initial concentration) to 0.95 mg $L^{-1}$ (final concentration).

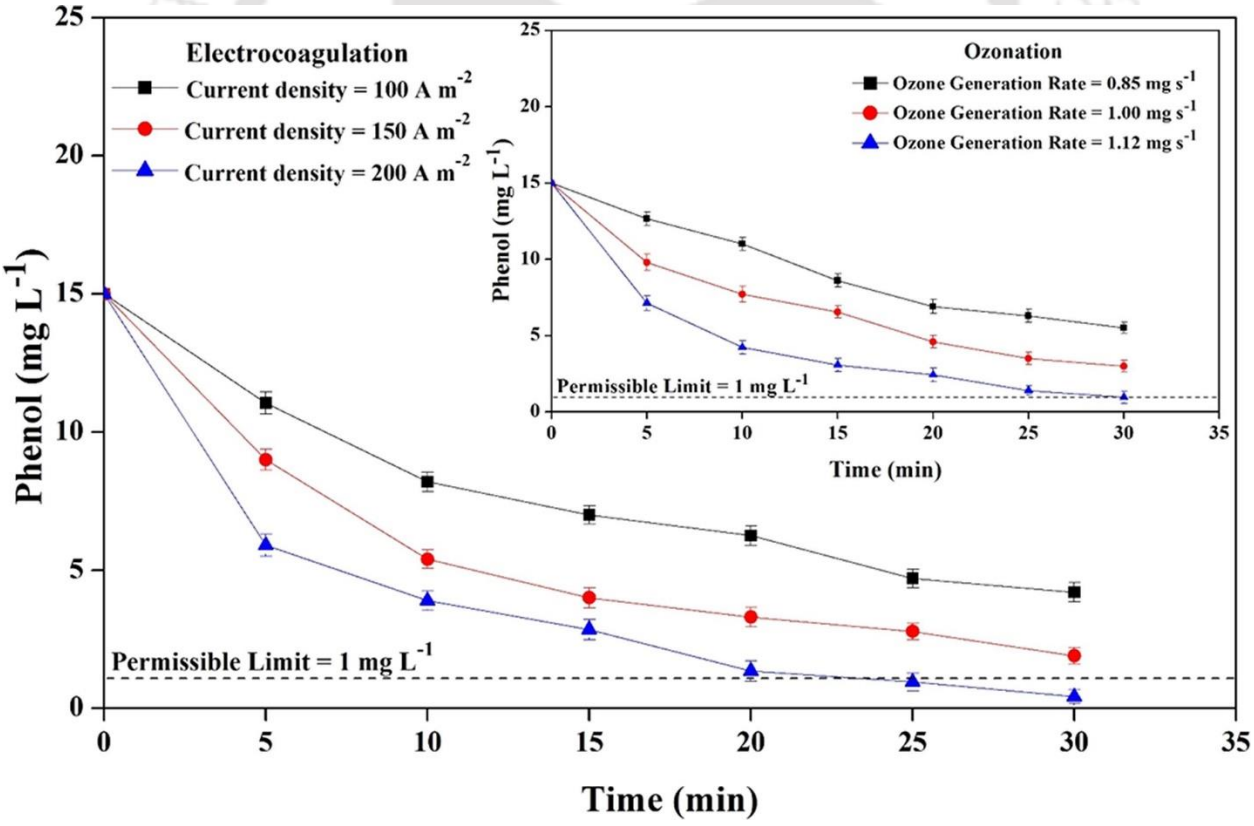


**Fig. 5.1:** Effect of electrocoagulation and ozonation on phenol removal. Inset: ozonation process, Outset: electrocoagulation process

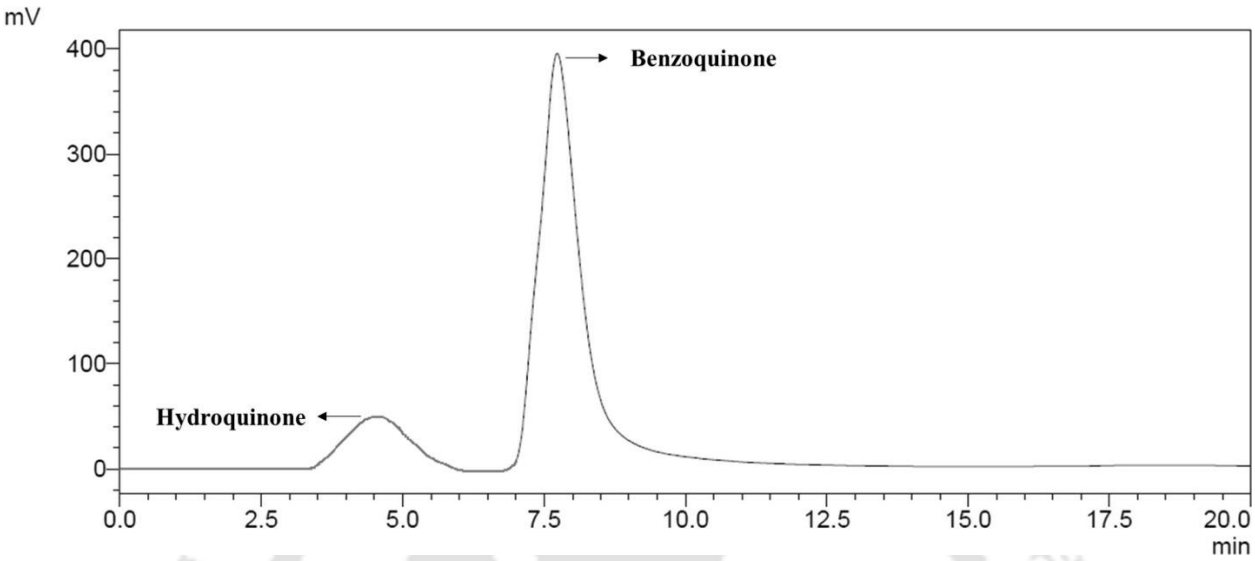


**Fig. 5.2:** Typical HPLC chromatogram showing the intermediates formed during phenol oxidation

From Figure 5.1 (Outset), it is seen that as the current density is increased from 100 to 200 A $m^{-2}$, the efficiency of phenol reduction also increases from 70% to 98% after 30 min of operation. During electrocoagulation, the phenol reduction efficiency was found to increase with respect to electrolysis time using aluminum electrodes. Various literatures have reported the generation of insoluble species by the integrated complexation, coagulation, and precipitation processes, resulting from the chemical synergy of trivalent cations with phenols and its compounds. Also, phenol, along with other organic substances, tends to incline towards the aqueous solution. The hydrolyzed products formed during electrocoagulation adsorbed the phenolic compounds on its surface (coagulation process), followed by the formation of flocs due to the physical interaction of the resulting particulate compounds (flocculation process). Due to current density, phenol and its various by-products get reduced to smaller organic molecules at the cathode surface [9]. The aluminum flocs along with other polymeric and monomeric hydroxides generated in situ adsorb

the formed organic molecules onto its surface, followed by precipitation at the bottom or flotation due to the $H_2$ bubble evolution. The current density was increased due of an increase in the bubble density of $H_2$ as well as a simultaneous reduction in the bubble size during the experiment. As such, the removal efficiency gets intensified due to higher upward flux and thereby leading to an increase in the floc floatation. Moreover, the in-situ generation of aluminum hydroxide flocs gets enhanced due to high current density, which eventually resulted in a higher amount of floc precipitation, thereby facilitating in the reduction of phenol concentration [10]. Thus, from the experiments conducted at an optimum treatment time of 30 min and a current density of 200 A $m^{-2}$, it was found that the phenol content reduces from 15 mg $L^{-1}$ (initial concentration) to 0.3 mg $L^{-1}$ (final concentration).

### 5.2.3 Effect of ozonation and electrocoagulation processes on iron removal

Figure 5.3 (inset) represents the change in reducing iron content in the effluent with varying ozone generation rates. From Figure 5.3 (inset), it is observed that iron reduction efficiency increases from 58.5% to 86.5% as the ozone generation rate is increased from 0.85 to 1.12 mg $s^{-1}$, respectively, after 30 min of operation. During the experiment, ozone oxidation converted the ferrous ions ($Fe^{2+}$) into the ferric state ($Fe^{3+}$), with subsequent formation of ferric hydroxide due to the precipitation of the oxidized salts. As shown in Eq. 3 and Eq. 4, $Fe^{2+}$ gets rapidly oxidized into $Fe^{3+}$ under acidic conditions. During ozone decomposition, $Fe^{2+}$ played the role of a catalyst for the production of $HO^{\bullet}$ radicals. Also, the formation of an intermediate species $FeO^{2+}$, during $Fe^{2+}$ oxidation, quickly gets transformed into $HO^{\bullet}$ [11]. Various reactions involving oxidation of $O_3$ with $Fe^{2+}$ are as follows [12]:

$$Fe \rightarrow Fe^{2+}(aq) + 2e^{-} \quad (5.2)$$

$$Fe^{2+} + O_3 \rightarrow FeO^{2+} + O_2 \quad (5.3)$$

$$FeO^{2+} + H_2O \rightarrow HO^{\bullet} + Fe^{3+} + OH^{-} \quad (5.4)$$

$$Fe^{3+} + 3OH^{-} \rightarrow Fe(OH)_3 \quad (5.5)$$

$$2Fe^{2+} + O_3 + 5H_2O \rightarrow 2Fe(OH)_3 + O_2 + 4H^{+} \quad (5.6)$$

Based on the pH range, the $Fe^{3+}$ ions were converted into ferric hydroxides (Eq. 5), followed by its precipitation at the bottom of the reactor. Thus, the generation of ferric hydroxide and its subsequent precipitation, owing to the soluble form's oxidation into insoluble oxides, was primarily responsible for the removal of iron content in the effluent. Under equilibrium condition, it was considered that as ferric hydroxides were insoluble in water, it gradually descended to the bottom of the reactor without participating in any type of reaction and, as such, can be effortlessly sieved out of the solution. The clear solution was then examined for residual $Fe^{2+}$. Also, ozone solubility was much higher in the water at lower temperatures [13]. Higher the ozone solubility in water, more will be the oxidation of soluble iron salts, and as such, the removal efficiency of $Fe^{2+}$ from the solution increases. Thus, at an optimum treatment time of 30 min and an ozone generation rate of 1.12 mg $s^{-1}$, the iron content reduces from 6.0 mg $L^{-1}$ (initial concentration) to 0.8 mg $L^{-1}$ (final concentration).

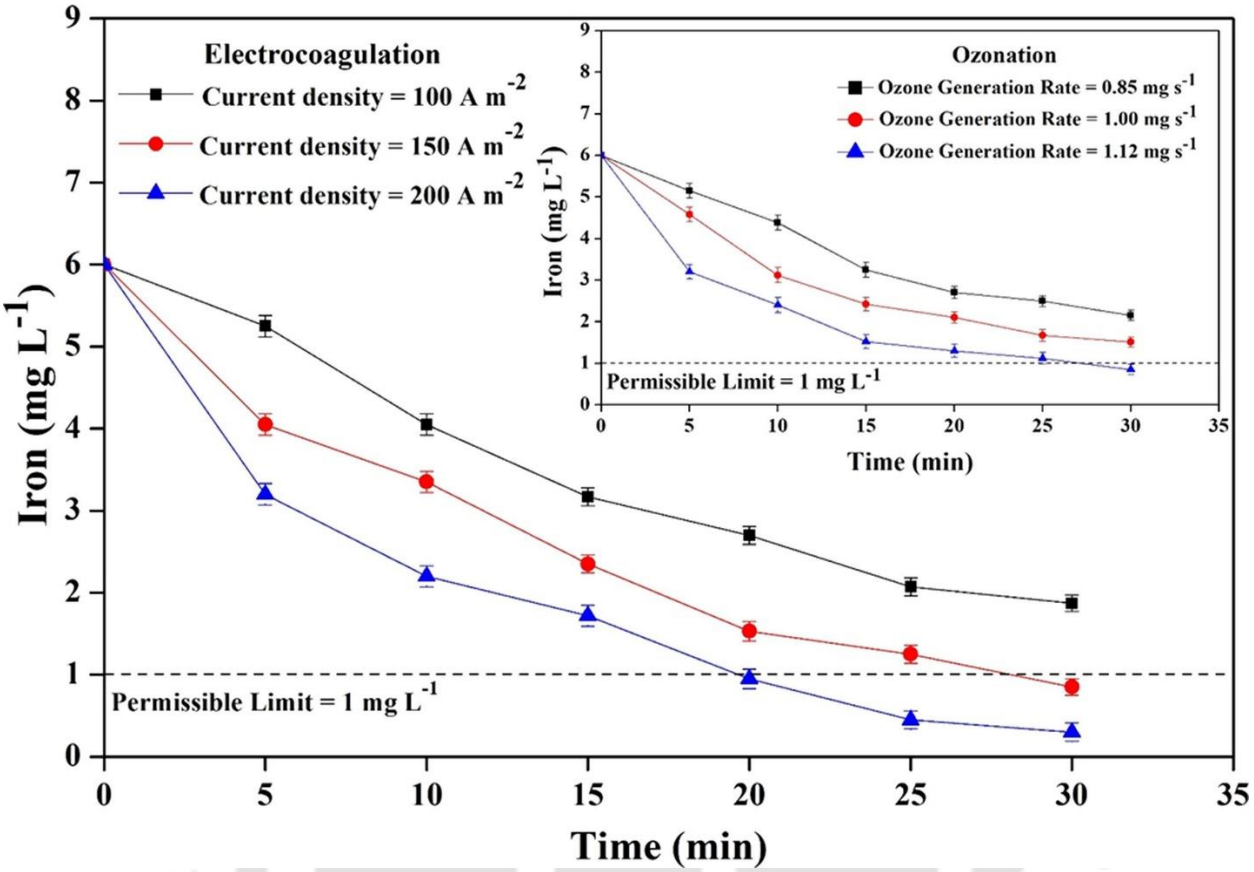


**Fig. 5.3:** Effect of electrocoagulation and ozonation on iron removal. Inset: ozonation process, Outset: electrocoagulation process

From Figure 5.3 (Outset), it is seen that with an increase in current density from 100 to 200 A $m^{-2}$, the efficiency of iron reduction also increases from 65% to 97.5% after 30 min of operation. The principal cause of iron removal via electrocoagulation was the adsorption of $Fe^{2+}$ ions on the surface of the in-situ generated $Al(OH)_3$ flocs. The state of iron was mainly governed by both the redox potential and the solution pH. The dissolved species of iron are usually divalent as long as the solution pH remains above 4. The transport of the $Fe(OH)_2$ particles produced in situ to the liquid bulk remained insoluble, even after the bulk pH remained well beneath the value signifying

the product solubility. Thus, an increase in iron reduction efficiency was primarily because of the adsorption of $Fe(OH)_2$ on Al flocs surface [14]. Moreover, as the current density was increased, the in-situ production of aluminum hydroxide flocs also gets increased, and as such, iron adsorption on its surface was enhanced. As such, the available binding sites played a significant part in the adsorption process of iron. During the hydrolysis reaction, $Al(OH)_3$ produced leads to the generation of reactive Al(III)–Fe(II) complexes, thus enhancing the oxidation of $Fe^{2+}$. $Fe^{2+}$ hydrolyses and forms precipitates as the pH of the solution increases. Thus, it may be inferred that as the pH increases, the reduction of iron was mainly because of the generation of in situ Al(OH)3 flocs, resulting in an enhanced $Fe(OH)_2$ adsorption on its surface, which later settled down as precipitates in the form of reddish-brown sludge at the bottom of the reactor and can be easily separated [15]. From the experiments conducted at an optimum treatment time of 30 min and a current density of 200 A $m^{-2}$, it was found that the iron content reduces from 6.0 mg $L^{-1}$ (initial concentration) to 0.15 mg $L^{-1}$ (final concentration).

### 5.2.4 Effect of ozonation and electrocoagulation processes on oil & grease content

Figure 5.4 (inset) depicts the reduction of oil concentration in the effluent during ozonation, with three different ozone generation rates viz. 0.85, 1.00 and 1.12 mg $s^{-1}$. From Figure 5.4 (inset), it is observed that oil reduction efficiency increases from 32% to 62% as the ozone generation rate is increased from 0.85 to 1.12 mg $s^{-1}$, respectively, after 30 min of operation. The oily contaminants found in industrial effluents are primarily aliphatic hydrocarbons. During ozonation, the aliphatic hydrocarbons get oxidized, with the cleavage of σ-bond between the carbon and hydrogen atom through the formation of free radicals. These moieties on interaction with the hydroxyl ion resulted

in the generation of alcohols, carboxylic acids, and ketones as intermediates [16]. Reactions of $O_3$ with saturated hydrocarbons are as follows [17]:

$$RH + O_3 \rightarrow RO^{\bullet} + HOO^{\bullet} \quad (5.7)$$

$$RH + O_3 \rightarrow R^{\bullet} + O_2 + HO^{\bullet} \rightarrow R_2C = O + RCOOH \quad (5.8)$$

$$RH + O_3 \rightarrow RO_2^{\bullet} + HO^{\bullet} \quad (5.9)$$

$$RH + O_3 \rightarrow R^{\bullet} + HO_3^{\bullet} \rightarrow ROH + O_2^{\bullet} \quad (5.10)$$

$$RH + O_3 \rightarrow R^{\bullet} + HO_3^{\bullet} \rightarrow ROOOH \quad (5.11)$$

The $HO_3^{\bullet}$ radical is produced when the ozone molecule abstracts the hydrogen atom from the carbon-hydrogen single bond system. The hydrotrioxide radical upon reaction with alkane again abstracts an H-atom to produce an alkyl radical, leading to the transient intermediate hydrotrioxide ROOOH molecule, and HOOOH, which finally decomposes into $H_2O$ and $CO_2$. The above mechanism completely mineralizes the intermediate hydrophilic compounds such as ROH, $R_2C$ = O, and RCOOH [18]. However, the mineralization reactions are kinetically sluggish than the precursors due to the functional group's inductive effect on the electron cloud distribution in the molecule. The $HO^{\bullet}$ radicals produced, when ozone interacts in the aqueous phase, can abstract hydrogen atoms from the saturated hydrocarbons, albeit straight-chained or branched alkanes, or even cycloalkanes. Oxidation by $HO^{\bullet}$ via abstraction of H atom results in the formation of the alkyl radical, which further react to form hydrophilic compounds and eventually reduces the oil content in the solution as shown by the following equation [19]:

$$RH + HO^{\bullet} \rightarrow R^{\bullet} + H_2O \quad (5.12)$$

The above-discussed pathway is predominant at low pH due to reaction selectivity. Thus, the experiments performed showed that at an optimum treatment time of 30 min and an ozone generation rate of 1.12 mg $s^{-1}$, the oil content reduces from 25 mg $L^{-1}$ (initial concentration) to 9.5 mg $L^{-1}$ (final concentration).

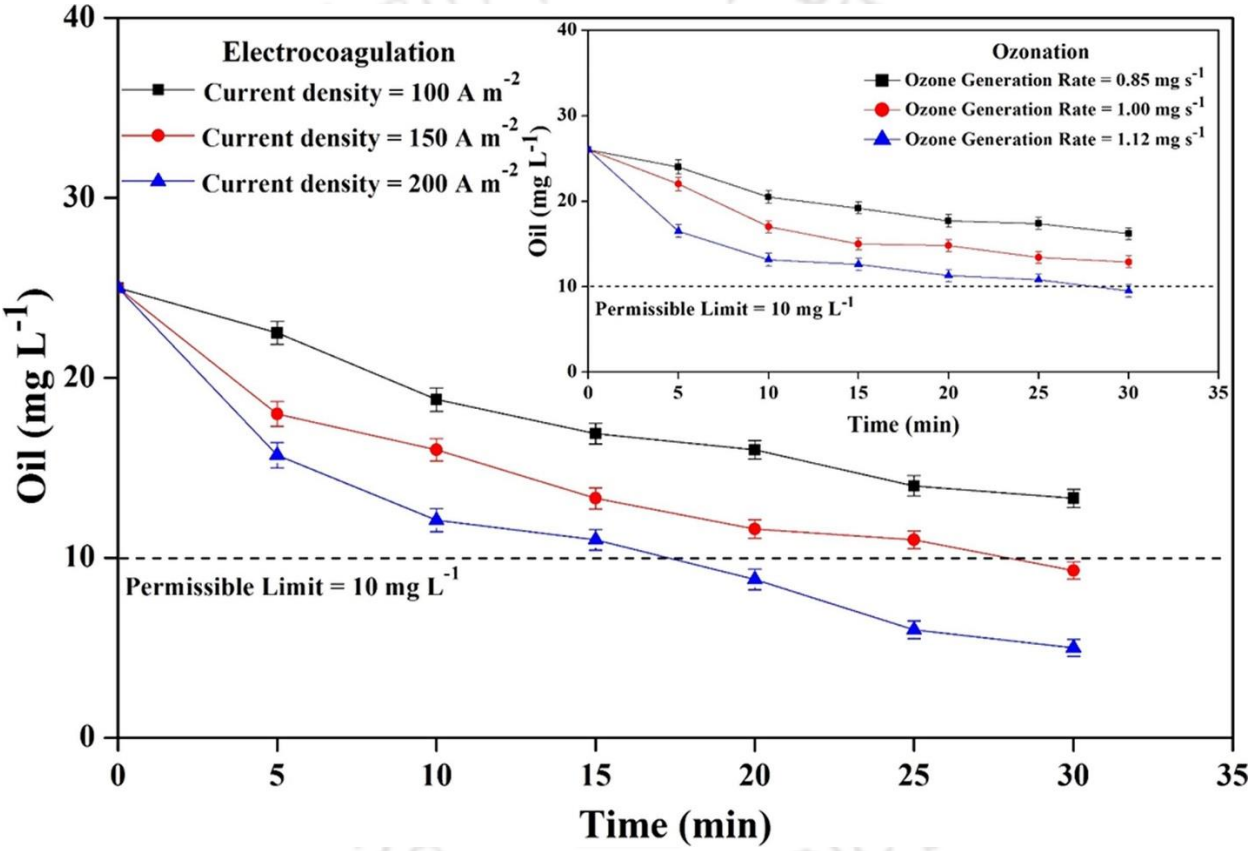


**Fig. 5.4:** Effect of electrocoagulation and ozonation on oil & grease removal. Inset: ozonation process, Outset: electrocoagulation process

From Figure 5.4 (Outset), it is seen that with an increase in current density from 100 to 200 A $m^{-2}$, the efficiency of oil reduction also increases from 40% to 88% after 30 min of operation. During electrocoagulation, it was found that the efficacy of oil removal increases as the current density

increases from 100 to 200 A $m^{-2}$. An increase in current density was realized by increasing the current supplied to the electrodes, because a hike in the supplied current eventually increased the dissolution of $Al^{3+}$ from the anode, as per Faraday's law of electrolysis [20]. The emulsified oil droplets are known to have a high negative surface charge, which, when neutralized by the positively charged $Al^{3+}$ ions, coalesce. Moreover, flocs of amorphous $Al(OH)_3$, $Al(OH)_4^-$, and its polymers that get generated in the electrocoagulation process having large surface areas, aided in the adsorption of the oil droplets, followed by its subsequent precipitation at the bottom of the container [21]. Also, $O_2$ and $H_2$ gases formed at the vicinity of anode and cathode, respectively, helped in the floatation of both oil droplets and flocs due to its higher upward flux, which increased the probability of adsorption and thus assisted in the reduction of oil content from the solution [22]. Further, it was seen from the experiments that, at an optimum treatment time of 30 min and a current density of 200 A $m^{-2}$, it was found that the oil content reduces from 25 mg $L^{-1}$ (initial concentration) to 3 mg $L^{-1}$ (final concentration).

### 5.2.5 Effect of ozonation and electrocoagulation processes on COD removal

Figure 5.5 (inset) shows the change in reduction of COD content in the effluent with varying ozone generation rates. From Figure 5.5 (inset), it is seen that COD reduction efficiency increases from 50.5% to 70% as the ozone generation rate is increased from 0.85 to 1.12 mg $s^{-1}$, respectively, after 30 min of operation. The contaminants present in the effluent get oxidized during ozonation, which lowered both the COD and the BOD content. Ozone oxidation followed two pathways: either radical oxidation by $HO^{\bullet}$ radicals, which were less selective and prevailed under alkaline state or direct oxidation by molecular ozone ($O_3$) having more selectivity, which prevailed under

acidic state [23]. Owing to the predomination of indirect hydroxyl radical-mediated reactions, there may be a potential for a considerable amount of ozone wastage through the scavenging activity with both inorganic and organic content of the effluent under alkaline conditions. However, the molecular ozone predominated under acidic conditions, and as such, the ozone wastage was substantially low via scavenging reactions in the solution in comparison to the $HO^{\bullet}$ radicals. Thus, the removal rates of both COD and BOD were increased at lower pH [24]. Moreover, at an optimum reaction time of 30 min and an ozone generation rate of 1.12 mg $s^{-1}$, the COD content reduces from 750 mg $L^{-1}$ (initial concentration) to 225 mg $L^{-1}$ (final concentration).

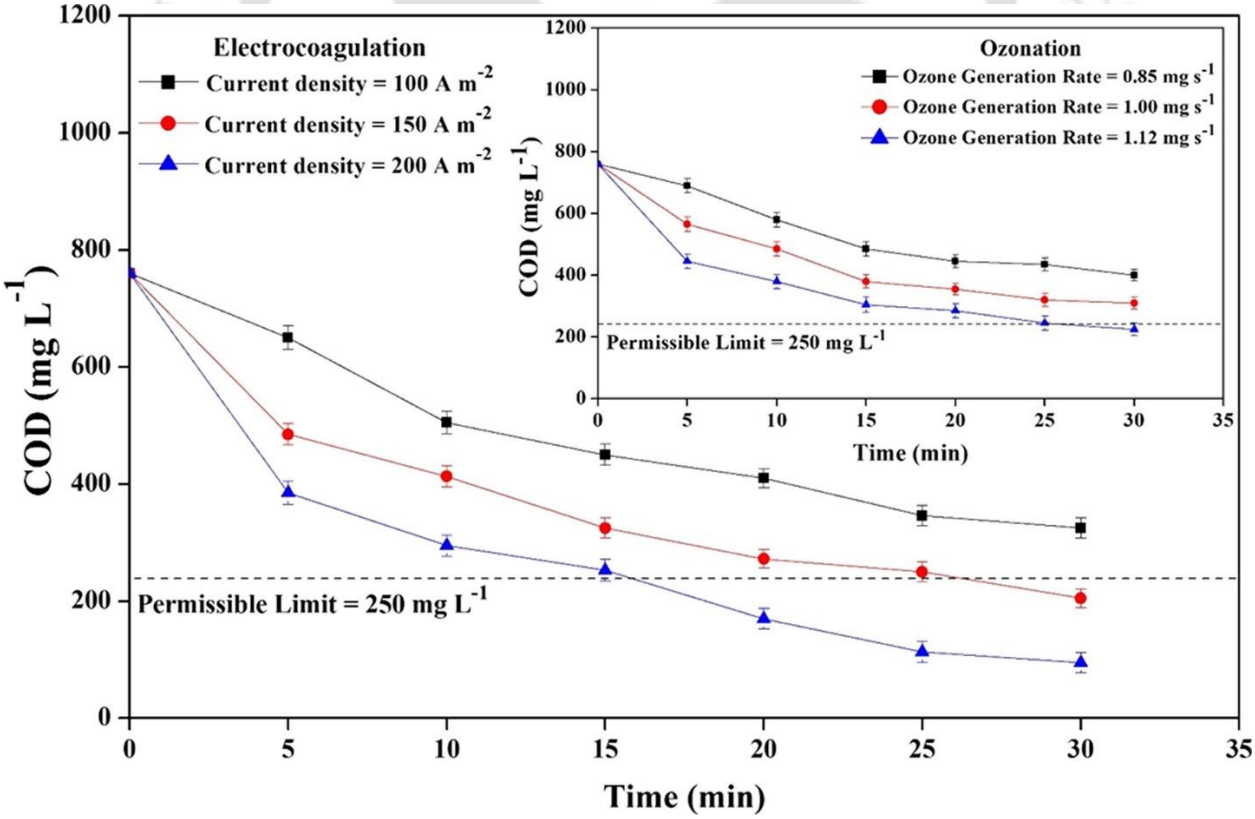


**Fig. 5.5:** Effect of electrocoagulation and ozonation on COD removal. Inset: ozonation process, Outset: electrocoagulation process

From Figure 5.5 (Outset), it may be seen that with an increase in current density from 100 to 200 A $m^{-2}$, the COD reduction efficiency also increases from 58.5% to 90.5% after 30 min of operation. During electrocoagulation, the absorptive nature of $OH^-$ ions generated at the surface of the cathodes helped in decreasing the COD content present in the effluent. At low pH, free cation, i.e., $Al^{3+}$ ions, was the most predominant solution. The decrease in COD content of the solution was attributed to both pollutant adsorptions into the insoluble metal hydroxide species and charge neutralization of colloids. The removal of pollutants increased as the cationic metal ion concentration was increased [25]. Thus, an increase in current density enhanced the reduction percentage of COD content in the solution. Also, it can be seen from the experiments that, at an optimum treatment time of 30 min and a current density of 200 A $m^{-2}$, the COD content reduces from 750 mg $L^{-1}$ (initial concentration) to 70 mg $L^{-1}$ (final concentration).

Also, Figure 5.6 shows a similar decreasing trend for BOD content in the solution. In both the ozonation and electrocoagulation processes, the reduction efficiencies of BOD content were found to be 74.3% and 85.7%, respectively, for the optimum experimental conditions obtained. Similar to the COD, phenomena such as oxidation (during ozonation) and flocculation (during electrocoagulation) are primarily responsible for the BOD content's declination trend in the wastewater [26,27].

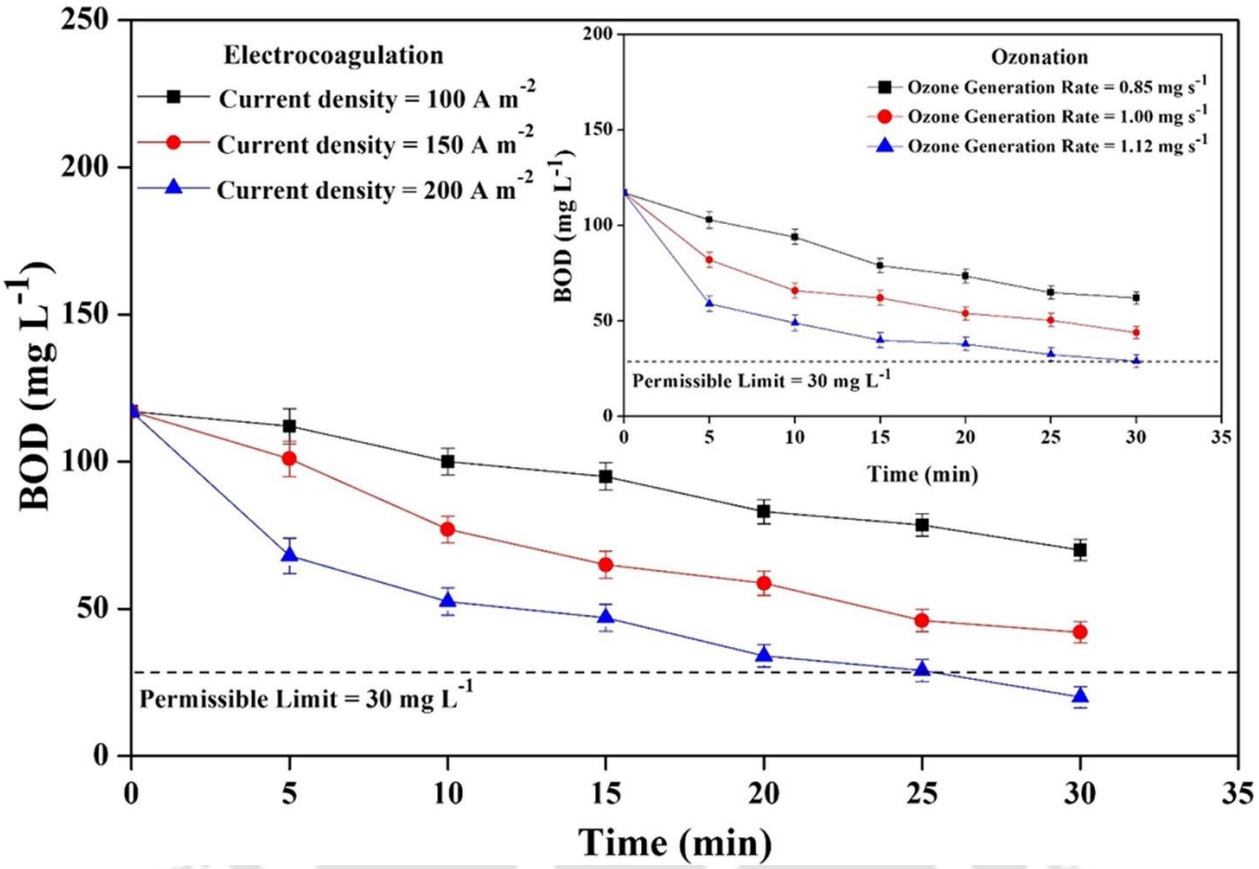


**Fig. 5.6:** Effect of electrocoagulation and ozonation on BOD removal. Inset: ozonation process, Outset: electrocoagulation process

Furthermore, the feed composition and the pollutant reduction efficiency of both ozonation and electrocoagulation processes for phenol, COD, BOD, oil & grease, and iron concentration are shown in Table 5.1, as per the WHO permissible guidelines for surface water. Table 5.2 depicts a comparative analysis between the removal efficiencies of different wastewater treatment methods reported in the literature and the present methods (electrocoagulation and ozonation) used in this study.

**Table 5.1:** Comparison of pollutant removal efficiency between ozonation and electrocoagulation process

| Pollutants | Initial concentration ($mg\ L^{-1}$) | Ozonation | | | Percent Removal* (%) | Electrocoagulation | | | Percent Removal* (%) | Permissible Limit ($mg\ L^{-1}$) [WHO] |
|---|---|---|---|---|---|---|---|---|---|---|
| | | Analysis Time = 30 min | | | | Analysis Time = 30 min | | | | |
| | | 0.85 $mg\ s^{-1}$ | 1.00 $mg\ s^{-1}$ | 1.12 $mg\ s^{-1}$ | | 100 $A\ m^{-2}$ | 150 $A\ m^{-2}$ | 200 $A\ m^{-2}$ | | |
| Phenol | 15 | 5.5 ± 1 | 3 ± 0.5 | 0.95 ± 0.1 | 93.5 | 4.5 ± 1 | 2 ± 1 | 0.3 ± 0.1 | 98.0 | 1 |
| COD | 750 | 370 ± 5 | 290 ± 3 | 225 ± 3 | 70.0 | 310 ± 4 | 200 ± 5 | 70 ± 2 | 90.5 | 250 |
| BOD | 105 | 64 ± 3 | 42 ± 3 | 27 ± 2 | 74.3 | 60 ± 2 | 35 ± 3 | 15 ± 1 | 85.7 | 30 |
| Iron | 6.0 | 2.5 ± 0.5 | 1.75 ± 0.5 | 0.8 ± 0.2 | 86.5 | 2.1 ± 0.5 | 0.85 ± 0.3 | 0.15 ± 0.2 | 97.5 | 1 |
| Oil | 25 | 17 ± 2 | 14 ± 2 | 9.5 ± 0.5 | 62.0 | 15 ± 2 | 9.5 ± 1 | 3 ± 1 | 88.0 | 10 |

***** At the optimum ozone generation rate of 1.12 $mg\ s^{-1}$ and current density of 200 $A\ m^{-2}$.

**Table 5.2:** Comparison of pollutant removal efficiencies by different wastewater treatment methods

| Methods used | Type of wastewater | Pollutant Removal efficiency | Reference |
|---|---|---|---|
| Ozonation | Olive mill wastewater | 80% phenols in 40 min | [28] |
| Electrocoagulation | Olive mill wastewater | 91% phenols in 25 min | [9] |
| Bio mineralization | Natural Groundwater | 47.86% iron in 10 min | [29] |
| Adsorption | Alau Dam reservoir water | 90.35% iron in 70 min | [30] |
| Biological digestion | Synthetic wastewater | 85.3% iron in 24 h | [31] |
| Ozonation | Textile wastewater | 64% COD in 90 min | [32] |
| Electrocoagulation | Simulated laundry wastewater | 62% COD in 40 min | [33] |
| Coagulation-flocculation | Paper mill wastewater | 76% COD in 31 min | [34] |
| Electrocoagulation Ozonation | Steel plant wastewater | 98.0% and 93.5% (phenol), 90.5% and 70% (COD), 97.5% and 86.5% (iron) and 88% and 62% (Oil) in 30 min | **Present Work** |

## 5.3 Electrode and sludge characterization

Figure 5.7 (a) and Figure 5.7 (b) shows the FESEM image of the electrode before and after the electrocoagulation treatment. It can be seen from both the figures that before the application of the electrocoagulation process, the electrode surface appears to be smooth with few indentations that may have occurred due to acid cleaning, whereas after the treatment, the electrode appears to be rough and contoured due to the uneven deposition of cations and sludge on its surface. The sludge generated during the experiment was monitored by evaluating its dry (70 mg) and wet weight (10 mg), structural morphology, particle size distribution, and the types of bonds present. Figure 5.7 (c) shows the FESEM image of the dried sludge, which indicates that the sludge does not inherit any specific shape after electrocoagulation treatment. Also, Figure 5.7 (d) indicates the size of the generated sludge, determined with the help of a particle size analyzer (Delsa nano). It is observed that the sludge size varies from 211 to 387 µm with a variation in treatment time from 10 to 30 min. The increase in sludge size indicates the formation of more amount of Al $(OH)_3$ sludge, which assists in the reduction of pollutants from the effluent by the phenomenon of adsorption followed by sedimentation. Furthermore, Figure 5.7 (e) shows the FT-IR spectra of the dried sludge. Absorption bands at 3550 and 1015 $cm^{-1}$ corresponds to the −OH and −Al−O stretching mode of vibration, respectively. An absorption band at 2100 $cm^{-1}$ was assigned due to alkyne C−C stretching present in the aliphatic chain. Also, the distinguishing peak at 1640 $cm^{-1}$ corresponds to C=C bond stretching. Also, the absorption band at 1310 $cm^{-1}$ represents the bending mode of vibration of −OH group due to phenol, and 680 $cm^{-1}$ confirms the presence of hydrous metal oxide (Fe−O) bond present in the complex. The sludge produced during the EC process can be easily removed either by the decantation process or with the help of a filter paper.

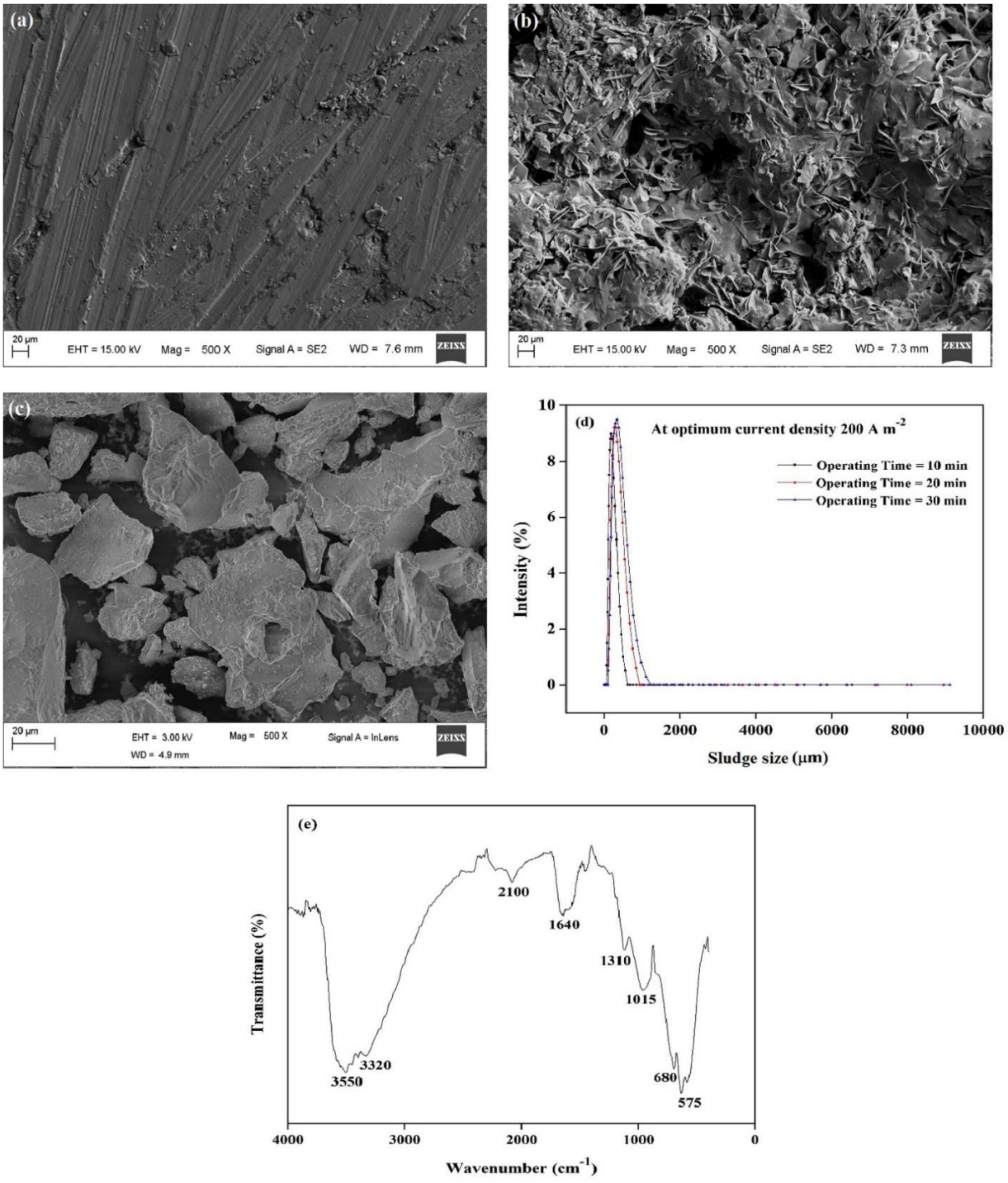


**Fig. 5.7:** Characterization of electrodes and sludge. FESEM images of (a) electrodes before EC treatment, (b) electrodes after EC treatment, and (c) dried EC sludge. Particle size analysis of (d) sludge produced during EC treatment, and FT-IR spectra of (e) dried EC sludge.

## 5.4 Kinetic modelling of phenol, iron, oil and COD reduction

Pseudo first-order reaction was effectively utilized to explain the degradation of pollutants during ozonation [35].

$$\frac{dC_p}{dt} = -k_{obs}\, C_p \quad (5.13)$$

Integration of Eq. (13) gives:

$$C_p = C_p^0\, e^{-k_{obs}t} \quad (5.14)$$

here, $C_p$ = pollutant concentration (mg $L^{-1}$), $C_p^0$ = Initial pollutant concentration (mg $L^{-1}$), t = residence time (min) and $k_{obs}$ = observed first-order rate constant ($min^{-1}$). As such, the plot of residence time versus regression of ln $C_p$ was used to evaluate the rate constant ($k_{obs}$). The values of $R^2$ and $k_{obs}$ at three ozone generation rates such as 1.12, 1.00, and 0.85 mg $s^{-1}$ for phenol, COD, BOD, iron, and oil are shown in Table 5.3. From the kinetic study conducted, it was observed that the reduction in pollutant efficiency gets enhanced as the ozone generation rate is increased. Thus, an improved reduction in pollutant concentration at 1.12 mg $s^{-1}$ compared to 0.85 mg $s^{-1}$ is primarily because of the existence of a high amount of dissolved quantity of ozone in the solution, resulting in higher oxidation of pollutants. At 1.12 mg $s^{-1}$, $k_{obs}$ for phenol (0.0705 $min^{-1}$) was found to be the highest, whereas $k_{obs}$ starts decreasing for 1.00 mg $s^{-1}$ (0.0548 $min^{-1}$) and 0.85 mg $s^{-1}$ (0.0352 $min^{-1}$), respectively. Likewise, the highest $k_{obs}$ for COD (0.0817 $min^{-1}$), BOD (0.1136 $min^{-1}$), iron (0.1121 $min^{-1}$), and oil content (0.0492 $min^{-1}$) were found at 1.12 mg $s^{-1}$. However, with a decline in the ozone generation rate from 1.00 to 0.85 mg $s^{-1}$, the rate constant $k_{obs}$ also decreases, as observed from Table 5.3. Also, the highest $R^2$ of 0.99 for phenol, iron, BOD and COD and 0.98 for oil and grease, respectively, was obtained at 1.12 mg $s^{-1}$. As a result,

reaction kinetics displayed that both the cations and the anions acknowledged the fitting of the kinetic model perfectly. Therefore, it can be inferred that all the compounds present in the effluent responded quite significantly to the pseudo first-order kinetic model.

**Table 5.3:** Observed reaction rate and $R^2$ values for different pollutants at three ozone generation rates.

| **Parameters** | **1.12 mg $s^{-1}$** | | **1.00 mg $s^{-1}$** | | **0.85 mg $s^{-1}$** | |
|---|---|---|---|---|---|---|
| | **$k_{obs}$ ($min^{-1}$)** | **$R^2$** | **$k_{obs}$ ($min^{-1}$)** | **$R^2$** | **$k_{obs}$ ($min^{-1}$)** | **$R^2$** |
| Phenol | 0.0705 | 0.99 | 0.0548 | 0.99 | 0.0352 | 0.99 |
| COD | 0.0817 | 0.99 | 0.0657 | 0.99 | 0.0484 | 0.99 |
| BOD | 0.1136 | 0.99 | 0.0780 | 0.99 | 0.0613 | 0.99 |
| Iron | 0.1121 | 0.99 | 0.0909 | 0.99 | 0.0676 | 0.99 |
| Oil | 0.0492 | 0.98 | 0.0304 | 0.98 | 0.0247 | 0.98 |

## 5.5 Mass transfer study of ozone

The conversion of gaseous ozone into the liquid phase along with its self-decomposition reaction governs the phenomenon of volumetric mass transfer coefficient ($K_l$ a) of ozone. The ozone mass transfer study was investigated to determine ozone transport from the gaseous phase into the aqueous phase. This phase change solely depends upon the $K_l$ a values. Two phenomena are involved in evaluating the $K_l$ a values of ozone, viz. self-decomposition rate of ozone absorbed into the solution, and mass transfer of the gaseous ozone into the aqueous phase [36]. The details of the mass transfer equations have been elaborately reported in chapter 3. The experiments were

carried out at 20 °C. The diffusion coefficient ($k_d$) for various pH ranges were determined using the correlation mention by Sotelo et al. (1987) [37]. At pH 3.5, the values of $K_l a$ were found to be $0.26 \times 10^3$ $s^{-1}$, $0.43 \times 10^3$ $s^{-1}$, and $0.55 \times 10^3$ $s^{-1}$, for ozone generation rates of 0.85 mg $s^{-1}$, 1.00 mg $s^{-1}$, and 1.12 mg $s^{-1}$ respectively, when $k_d$ was $2.6 \times 10^4$ $s^{-1}$. It can be concluded that an increase in $K_l a$ with respect to ozone generation rates corresponds to the enhanced mass transfer of gaseous ozone into the liquid phase i.e. the ozone generation rate is directly proportional to $K_l a$. Thus, the amount of dissolved ozone concentration increases in the solution, with an increase in the ozone generation rate from 0.85 to 1.12 mg $s^{-1}$, as shown in Figure 5.8.

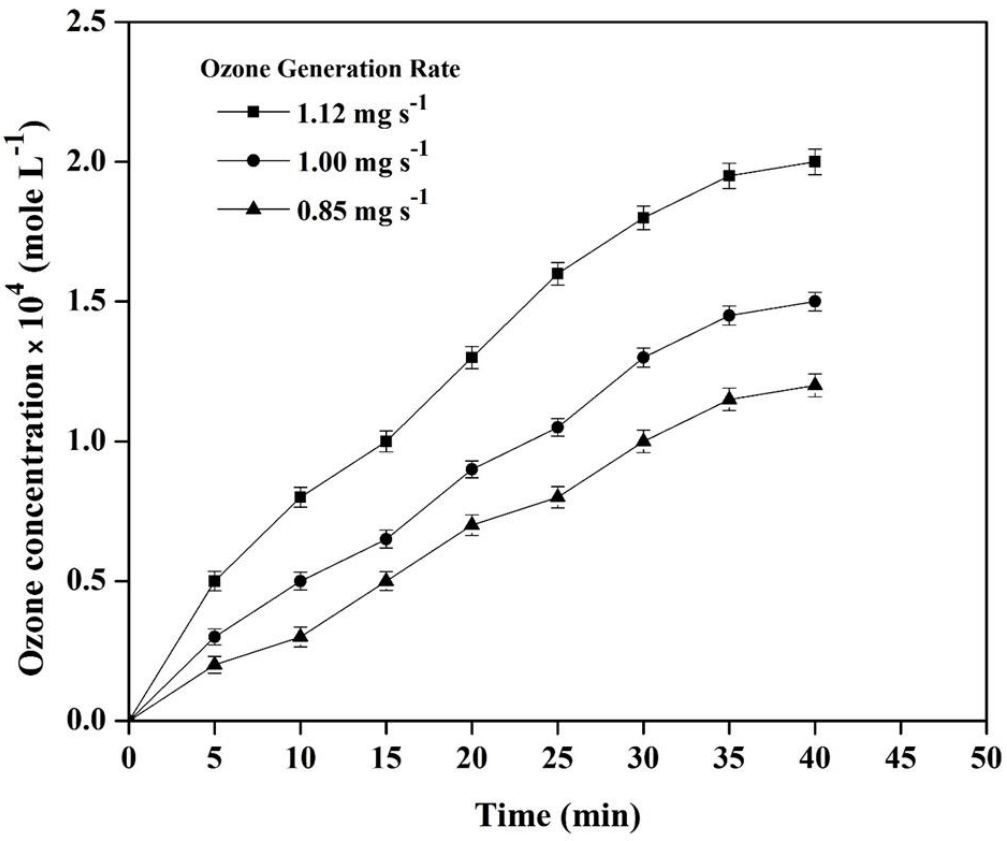


**Fig. 5.8:** Concentration profile of ozone at different ozone generation rates

## 5.6 Estimation of energy consumption and operating cost of each process

During the lab scale (batch operation) application of ozonation process, the economic aspect is investigated by the evaluation of electrical energy per order ($E_{EO}$). The figures-of-merit for technical development, based on the electrical energy per order ($E_{EO}$) (also termed as the efficiency index) was calculated. $E_{EO}$ is the amount of electrical energy required in kWh for decreasing the pollutant content by 1 order of magnitude in 1 $m^3$ of contaminated water. For pseudo-first order reactions, the $E_{EO}$ (kWh $m^{-3}$) values for batch operations was calculated with the help of following equation [38]:

$$E_{EO} = \frac{P \times t \times 1000}{V \times \log_{10} \frac{C_i}{C_f}} \quad (5.15)$$

where P = power required for the process (kWh), t = reaction time (h), V = volume of sample treated, $C_i$ and $C_f$ are the initial and final concentration of the pollutants. In ozonation, the $E_{EO}$ values for the pollutants are as follows: for COD, $E_{EO}$ = 69.32 kWh $m^{-3}$, for BOD $E_{EO}$ = 61.4 kWh $m^{-3}$, for phenol $E_{EO}$ = 30.25 kWh $m^{-3}$, for iron $E_{EO}$ = 41.40 kWh $m^{-3}$, for oil $E_{EO}$ = 86.25 kWh $m^{-3}$. Similarly, in case of electrocoagulation the values of $E_{EO}$ obtained are as follows: for COD, $E_{EO}$ = 43.70 kWh $m^{-3}$, for BOD $E_{EO}$ = 53.25 kWh $m^{-3}$, for phenol $E_{EO}$ = 26.52 kWh $m^{-3}$, for iron $E_{EO}$ = 28.05 kWh $m^{-3}$, for oil $E_{EO}$ = 48.85 kWh $m^{-3}$. It is clearly evident that electrical energy per order for electrocoagulation is lower than that of ozonation, indicating that the electrocoagulation process is more energy-efficient with respect to the removal of specified pollutants.

Furthermore, in the present work, the cost estimation for ozonation primarily considered the cost of energy requirement during the entire operation (US$ $m^{-3}$ of solution). The operational cost was calculated from the equation below:

$$\text{Operating cost}_{(\text{ozonation})} = q \times Q_{\text{energy}} \quad (5.16)$$

here, q = Electricity cost (0.0948 US$ $kWh^{-1}$) and $Q_{energy}$ = Electrical energy consumption for pollutant removal. The electricity cost was considered in accordance with its price for Assam (India) in the year 2020. Considering the power utilization to be 33, 51, and 72.5 W at 0.85, 1.00, and 1.12 mg $s^{-1}$, the price of electrical energy was observed to be 14.11, 27.50, and 44.75 US$ $m^{-3}$, respectively. As such, the cost of operation for the ozone generation rate of 0.85, 1.00, and 1.12 mg $s^{-1}$ was calculated as 1.36, 2.65, and 4.30 US$ $m^{-3}$, respectively at the end of 30 min.

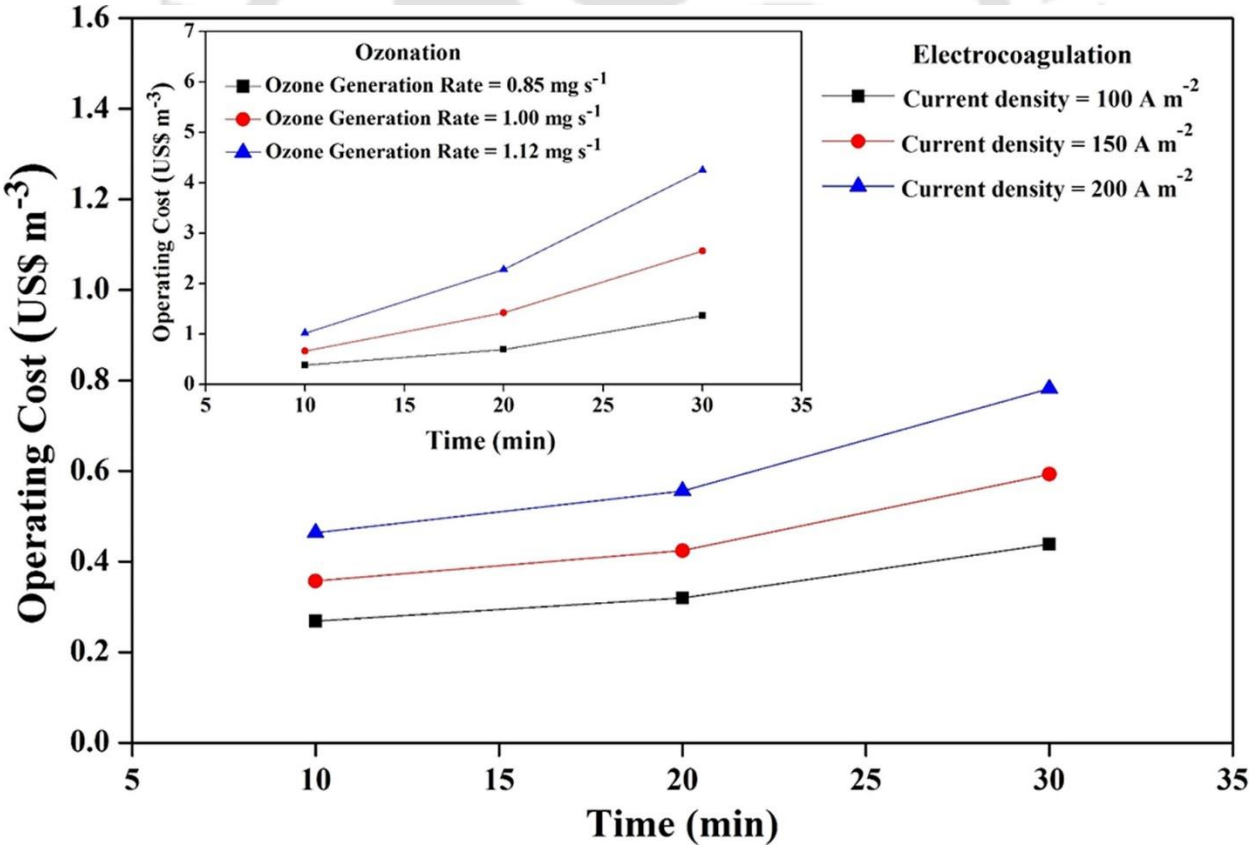


**Fig. 5.9:** Effect of electrocoagulation and ozonation on operating cost. Inset: ozonation process, Outset: electrocoagulation process

The cost of operation for electrocoagulation consists of sludge disposal cost, fixed cost, cost of chemicals, electricity, and electrode cost. Nevertheless, for simplicity, the cost estimation in this study mainly involved the rate of electricity and the electrode cost. The operating cost was determined from the equation given below [39]:

$$\text{Operating cost}_{(\text{electrocoagulation})} = p \times Q_{\text{electrode}} + q \times Q_{\text{energy}} \quad (5.17)$$

Here, $Q_{\text{energy}}$ = Electrical energy consumption for pollutant removal, $Q_{\text{electrode}}$ = Electrode materials consumption, p = Cost of electrode (2.0475 US$ $kg^{-1}$ of aluminum) and q = Cost of electricity (0.0948 US$ $kWh^{-1}$). The equation for electrical energy consumption is given as:

$$Q_{\text{energy}} = \frac{I \times V \times t}{V_L} \quad (5.18)$$

Here, I = Current (A), V = Voltage (V), t = treatment time (s) and $V_L$ = Wastewater volume ($m^3$). However, consumption of electrodes was evaluated from the equation below (Faraday's law) [15]:

$$Q_{\text{electrode}} = \frac{I \times t \times M.W}{F \times z \times V_L} \quad (5.19)$$

Here, M.W = Molar mass of aluminum (26.98 g $mol^{-1}$), F = Faraday's constant (96,487 C $mol^{-1}$) and z = Number of transferred electrons (z = 3). The work done showed that, with an enhanced current density, both the cost of energy and the electrodes was increased. The reason can be attributed to higher anodic oxidation and energy consumption during the process. Thus, with a rise in current density from 100 to 200 A $m^{-2}$, the cost of electrodes as well as the cost of energy varied from 0.00106 to 0.00242 US$ $m^{-3}$ and 2.82 to 6.5 US$ $m^{-3}$, respectively. The operating cost as such was calculated to be 0.381, 0.553, and 0.742 US$ $m^{-3}$ for a current density of 100, 150, and 200 A $m^{-2}$, respectively after a reaction time of 30 min. Figure 5.9 shows the cost of operation for both ozonation and electrocoagulation processes. It is seen from Figure 5.9 that electrocoagulation

is much more economical compared to the ozonation process. Also, the operational cost for this study was found to be economical for both the processes, when compared with other reported treatment methods, as shown in Table 5.4.

**Table 5.4:** Comparison of cost estimation for the ozonation and electrocoagulation process in treating different types of wastewater

| **Methods used** | **Types of wastewater** | **Operating cost** | **References** |
|---|---|---|---|
| Electrocoagulation | Metalworking wastewater | 4.74 US$ $m^{-3}$ | [40] |
| Electrocoagulation | Synthetic wastewater | 1.62 US$ $m^{-3}$ | [41] |
| Electrocoagulation | Kraft pulp bleaching filtrates | 14.21 US$ $m^{-3}$ | [42] |
| Electrocoagulation | Synthetic wastewater | 6.05 US$ $m^{-3}$ | [15] |
| Ozonation | Microalgae lipid strain slurry | 7.44 US$ (kg of dry algal mass)$^{-1}$ | [43] |
| Ozonation | Textile dye wastewater | 63.5 US$ $m^{-3}$ | [44] |
| Ozonation | Olive oil mill wastewater | 95 US$/$m^3$ | [45] |
| Ozonation | Municipal wastewater | 4.50 US$ $m^{-3}$ | [46] |
| Electrocoagulation<br>Ozonation | Cold rolling mill wastewater | EC = 0.742 US$ $m^{-3}$<br>$O_3$ = 4.30 US$ $m^{-3}$ | **Present Work** |

## 5.7 Feasibility study of the ozonation and electrocoagulation processes

The economic advantage of operating an electrocoagulation setup over an ozonation unit is quite evident. A preliminary cost analysis study was also conducted for both the processes, which indicated that the electrocoagulation process is much more economical than ozonation, as shown in Figure 5.9. The capital cost of setting up an ozonation unit will be higher due to the greater complexity of fabrication and erection than an electrocoagulation unit. Moreover, the efficacy of the electrocoagulation process is remarkably higher for reducing all the available pollutants in the effluent compared to the ozonation process, as evident from Figure 5.10. Besides, there are other downsides of ozonation, such as the treated water stream is highly acidic, complete mineralization of complex contaminants is sometimes not possible, and generation of toxic intermediates can cause more damage [47]. On the other hand, the degraded products formed during electrocoagulation get adsorbed and securely locked in the generated sludge, which the decantation process can easily separate. The stream coming out of the electrocoagulation chamber is non-corrosive and slightly alkaline. Moreover, there is no risk of releasing noxious fumes from an electrocoagulation chamber, while proper precautions must be taken to prevent an accidental release of ozone. Hence, the targeted effluent electrocoagulation process is more suitable than ozonation, owing to its better performance efficiency and utilization of a lesser amount of current. The results reported here depicted the feasibility of the techniques considered herein and not scalable to continuous operation at the level of 10–30 m3 h−1. However, the range of values of crucial factors like; the current density, residence time within the reactor, inter-electrode distance, and electrode materials considered herein might be helpful to design a continuous flow reactor. For example, the reactor volume for a 30 m3 h−1 capacity treatment plant can only be known from

the residence time obtained from this study. However, the hydrodynamic and mixing properties of the reactors must be taken care of before designing the reactor for a continuous mode of operation.

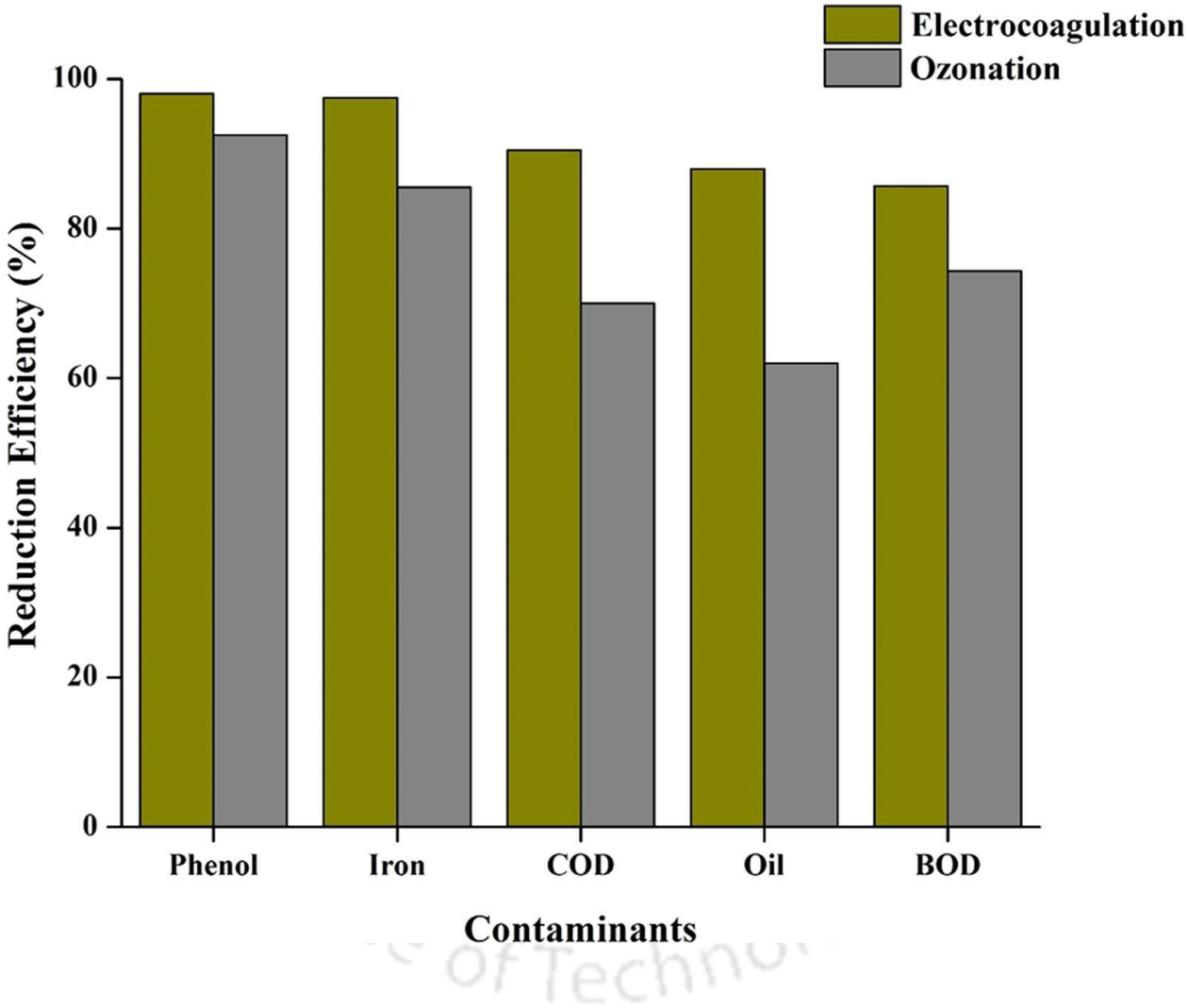


**Fig. 5.10:** Comparison of pollutant reduction efficiency by electrocoagulation and ozonation.

## 5.8 Summary of work

This study focuses on the standalone application of ozonation and electrocoagulation processes for the removal of phenol, COD, BOD, iron, and oil content from the CRM wastewater of Tata Steel industry (India). Ozonation leads to a decrease in initial pH from 7.8 to 3.5 due to the formation of various derivatives of acidic character. Nevertheless, the pH increases from 7.8 to 8.5 during electrocoagulation, owing to the generation of $OH^-$ ions at the cathode surface. The optimum operating conditions of 1.12 mg $s^{-1}$ (ozone generation rate), 200 A $m^{-2}$ (current density), and 30 min (treatment time) were sufficient in lowering all the target contaminants below their respective permissible limits, thus fulfilling the environmental requirement for its discharge/reuse. Also, at the optimized operating conditions, the electrocoagulation process was found to achieve better removal efficiency for all the target contaminants (phenol, iron, COD, BOD, and oil & grease) compared to ozonation. Besides, if the ozone generation rate was increased above 1.12 mg $s^{-1}$ (optimized condition), there is only a slight increase in the pollutant removal efficiency, whereas a significant increase in the operational cost was observed. Further, the decomposition of pollutants pursues pseudo first-order kinetics, in which the highest rate constant ($k_{obs}$) for all the target contaminants was achieved at the optimum ozone generation rate of 1.12 mg $s^{-1}$. Particle size analysis showed that the size of electrogenerated sludge increases with an increase in electrolysis time. The increase in sludge size indicates the formation of more amount of $Al(OH)_3$ with respect to electrolysis time. Additionally, the preliminary cost estimation showed that the operating cost of ozonation (4.30 US$ $m^{-3}$) was about six times than that of electrocoagulation (0.742 US$ $m^{-3}$) for the CRM wastewater. Thus, it may be concluded that electrocoagulation is highly economical and showed better pollutant removal efficiency than ozonation for the target wastewater.

## Chapter 5

## References


[1] S. Venkatesh, N.D. Pandey, A.R. Quoff, Decolorization of synthetic dye solution containing congo red by Advanced Oxidation Process (AOP), Int. J. Adv. Res. Civil,Structural,Environment Infrastruct. Eng. Dev. 2 (2014) 49–55. https://doi.org/10.1016/ijarcsei.2014.106115.

[2] S.M. de A.G.U. de Souza, K.A.S. Bonilla, A.A.U. de Souza, Removal of COD and color from hydrolyzed textile azo dye by combined ozonation and biological treatment, J. Hazard. Mater. 179 (2010) 35–42. https://doi.org/10.1016/j.jhazmat.2010.02.053.

[3] Y. Meas, J.A. Ramirez, M.A. Villalon, T.W. Chapman, Industrial wastewaters treated by electrocoagulation, Electrochim. Acta. 55 (2010) 8165–8171. https://doi.org/10.1016/j.electacta.2010.05.018.

[4] S. Enami, M.R. Hoffmann, A.J. Colussi, How phenol and a-tocopherol react with ambient ozone at gas/liquid interfaces, J. Phys. Chem. A. 113 (2009) 7002–7010. https://doi.org/10.1021/jp901712k.

[5] M.K. Ramseier, U. von Gunten, Mechanisms of phenol ozonation-kinetics of formation of primary and secondary reaction products, Ozone Sci. Eng. 31 (2009) 201–215. https://doi.org/10.1080/01919510902740477.

[6] L.P. Yang, W.Y. Hu, H.M. Huang, B. Yan, Degradation of high concentration phenol by ozonation in combination with ultrasonic irradiation, Desalin. Water Treat. 21 (2010) 87–95. https://doi.org/10.5004/dwt.2010.1233.

[7] Y. Du, M. Zhou, L. Lei, Role of the intermediates in the degradation of phenolic compounds by Fenton-like process, J. Hazard. Mater. 136 (2006) 859–865. https://doi.org/10.1016/j.jhazmat.2006.01.022.

[8] S. Esplugas, J. Giménez, S. Contreras, E. Pascual, M. Rodríguez, Comparison of different advanced oxidation processes for phenol degradation, Water Res. 36 (2002) 1034–1042. https://doi.org/10.1016/S0043-1354(01)00301-3.

[9] N. Adhoum, L. Monser, Decolourization and removal of phenolic compounds from olive mill wastewater by electrocoagulation, Chem. Eng. Process. Process Intensif. 43 (2004) 1281–1287. https://doi.org/10.1016/j.cep.2003.12.001.

[10] M. Uğurlu, A. Gürses, Ç. Doğar, M. Yalçin, The removal of lignin and phenol from paper mill effluents by electrocoagulation, J. Environ. Manage. 87 (2008) 420–428. https://doi.org/10.1016/j.jenvman.2007.01.007.

[11] J. Sallanko, E. Lakso, J. Röpelinen, Iron behavior in the ozonation and filtration of groundwater, Ozone Sci. Eng. 28 (2006) 269–273. https://doi.org/10.1080/01919510600721795.

[12] R. El Araby, S. Hawash, G. El Diwani, Treatment of iron and manganese in simulated groundwater via ozone technology, Desalination. 249 (2009) 1345–1349. https://doi.org/10.1016/j.desal.2009.05.006.

[13] N. Kishimoto, S. Ueno, Catalytic Effect of Several Iron Species on Ozonation, J. Water Environ. Technol. 10 (2012) 205–215. https://doi.org/10.2965/jwet.2012.205.

[14] A. Doggaz, A. Attour, M. Le Page Mostefa, M. Tlili, F. Lapicque, Iron removal from waters by electrocoagulation: Investigations of the various physicochemical phenomena involved, Sep. Purif. Technol. 203 (2018) 217–225. https://doi.org/10.1016/j.seppur.2018.04.045.

[15] D. Ghosh, H. Solanki, M.K. Purkait, Removal of Fe(II) from tap water by electrocoagulation technique, J. Hazard. Mater. 155 (2008) 135–143. https://doi.org/10.1016/j.jhazmat.2007.11.042.

[16] P.K.A. Hong, T. Xiao, Treatment of oil spill water by ozonation and sand filtration, Chemosphere. 91 (2013) 641–647. https://doi.org/10.1016/j.chemosphere.2013.01.010.

[17] L.G. De Araujo, E.S.A.P. Prado, F. De Souza Miranda, R. Vicente, A.S. Da Silva Sobrinho, G.P. Filho, J.T. Marumo, Physicochemical modifications of radioactive oil sludge by ozone treatment, J. Environ. Chem. Eng. 8 (2020) 104128. https://doi.org/10.1016/j.jece.2020.104128.

[18] J. Cerkovnik, E. Eržen, J. Koller, B. Plesničar, Evidence for HOOO radicals in the formation of alkyl hydrotrioxides (ROOOH) and hydrogen trioxide (HOOOH) in the ozonation of C - H bonds in hydrocarbons, J. Am. Chem. Soc. 124 (2002) 404–409. https://doi.org/10.1021/ja017320i.

[19] R. Lee, M.L. Coote, Mechanistic insights into ozone-initiated oxidative degradation of saturated hydrocarbons and polymers, Phys. Chem. Chem. Phys. 18 (2016) 24663–24671. https://doi.org/10.1039/c6cp05064f.

[20] V.L. Dhadge, C.R. Medhi, M. Changmai, M.K. Purkait, House hold unit for the treatment of fluoride, iron, arsenic and microorganism contaminated drinking water, Chemosphere. 199 (2018) 728–736. https://doi.org/10.1016/j.chemosphere.2018.02.087.

[21] M. Changmai, M. Pasawan, M.K. Purkait, Treatment of oily wastewater from drilling site using electrocoagulation followed by microfiltration, Sep. Purif. Technol. 210 (2019) 463–472. https://doi.org/10.1016/j.seppur.2018.08.007.

[22] M.H. Abdel-Aziz, E.S.Z. El-Ashtoukhy, M.S. Zoromba, M. Bassyouni, Oil-in-water emulsion breaking by electrocoagulation in a modified electrochemical cell, Int. J. Electrochem. Sci. 11 (2016) 9634–9643. https://doi.org/10.20964/2016.11.53.

[23] C.D. Adams, S. Gorg, Effect of pH and Gas-Phase Ozone Concentration on the Decolorization of Common Textile Dyes, J. Environ. Eng. 128 (2002) 293–298. https://doi.org/10.1061/(asce)0733-9372(2002)128:3(293).

[24] V. Preethi, K.S. Parama Kalyani, K. Iyappan, C. Srinivasakannan, N. Balasubramaniam, N. Vedaraman, Ozonation of tannery effluent for removal of cod and color, J. Hazard. Mater. 166 (2009) 150–154. https://doi.org/10.1016/j.jhazmat.2008.11.035.

[25] M. Priya, J. Jeyanthi, Removal of COD, oil and grease from automobile wash water effluent using electrocoagulation technique., Microchem. J. 150 (2019) 104070. https://doi.org/10.1016/j.microc.2019.104070.

[26] S. Baig, P.A. Liechti, Ozone treatment for biorefractory COD removal, Water Sci. Technol. 43 (2001) 197–204. https://doi.org/10.2166/wst.2001.0090.

[27] Q.H. Nguyen, T. Watari, T. Yamaguchi, Y. Takimoto, K. Niihara, J.P. Wiff, T. Nakayama, COD removal from artificial wastewater by electrocoagulation using aluminum electrodes, Int. J. Electrochem. Sci. 15 (2020) 39–51. https://doi.org/10.20964/2020.01.42.

[28] O. Chedeville, M. Debacq, C. Porte, Removal of phenolic compounds present in olive mill wastewaters by ozonation, Desalination. 249 (2009) 865–869. https://doi.org/10.1016/j.desal.2009.04.014.

[29] J.A. Diaz-Alarcón, M.P. Alfonso-Pérez, I. Vergara-Gómez, M. Díaz-Lagos, S.A. Martínez-Ovalle, Removal of iron and manganese in groundwater through magnetotactic bacteria, J. Environ. Manage. 249 (2019) 109381. https://doi.org/10.1016/j.jenvman.2019.109381.

[30] M. Aji, B. Gutti, B. Highina, Application of Activated Carbon in Removal of Iron and Manganese from Alau Dam water in Maiduguri, Colomb J Life Sci. 17 (2015) 35–39. https://doi.org/10.1016/cjls.2015.155641.

[31] M.E. Torbaghan, G.H. Khalili Torghabeh, Biological removal of iron and sulfate from synthetic wastewater of cotton delinting factory by using halophilic sulfate-reducing bacteria, Heliyon. 5 (2019) e02948. https://doi.org/10.1016/j.heliyon.2019.e02948.

[32] H. Selçuk, G. Eremektar, S. Meriç, The effect of pre-ozone oxidation on acute toxicity and inert soluble COD fractions of a textile finishing industry wastewater, J. Hazard. Mater. 137 (2006) 254–260. https://doi.org/10.1016/j.jhazmat.2006.01.055.

[33] C.T. Wang, W.L. Chou, Y.M. Kuo, Removal of COD from laundry wastewater by electrocoagulation/electroflotation, J. Hazard. Mater. 164 (2009) 81–86. https://doi.org/10.1016/j.jhazmat.2008.07.122.

[34] M. Irfan, T. Butt, N. Imtiaz, N. Abbas, R.A. Khan, A. Shafique, The removal of COD, TSS and colour of black liquor by coagulation–flocculation process at optimized pH, settling and dosing rate, Arab. J. Chem. 10 (2017) S2307–S2318. https://doi.org/10.1016/j.arabjc.2013.08.007.

[35] P. Mondal, M.K. Purkait, Green synthesized iron nanoparticles supported on pH responsive polymeric membrane for nitrobenzene reduction and fluoride rejection study: Optimization approach, J. Clean. Prod. 170 (2018) 1111–1123. https://doi.org/10.1016/j.jclepro.2017.09.222.

[36] S. Khuntia, S.K. Majumder, P. Ghosh, Removal of ammonia from water by ozone microbubbles, Ind. Eng. Chem. Res. 52 (2013) 318–326. https://doi.org/10.1021/ie302212p.

[37] J.L. Sotelo, F.J. Beltran, F.J. Benitez, J. Beltran-heredia, Ozone Decomposition in Water: Kinetic Study, Ind. Eng. Chem. Res. 26 (1987) 39–43. https://doi.org/10.1021/ie00061a008.

[38] J.R. Bolton, K.G. Bircher, W. Tumas, C.A. Tolman, Figures-of-merit for the technical development and application of advanced oxidation technologies for both electric- and solar-driven systems (IUPAC Technical Report), Pure Appl. Chem. 73 (2001) 627–637. https://doi.org/doi:10.1351/pac200173040627.

[39] M. Changmai, P.P. Das, P. Mondal, M. Pasawan, A. Sinha, P. Biswas, S. Sarkar, M.K. Purkait, Hybrid electrocoagulation–microfiltration technique for treatment of nanofiltration rejected steel industry effluent, Int. J. Environ. Anal. Chem. 102 (2022) 62–83. https://doi.org/10.1080/03067319.2020.1715381.

[40] M. Kobya, P.I. Omwene, Z. Ukundimana, Treatment and operating cost analysis of metalworking wastewaters by a continuous electrocoagulation reactor, J. Environ. Chem. Eng. 8 (2020) 103526. https://doi.org/10.1016/j.jece.2019.103526.

[41] M.A. Madhavan, S.P. Antony, Effect of polarity shift on the performance of electrocoagulation process for the treatment of produced water, Chemosphere. 263 (2021) 128052. https://doi.org/10.1016/j.chemosphere.2020.128052.

[42] E.C.L. Coimbra, A.H. Mounteer, A.L.V. do Carmo, M.J.F. Michielsen, L.A. Tótola, J.P.F. Guerino, J.G.A.N. Gonçalves, P.R. da Silva, Electrocoagulation of kraft pulp bleaching filtrates to improve biotreatability, Process Saf. Environ. Prot. 147 (2021) 346–355. https://doi.org/10.1016/j.psep.2020.09.039.

[43] M.F. Kamaroddin, A. Rahaman, D.J. Gilmour, W.B. Zimmerman, Optimization and cost estimation of microalgal lipid extraction using ozone-rich microbubbles for biodiesel production, Biocatal. Agric. Biotechnol. 23 (2020) 101462. https://doi.org/10.1016/j.bcab.2019.101462.

[44] A.M. El-Dein, J. Libra, U. Wiesmann, Cost analysis for the degradation of highly concentrated textile dye wastewater with chemical oxidation H2O2/UV and biological treatment, J. Chem. Technol. Biotechnol. 81 (2006) 1239–1245. https://doi.org/https://doi.org/10.1002/jctb.1531.

[45] P. Cañizares, R. Paz, C. Sáez, M.A. Rodrigo, Costs of the electrochemical oxidation of wastewaters: A comparison with ozonation and Fenton oxidation processes, J. Environ. Manage. 90 (2009) 410–420. https://doi.org/10.1016/j.jenvman.2007.10.010.

[46] R. Irani, A.B. Khoshfetrat, M. Forouzesh, Real municipal wastewater treatment using simultaneous pre and post-ozonation combined biological attached growth reactor: Energy consumption assessment, J. Environ. Chem. Eng. 9 (2021) 104595. https://doi.org/10.1016/j.jece.2020.104595.

[47] A.H. Konsowa, M.E. Ossman, Y. Chen, J.C. Crittenden, Decolorization of industrial wastewater by ozonation followed by adsorption on activated carbon, J. Hazard. Mater. 176 (2010) 181–185. https://doi.org/10.1016/j.jhazmat.2009.11.010.

# Chapter 6

# Conclusions and Future scope of work

# Chapter 6
# Conclusions and Future scope of work

*The present chapter has been categorized into two sections: first section contains the conclusions of all the experimental results presented in this thesis and the inferences drawn from it, while the second section includes recommendations towards scope for future work.*

## 6.1 Conclusion

**Chapter 1** addresses the state of the art literature, research motivation of present work, possible scope of research, along with the objectives and organization of the thesis. **Chapter 2** describes the materials and experimental methods used for the thesis work. The mechanism and reactor set-up of both ozonation and electrocoagulation methods were discussed. It also includes the characterization techniques used for the analysis of the wastewater samples.

**Chapter 3: Hybrid ozone assisted electrocoagulation technique for the treatment of cyanide and phenol rich steel plant wastewater.**

1. During ozonation, the pH of the effluent rapidly decreases from an initial pH of 7.72 to 3.0. However, the pH later increases up to 8.30 at the end of the electrocoagulation process.
2. The hybrid ozone assisted electrocoagulation process was very effective in reducing the concentration of cyanide, phenol, COD, BOD, and chloride up to 0.1 mg $L^{-1}$ (99.8 %), 0.5 mg $L^{-1}$ (99.5 %), 110 mg $L^{-1}$ (94.7 %), 24 mg $L^{-1}$ (95.0 %), and 975 mg $L^{-1}$ (46.5 %), respectively, which is well below their respective permissible limit of surface water.

3. The kinetic study performed indicated that the degradation of all the target contaminants can be well explained by the pseudo first-order kinetic model. The highest contaminant reduction with rate constant ($k_{obs}$) of 0.1208, 0.1401, 0.0309, 0.0338, and 0.0125 $min^{-1}$ and $R^2$ values of 0.99 were obtained for cyanide, phenol, COD, BOD, and chloride, respectively, at an ozone generation rate of 1.33 mg $s^{-1}$.
4. Mass transfer study showed that an increase in the ozone generation rate increases the volumetric mass transfer coefficient ($K_l$ a), resulting in an increased ozone concentration.
5. The hybrid ozone assisted electrocoagulation process showed an operating cost of 5.801 US$ $m^{-3}$.

**Chapter 4: Removal of ammonia-N, iron and colour from steel plant generated biological oxidation treated (BOT) wastewater via hybrid ozone assisted electrocoagulation.**

1. An optimum ozone generation rate of 1.33 mg $s^{-1}$ was sufficient to reduce the colour content up to 45 mg $L^{-1}$ (98.2 %). However, a combination of ozone assisted electrocoagulation process was required to lower the concentration of iron, and ammonia-N up to 0.6 mg $L^{-1}$ (90.6 %), and 48.5 mg $L^{-1}$ (62.8 %), respectively, which was well below their permissible limit of surface water. Even though the removal rate of ammonia-N was found to be much lower, no further treatment was carried out since the WHO permissible limit of the pollutant has already been reached.
2. The kinetic modelling showed that the degradation of the target contaminants followed the pseudo first-order kinetic model. The highest contaminant reduction with rate constant ($k_{obs}$) of 0.022, 0.010, and 0.095 $min^{-1}$ as well as $R^2$ values of 0.988, 0.985, and 0.977 were

obtained for iron, ammonia, and colour, respectively, at an ozone generation rate of 1.33 mg $s^{-1}$.

3. Size determination study of the ozone microbubbles showed that the bubble size varied between 20 µm and 650 µm, with the sauter mean diameter of 425 µm.
4. The corrosion increased from 27.2 to 45.1 mg with an increase in current density from 50 to 150 A $m^{-2}$. Further, an increase in film thickness was observed from 6.1 to 8.8 µm over the electrode surface as current density proceeds from 50 to 150 A $m^{-2}$.
5. Preliminary cost analysis for the hybrid ozone assisted electrocoagulation process was found to be 5.822 US$ $m^{-3}$.

**Chapter 5: Treatment of oil, phenol, and iron rich cold rolling mill (CRM) wastewater of steel plant by standalone electrocoagulation and ozonation techniques.**

1. Ozonation leads to a decrease in the initial pH from 7.8 to 3.5. On the other hand, the pH increases from 7.8 to 8.5 during electrocoagulation.
2. At the optimized conditions, electrocoagulation was found to achieve better removal efficiency for all the target contaminants viz. 98% phenol, 97.5% iron, 90.5% COD, 85.7% BOD, and 88% oil & grease; whereas the ozonation process showed relatively lower removal rates of 93.5% phenol, 86.5% iron, 70% COD, 74.3% BOD, and 62% oil & grease.
3. The degradation of the target contaminants pursues pseudo first-order kinetics. The highest contaminant reduction with rate constant ($k_{obs}$) of 0.0705, 0.1121, 0.0817, 0.1136, and 0.0492 $min^{-1}$ and $R^2$ values of 0.99 were obtained for phenol, iron, COD, BOD, and oil & grease, respectively, at an ozone generation rate of 1.12 mg $s^{-1}$.

4. Particle size analysis showed that the sludge size increases from 211 to 387 µm with a variation in treatment time from 10 to 30 min. The increase in sludge size indicates the formation of more amount of $Al(OH)_3$ with respect to electrolysis time.
5. The operating cost of ozonation (4.30 US$ $m^{-3}$) was found to be about six times than that of electrocoagulation (0.742 US$ $m^{-3}$) during the treatment of the CRM wastewater.

## 6.2 Future scope of work

Research findings of this thesis work provided a good number of insights on both electrocoagulation and ozonation techniques used for the treatment of industrial wastewater. Few recommendations for future work are outlined below:

**Electrocoagulation:**

1. Though the combination of electrocoagulation with other technique resulted in high process performance, yet factors like non-uniform coagulant dosing and electrode passivation continue to restrict its industrial application. However, this can be resolved by the use of alternate current and reverse polarization. Future studies should extensively focus on minimizing the electrode passivation rate as it greatly determines the removal efficiency of the process.
2. Further research must be carried out to reduce the electrode consumption and increase the pollutant reduction efficiency of the process. This might be achieved by evaluating the performance of dielectrophilic improved electrodes, which are projected to minimize the electrode consumption while also improving the water quality of permeates. Such research

would assist in understanding the fouling control mechanism by the electrocoagulation process along with future reactor design of the combined techniques.

3. Significant importance should be given to the development of simulation and modelling approach such as artificial neural network (ANN) and Taguchi models for the prediction of pollutant removal efficiency in complex wastewaters. The use of machine learning tools viz. AutoCAD and Python is another emerging area which could be explored for designing the process reactor and operational control of the EC system.
4. It is highly recommended to develop a sustainable approach for the utilization of generated $H_2$ gas and proper disposal of sludge formed during the EC process. This can significantly make the process more efficient, eco-friendly and cost-effective apart from providing a feasible alternative for the degradation of different wastewater contaminants.

**Ozonation:**

5. Although the ozone-based treatment processes showed higher pollutant degradation efficiency; however, the removal mechanism for most of the refractory organic contaminants has not yet been established. As such, major attention should be given on the development of rate expressions, water chemistry correlation, aspects of mineralization, and selection of scale-up parameters based on established reaction mechanisms.
6. Further studies should be conducted on the evaluation of electrical energy required to oxidize different types of pollutants during ozone-based treatment of real wastewater so that a perceptible comparison could be achieved. The application of solar energy may be a cost-effective solution to treat and reuse different wastewater, which could present ozonation as an economically feasible process.

7. More studies need to be carried out on the implementation of real-time monitoring and control systems to adjust the ozone dosing based on variations in wastewater properties. This ensures that the process remains efficient and effective under changing conditions. Also, optimizing the method of ozone delivery, via fine bubble diffusion or the use of ozone-resistant diffusers, is another emerging area which could be explored to ensure maximum contact between the ozone gas and water samples.
8. Prolonged reaction time can result in higher energy consumption, thereby increasing the overall operating cost of the process. Further studies should be conducted on the use larger reaction tanks or increase the flow rate of water through these reaction tanks, which can significantly improve the mass transfer of ozone from its gaseous phase into aqueous phase, thus reducing the reaction time of the process.
9. Based on the results obtained from the treatment of steel industry effluents, a pilot plant study is strongly recommended to treat different types of wastewater and to investigate its feasibility in industrial scale.

# *Appendix A: Determination of oil and grease concentration using UV-Vis spectrophotometer*

The concentration of oil and grease in both the ozonated and electrocoagulated samples is determined by first creating a calibration curve. The oil and grease concentration in the CRM wastewater was 25 mg $L^{-1}$. In view of this, millipore water and particular volumes of wastewater samples were used to create standard oil and grease emulsions with concentrations ranging from 10 to 25 mg $L^{-1}$. The prepared standards were sonicated for 7-8 hours before analysis. The absorbance of the resulting emulsions at various concentrations was measured using a UV-Vis spectrophotometer at a wavelength of 235 nm. The measured absorbance values were then plotted against variations in emulsion solution concentration. Since the absorbance varied linearly with changes in the proportion of oil and grease, the concentration of both the ozonated and electrocoagulated samples were determined by calculating the absorbance using the calibration curve that was created.

# *Appendix B: Determination of metal ion concentration using atomic absorbance spectrophotometer*

The determination of metal ion concentration in the treated samples is carried out by first preparing a fresh stock solution of 1000 mg $L^{-1}$ for the target metal ion. Standard solutions in the range of 10-100 mg $L^{-1}$ as per requirement were prepared from the stock solution. The obtained standard solutions with varied concentrations were analyzed for their absorbance using atomic absorbance spectrophotometer at the corresponding wavelength for the target metal ion to fit the calibration values in the software analyzing the standard samples. The obtained absorbance values were plotted with respect to variations in solution concentration. Subsequently, the calibration values were used in measuring the unknown concentration of the treated samples. The AAS method detection limit for metal of interest (iron in this study) ranges between 0.06 to 15 μg/mL at a wavelength of 248.3 nm.

# *Appendix C: Calibration standard curve for particle size analyzer*

The particle size analyzer typically works on the principle of dynamic light scattering (DLS). The particle size diameter of the electrocoagulated samples is determined by first creating a calibration standard curve. The measurement cell for the analysis was made of glass and the measurement angle was automatically set to back scatter. The filter optical density and the focus position were taken as 4.039 and 3.1 mm respectively. The solvent used was water, having a refractive index of 1.3303 and the time for each run was 10 sec. The particle size distribution peak was then plotted against variations in particle size diameter. The average hydrodynamic diameter of the standard curve was found to be 63.25 nm with a mean intensity of 290.4 kcounts/s. Also, a diffusion coefficient of 7.4 $\mu m^2/s$ was reported for the standard curve.

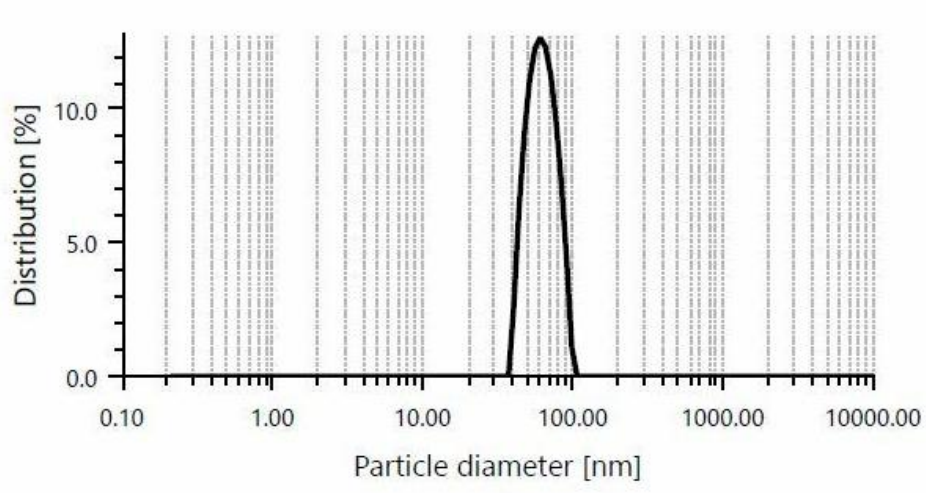


**Fig. A1:** Calibration curve for the standard solution during particle size analysis

# *Appendix D: Hypothesis test to demonstrate the synergy for the ozone-electrocoagulation process*

A hypothesis test based on mean efficiency calculation has been developed to demonstrate the synergy for the integrated process. The mean efficiency of the integrated process ($O_3$/EC) was significantly higher than the standalone processes (EC and $O_3$).

To quantify this, t-statistical test was conducted using a two-sample ANNOVA. The null hypothesis assumes that the difference in the mean value of the standalone and the integrated processes is the same, while the alternate hypothesis assumes both are significantly different. In this study, three samples are taken from the experimental data for both standalone and integrated processes. As the sample size is low, "t" statistics are considered instead of the "z" distribution. Also, the value of "α" was considered to be 0.005 since the difference of the means has a greater significance. While comparing the mean efficiency of standalone ozonation with the integrated process, the t-stat was found to be 8.98 with a p value < 0.0001. As the p-value is drastically lower than α, the null hypothesis could be rejected with good conviction. Further, comparing the mean efficiency of standalone electrocoagulation with the integrated process showed a t-stat of 13.04 with a p value < 0.0001, which again rejects the null hypothesis. Thus, in both the cases, the alternate hypothesis can be adapted which implies that the synergy of the integrated process has a significant impact in enhancing the performance efficiency of the process compared to the standalone methods.

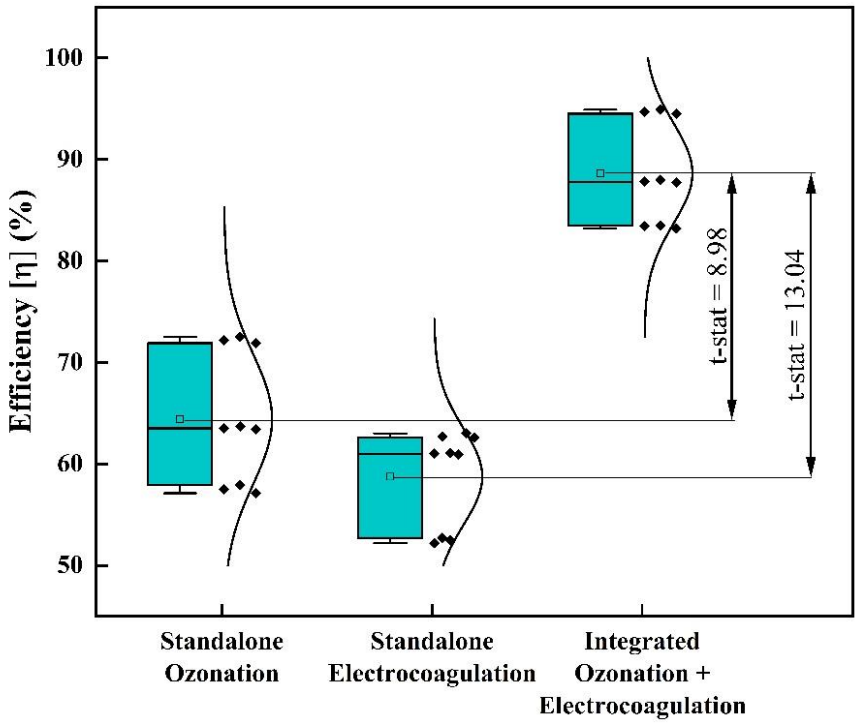


**Fig. A2:** Hypothesis testing establishing the synergy of the integrated process in enhancing the performance efficiency

# *Appendix E: Error analysis*

The errors in experimentally measured quantities and in parameters calculated from those measurements are important in that they determine the accuracy of calculation and predictions using those quantities. There are two types of errors viz. systematic error and random error. Systematic errors are the results of faulty assumptions or improper experimental measuring techniques. In this work, care was taken in eliminating systematic errors by appropriately designing the experiments and adopting qualified methods for analysis of the data. On the other hand, random errors result from variation in the precision of measuring parameters and the slight variations that occur in successive measurements made by the same observer under nearly identical conditions. Random errors cannot be eliminated. The focus of the error analysis presented in this section is on the random errors.

In most of the experiments performed in this work, the quantity that is measured directly is the pollutant concentrations, which is used to determine the removal (%) in the target wastewater samples.

**Error in the measurement of concentration of pollutants**

The pollutant concentrations in the solution were determined using atomic absorbance spectrophotometer and UV-Vis spectrophotometer. Calibration curves were prepared and the absorbance values at various concentrations was measured. From the calibration curves, it was observed that the standard deviation of the predicted value from actual value of concentration is 0.9917 for three different cases. Thus, every measurement of concentration is associated with an error of 0.80 % whose effect on the removal values can be ignored.